NMR STUDIES OF INTERNAL ROTATION

A thesis presented in partial fulfilment
of the requirements for the degree of
Doctor of Philosophy in Chemistry at
Massey University.

ALAN ROBERT FURNESS
1975

ABSTRACT

Density matrix theory has been used to develop a computer program for the solution of a four-nuclear spin system. A description of the theory used to develop this program is given in Chapter Three.

This theory has been used to study a range of p-substituted nitrosobenzenes. The activation parameters have been determined and for N,N-dimethyl-p-nitrosoaniline, a comparison has been made with previous studies which have used more approximate methods.

The solvent dependency of the barrier to rotation has been investigated in the N,N-dialkyl-p-nitrosoanilines and no significant solvent dependence found.

In the early stages of this thesis, attempts were made to find a tetrahedral cobalt (II) complex involving ligand exchange, but no such complex suitable for a detailed NMR investigation was found. The investigation, though unsuccessful, has been briefly reported. These findings may aid further work in this area.

LIST OF CONTENTS

LIST OF TABLES

LIST OF FIGURES

List of Symbols

B_0	external magnetic field in the + z direction
B_1	radiofrequency magnetic field
$\hbar$	Planck's constant divided by 2π
$\mathcal{H}$	Hamiltonian, or Spin Hamiltonian
I^+, I^-	raising and lowering operators
I_x, I_y, I_z	angular momentum operators in units of $h/2\pi$
i	$\sqrt{-1}$
J'_{ij}	Isotropic spin-spin coupling constant between nuclei i and j in terms of linear frequency. It is related to J_{ij} by the following expression, $J'_{ij} = \dfrac{2\pi J_{ij}}{\hbar}$
Tr	Trace
α β	spin functions
σ	sheilding constant
ρ	density matrix
ρ_{ij}	the ijth element of the density matrix
τ, τ'	mean lifetime of the nucleus in a given environment in units of s rad^{-1} and Hz^{-1} respectively.
T_2, T'_2	Transverse relaxation time in units of s rad^{-1} and Hz^{-1} respectively.
T_1, T'_1	Longitudinal relaxation time in units of s rad^{-1} and Hz^{-1} respectively.
Ψ ψ, Φ, ϕ	wave functions
ω_0, ω	angular frequencies

γ	Magnetogyric ratio
f	$\gamma B_1/4\pi$
ω_r	γB_1
$\otimes$	tensor product
k_B	Boltzmann constant
k	specific rotational rate
$K^{\ddagger}$	equilibrium constant
χ	transmission coefficient
ω_A	angular frequency of proton at site A
ω_B	angular frequency of proton at site B
$\langle I_{yT} \rangle$	total angular momentum in the y direction

CHAPTER ONE

An Introduction

to

Nuclear Magnetic Resonance

This thesis is concerned with the study of the internal rotation of molecules using nuclear magnetic resonance (NMR). The first NMR signals were observed almost simultaneously in 1945 by two separate groups led by Bloch[1] and Purcell[2]. Since 1945 instrumentation has developed to such an extent that NMR is now a very powerful tool for the investigation of molecular structure and molecular processes. Today, the NMR spectroscopist is concerned with not only the precise determination of high resolution spectra, but also the detailed elucidation of the NMR parameters from the spectra. His field of study also includes the interpretation and/or prediction of these parameters from the physical and theoretical models as well as applying this knowledge to problems such as the evaluation of kinetic parameters for processes where nuclei are interchanged, an example being rotation about a bond.

The purpose of this chapter is to provide a brief overview of some basic principles of NMR that will be encountered in reading this thesis.

1.1 Nuclear Spin

Pauli suggested the idea of nuclear spin in 1924[3] in order to explain the hyperfine structure in atomic spectra. He suggested that the hyperfine structure was due to nuclear spin angular momentum. The quantum number describing this energy is given the symbol I, and is called the spin quantum number. Table 1.1 lists the spin quantum number for some of the more common species.

TABLE 1.1 Spin properties for a selection of Nuclei[4].

Isotope	I	% Natural Abundance
^1H	$\frac{1}{2}$	99.98
^2D	1	0.016
^{11}B	3/2	81.17
^{13}C	$\frac{1}{2}$	1.11
^{14}N	1	99.64
^{19}F	$\frac{1}{2}$	100
^{31}P	$\frac{1}{2}$	100

1.2 Chemical Shifts

The main contributing factor to the phenomenon of the chemical shift is the shielding of the nucleus from the external magnetic field by the electrons. Electron circulations give rise to magnetic fields. The effect of an applied magnetic field on the electrons of a molecule is to produce localized induced magnetic fields. These induced magnetic fields operate against the field applied to the sample.

In order to attain the resonance condition, a proton shielded in this way by its associated electrons, requires a greater applied field than that required by an isolated proton. Such a proton will resonate at a higher applied external magnetic field than an unshielded proton. The measurement of the chemical shift position of nuclei in different chemical environments is a powerful tool in the elucidation of molecular structure.

1.3 Spin-spin Coupling

Proctor and Yu[5] were the first to make the observation that the chemically shifted peaks could themselves show fine structure. Gutowsky and McCall[6] showed that this fine structure may arise in any molecule containing two or more nuclei which resonate at different field strengths.

The NMR signal of a nucleus in a molecule can be influenced by the magnetic fields of other protons. This influence can either add to, or subtract from, the magnetic field required for resonance. For a particular nucleus A in a molecule AX_n the number of lines into which the A resonance is split is $2nI_x+1$, where I_x is the nuclear spin quantum number of X. If A and X each have a spin quantum of $\frac{1}{2}$ and the chemical shift difference is large compared to the coupling constant, the multiplet lines are equally spaced, and their relative intensities are given by the binomial coefficients.

The separation between the lines is known as the spin-spin coupling constant J_{AX}. This separation is independent of the applied field B_o. On the basis of their measurements, Hahn and Maxwell[7], and Gutowsky and McCall[6] proposed that these multiplets arose from an interaction between neighbouring nuclear spins which is proportional to the scalar product $I_{(1)} \cdot I_{(2)}$.

Ramsey and Purcell[8] first suggested that these interactions arise from an indirect coupling mechanism via the electrons in the molecule. For solids, the coupling is dependent on molecular orientation and is

determined by dipole-dipole interaction. In liquids
and gases, rapid molecular motion average out these
interactions and J is independent of molecular
orientation.

1.4 The spin Hamiltonian of the Multi-spin 1/2 System.

This section introduces the quantum mechanical
description of the spin Hamiltonian which will be used
in Chapter Three.

When an ensemble of identical spin nuclei is
subjected to a large stationary magnetic field B_o acting
in the -z direction, the spin Hamiltonian for each
magnetic nucleus may be written as

$$\mathcal{H} = (1-\sigma)\ \hbar\gamma B_o I_z \qquad\qquad ...(1.1)$$

where I_z is the spin angular momentum operator in the z
direction.

This Hamiltonian represents the quantum mechanical
equivalent of the potential energy $(-\bar{\mu}.\bar{B}_o)$ of a classical
bar magnet of magnetic moment $\bar{\mu}$ immersed in a magnetic
field $\bar{B}_o$.

In considering the spin Hamiltonian separately, the
spin state of the nucleus is assumed to be independent of
the electronic, rotational, and vibrational states of the
whole molecule but this is certainly not so. Thus the
necessity of including in equation (1.1), σ, the shielding
constant, which takes account of the effect of the
electrons about and near the nucleus. A tensor quantity,
$\bar{\sigma}$, should be used to take account of the shielding effect,
but for fluid samples the molecules undergo many
collisions during the lifetime of excited nuclear states,
so as the molecules tumble, the shielding effect can be

represented by the scalar $\sigma (=1/3 \; Tr \; \bar{\sigma})$.

The Hamiltonian of a molecule containing two or more magnetic nuclei assuming no spin-spin coupling is,

$$\sum_{i=1}^{n} \omega_{oi} \hbar I_{zi}$$

$$...(1.2)$$

where $\omega_{oi} = (1 - \sigma_i) \gamma B_o$

and the subscript i denotes the environment of the ith magnetic nucleus.

In taking account of spin-spin coupling the interaction between two magnetic nuclei m and n may be represented by the scalar product

$$V_{nm} = J'_{nm} \hbar^2 I_n \cdot I_m$$

I is the total spin operator and J' is the coupling constant measured in Joules. The coupling constant J which is measured in an NMR experiment is in Hertz and is related to J' by,

$$J = \frac{\hbar J'}{2\pi}$$

The scalar product of $I_n \cdot I_m$ gives

$$I_n \cdot I_m = I_{zn} I_{zm} + \tfrac{1}{2}(I_n^+ I_m^- + I_n^- I_m^+)$$

where

$$I_n^+ = I_{xn} + j I_{yn} \quad \text{and} \quad I_n^- = I_{xn} - j I_{yn}$$

For a molecule containing many magnetic nuclei the total spin-spin coupling energy is obtained by summing over all pairs of magnetic nuclei

$$V = \sum_n \sum_m \hbar^2 J'_{nm} I_n \cdot I_m \qquad ...(1.3)$$

The NMR spectrum is probed by applying a small radio-frequency magnetic field $2B_1 \cos \omega t$ along the x axis.

The total Hamiltonian is now

$$\mathcal{H} = -\sum_i (\gamma_i B_o (1-\sigma_i) I_{zi} - \hbar \gamma_i 2B_1 \cos\omega t \, I_{xi})$$
$$+ \sum_n \sum_m \hbar^2 J'_{nm} I_n \cdot I_m \qquad \ldots(1.4)$$

$2B_1 \cos\omega t$ may be resolved into a pair of circularly polarized fields rotating in opposite directions in the x-y plane giving

$$(2B_1 \cos\omega t)\bar{e}_x = B_1(\bar{e}_x\cos\omega t - \bar{e}_y\sin\omega t) + B_1(\bar{e}_x\cos\omega t +$$
$$\bar{e}_y\sin\omega t) \qquad \ldots(1.5)$$

where $\bar{e}_x$ and $\bar{e}_y$ are unit vectors in the x and y directions. Only one of these rotating magnetic field components has the same sense as the Larmor precession of the nuclear magnetic moment about B_o. The out of phase component can be neglected as it produces insignificant changes in the orientation of the magnetic moment of the spin $\frac{1}{2}$ nucleus. Only the "in phase" component need be considered in the contribution to the spin Hamiltonian as this is the component in the direction of B_x. If a rotating reference frame is used which has a set of axes rotating about the z axis the Hamiltonian becomes[9]

$$\mathcal{H} = -\omega\hbar\sum_i I_{zi} + \hbar\sum_i \omega_{oi} I_{zi} + \hbar\gamma B_1\sum_i I_{xi} + \hbar^2\sum_{n<m}\sum J'_{nm}I_n I_m$$
$$\ldots(1.6)$$

1.5 Relaxation

If there is a Boltzmann distribution of nuclei among the spin states, a net absorption of energy may be observed with low intensity irradiation at the resonance frequency. For an assembly of weakly coupled identical nuclei of spin $\frac{1}{2}$, the energy levels of an isolated nucleus may be applied to the assembly as a

whole. When there is thermal equilibrium throughout
the assembly the relative population of the two
energy levels is :

$$\frac{N_2}{N_1} = \exp\left(\frac{-\Delta E}{k_B T}\right)$$

N_2 and N_1 are the number of nuclei in the high and low
energy levels respectively.

The separation of the energy levels is given by
$\gamma \hbar B_o$, hence

$$\frac{N_2}{N_1} = \exp\left(\frac{-\gamma \hbar B_o}{k_B T}\right)$$

and since $\gamma \hbar B_o / k_B T$ is small

$$\frac{N_2}{N_1} \simeq 1 - \frac{\gamma \hbar B_o}{k_B T}$$

As can be seen by this equation it is important to
have the magnetic field used for resonance, B_o, as large
as possible. The effect of this is that the energy
levels become more widely spaced combined with an
increased sensitivity, because the excess population in
the lower state is increased. The observation of an
NMR signal depends upon the net absorption of energy by
this small population.

When an external field B_o is applied in the z
direction to a sample containing many identical spins,
M, the magnetization of the sample is given by the
equation

$$M = \sum_j \mu_j = \gamma \hbar \sum_j \langle \hat{I}_j \rangle \qquad \qquad \ldots(1.7)$$

where $\hbar \langle \hat{I} \rangle$ is the expectation value of the spin angular
momentum. The magnitude of M_o, the equilibrium value of
the magnetization, depends on the temperature and the
magnetic field, B_o. When the external magnetic field is

switched off, the magnetization decays from M_o to zero.
However upon removal of the B_1 field, B_o still on, M_z
decays to its equilibrium value with time constant, T_1,
which is called the spin-lattice relaxation time or the
longitudinal relaxation time. The transverse components
of magnetization, M_x and M_y, decay to zero with time
constant, T_2, which is known as the transverse
relaxation time or the spin-spin relaxation time. For
liquids T_1 and T_2 both arise from energy exchange between
the spin system and the lattice[10].

The full equations describing the change in the
components of the magnetization with time when a field
B_o is applied in the z direction and a small radiofrequency
field $2B_1\cos\omega t$ is applied along the x axis are called the
Bloch equations and in terms of an axis system rotating
with frequency ω_i can be written as[10] :

$$\frac{d\,M_z}{dt} = -\gamma B_1 v - (M_z - M_o)/T_1$$

$$\frac{du}{dt} = +(\omega_i - \omega)v + \frac{u}{T_2}$$

$$\frac{dv}{dt} = -(\omega_i - \omega)u + \gamma B_1 M_z - \frac{v}{T_2}$$

...(1.8)

where

$$u = M_x \cos\omega t - M_y \sin\omega t$$

$$v = M_x \sin\omega t - M_y \cos\omega t$$

$$\omega_i = \gamma B_o$$

In the usual continuous wave NMR experiment where
the out of phase component v is monitored by operating
the instrument in the absorption mode, the left-hand side
of equation (1.8) can be set equal to zero and the Bloch

equations can be solved to give the absorption line shape. These equations can be solved when spin-spin coupling effects are absent to yield the line shape of NMR resonances, provided exchange phenomena are not considered.

1.6 Saturation

As mentioned earlier the NMR spectrum of a molecule is probed using the oscillating field B_1, which is perpendicular to B_0. If the power in the oscillating field is too high, the intensity of the absorption spectrum decreases. This is a major hazard to be aware of when obtaining experimental spectra for line-shape analyses.

In a steady state experiment the time derivatives of the Bloch equations previously described, equal zero. The value obtained for v is[10] :

$$\frac{M_0 \gamma B_1 T_2^2 (\omega_0 - \omega)}{T_2^2 (\omega_0 - \omega)^2 + 1 + T_1 T_2 \gamma^2 B_1^2}$$

If B_1 increases to such a point that the term $T_1 T_2 \gamma^2 B_1^2$ is no longer much less than one, the intensity of the observed signal is decreased in a manner which is illustrated in the following spectra.
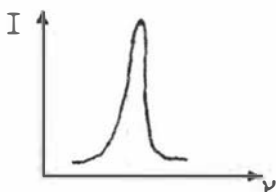
$$\gamma B_1 (T_1 T_2)^{\frac{1}{2}} \ll 1$$
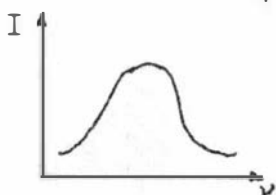
$$\gamma B_1 (T_1 T_2)^{\frac{1}{2}} = 1$$
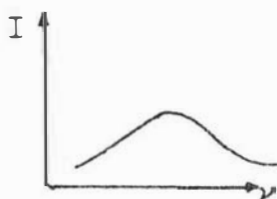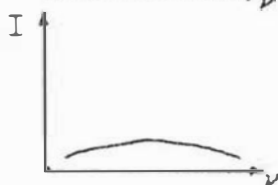
$$\gamma B_1 (T_1 T_2)^{\frac{1}{2}} = 2$$

$$\gamma B_1 (T_1 T_2)^{\frac{1}{2}} = 3$$

In all experiments carried out, great care was taken to ensure that the B_1 power output was kept to a minimum level to avoid such spectral distortions.

CHAPTER TWO

The application of NMR
to Kinetic Studies
involving Intramolecular Exchange

Barriers to internal rotation have been a subject of interest for almost 40 years and have been determined by a variety of techniques for a large number of molecules.[11]   Techniques such as electron diffraction, dipole moment measurements, infared, Raman, and microwave spectroscopy have been used.[12,13] NMR spectroscopy has made a significant contribution to this area, but all techniques are needed to understand the nature of the forces restricting intramolecular motions.

This chapter traces the development of magnetic resonance methods for the study of rate processes in chemistry.   The explicit rate process under consideration is intramolecular exchange.

Spectroscopy in all its forms measures physical properties that can be related to the concentrations of substances.   An application in the study of chemical kinetics is that of measuring the concentration of a reactant or product as a function of time.   However the use of the magnetic resonance technique provides information about reactions from measurements on systems that are chemically at equilibrium and in the case of intramolecular exchange, these measurements are made by following the spectral changes caused by different exchange rates.   Thus NMR spectroscopy has been used to study intramolecular exchange processes with activation energies of 20 to 100 kJ mol^{-1}.

2.1 <u>Relaxation Mechanisms</u>.[15]

The time scales in NMR are relatively slow for
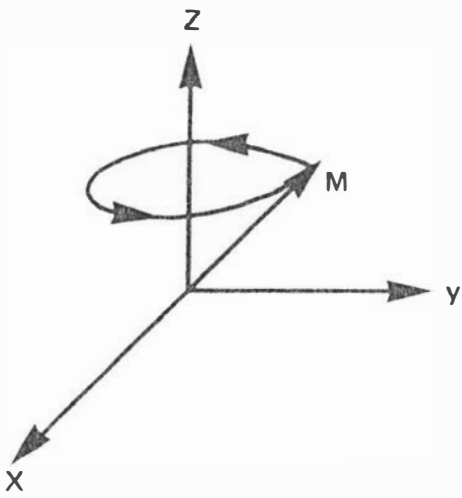
Figure 2.1

(a) In a laboratory frame M precesses about the Z axis at $\omega = \gamma B_o$
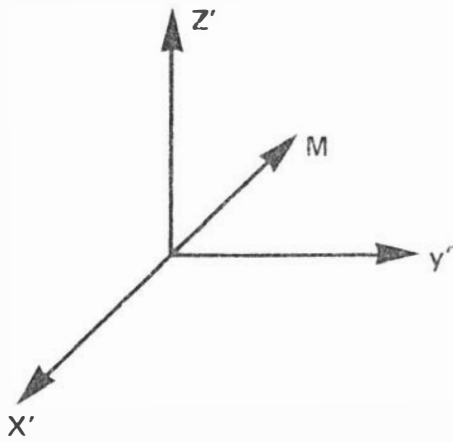
(b) In a frame rotating at a frequency ω_o. M is stationary.
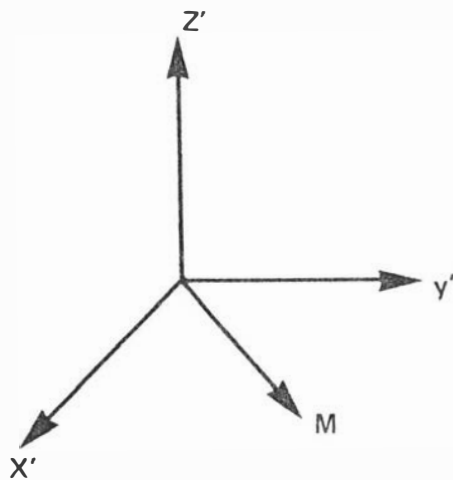
(c) When perturbed far from equilibrium, M is still stationary in the rotating frame.

microscopic processes. While molecules in a non-viscous liquid have frequency components from O to 10^{12}Hz, the classical precession frequency for protons is 60 MHz in an applied magnetic field of 1.4 Tesla.

The intensity of the rotational frequency components at the nuclear resonance frequency contribute directly to the relaxation mechanism. This can be illustrated by considering a macroscopic magnetization vector M slightly displaced from equilibrium precessing at a rate of $\omega_0 = \gamma B_0$ in reference to a laboratory frame (see Figure 2.1).

In a frame rotating at the precession frequency ω_0, M appears to be stationary. M relaxes because of the interaction with the microscopic magnetic moments of the nuclear spins. As the molecules move about in the liquid the motions of their nuclear magnetic moments generate fluctuating magnetic fields. These microscopic fields denoted by b are similar in behaviour to the B_1 field generated in an NMR instrument.

b is defined by b = $\underline{i}b_x$ + $\underline{j}b_y$ + $\underline{k}b_z$ A static b_z is static in both reference frames, but a b_x for a b_y rotates in a rotating frame. If M has been perturbed as in Figure 2.1(c), the processes which generate b fields that cause $M_{z'}$ to return to equilibrium are called T_1 processes. The processes that cause $M_{x'}$ and $M_{y'}$ to return to equilibrium are T_2 processes. For liquids, in the case of proton

magnetic resonance, $T_1 \geqslant T_2 \geqslant T_2^*$ where T_2^* is the relaxation process taking account of instrumental effects and viscosity broadening.

Generally for proton magnetic resonance in liquids $T_1 = T_2$ with the line-width being proportional to T_2^{-1}.

The torque acting on M is given by the vector cross product of b and M.

$$(b \times M) = i(b_y, M_z, - b_z, M_y,) + j(b_z, M_x, - b_x, M_z,) +$$
$$k(b_x, M_y, - b_y, M_x,)$$
$$...(2.1)$$

Whilst T_2 processes arise from components in all three directions, T_1 relaxation processes arise only from fluctuating magnetic fields in the x' and y' directions.

A static component of b in the z' direction (rotating frame) is equivalent to a static component of b_1 in the z direction (laboratory frame). Thus, in a laboratory frame there is a zero frequency contribution to T_2 processes. Conversely, a static component of b in the x' or y' direction corresponds to a high frequency component of b_1 in the x or y directions. Only high frequency processes can affect T_1 and also T_2. However it is the low frequency interaction that causes T_2 to be often appreciably shorter than T_1 when chemical exchange or other low frequency processes are present.

From the preceding discussion it can be seen that chemical or intramolecular exchange in the appropriate frequency range will produce observable changes in NMR

spectra. Methods and techniques have been
developed over the past twenty years for the
determination of useful kinetic parameters from
the observed line-widths and line shapes. The
rate processes that have been studied have
frequencies which fall in the range of 10^{-1} to 10^5
s^{-1} for diamagnetic substances.[16]

2.2   Thermodynamic Parameters of Intramolecular
         Exchange.

The thermodynamic parameters used in this thesis
are from the theory of absolute reaction rates.[17]
This theory and its relevant equations can be applied
to all NMR studies involving exchange if they are
treated as typical rate processes.[18]

The Arrhenius equation written as $k = Ae^{-E/RT}$ is
generally accepted as representing the temperature
dependence of the specific rates of most chemical
reactions and certain physical processes. Provided
that the temperature range is not large, the quantities
A and E are taken as constant. A is regarded as the
frequency factor for the reaction or rate process,
while E is termed the energy of activation.

Transition state theory is based on the premise
that a rate process is characterised by an initial
configuration which passes by continuous change of the
co-ordinates into the final configuration. This is
critical for the process, in the sense that if this
system is attained there is a high probability that
the reaction will continue to completion. The
expression "activated complex" is given to this

critical configuration.

The specific rotational rate (k) is defined by

$$k = \frac{k_B T}{h} \quad K^{\ddagger} \qquad \qquad ...(2.2)$$

The effective rate of crossing the energy barrier by the activated complexes is equal to $\frac{k_B T}{h}$, which is a universal frequency, dependent only on temperature and independent of the nature of the reactants and the type of reaction. There is a possibility that some systems will revert to the initial state after passing to the activated state. To take account of this, a factor called the transmission coefficient is used. In studies of this type a unit transmission coefficient is assumed. This is justified, as exchange effects are only seen when the system has rotated to its "product" state.

$K^{\ddagger}$ is analogous to other equilibria constants, and hence can be related to a standard free energy change $G^{\ddagger}$, and the corresponding enthalpy and entropy changes, $H^{\ddagger}$ and $S^{\ddagger}$, associated with the reactant activated complex equilibria being considered.

The constant $K^{\ddagger}$, for the equilibrium between the activated complex and the reactants, may be expressed thus

$$K^{\ddagger} = \exp \frac{-\Delta G^{\ddagger}}{RT} \qquad \qquad ...(2.3)$$

Substituting this into equation (2.2) an expression for the rotational rate is obtained.

$$k = \frac{k_B T}{h} \quad \exp \left(\frac{-\Delta G^{\ddagger}}{RT} \right) \qquad \qquad ...(2.4)$$

and as $\Delta G^{\ddagger} = \Delta H^{\ddagger} - T\Delta S^{\ddagger}$ $\qquad \qquad ...(2.5)$

then $k = \dfrac{k_B T}{h} \quad \exp\left(\dfrac{-\Delta H^{\ddagger}}{RT}\right) \quad \exp\left(\dfrac{\Delta S^{\ddagger}}{R}\right)$ $\qquad \ldots(2.6)$

Using the above equations it is possible to relate the measured rate of reaction to the free energy of activation $(\Delta G^{\ddagger})$.

2.2.1 Determination of E_a and A

The empirical relation of Arrhenius can be written in logarithmic form as

$\ln k = \dfrac{-E_a}{RT} + \ln A$ $\qquad \ldots(2.7)$

Provided k has been measured as a function of temperature, the empirical constants E_a and A can be deduced from the slope and intercept of a plot of k versus $\dfrac{1}{T}$.

2.2.2 Determination of $\Delta H^{\ddagger}$ and $\Delta S^{\ddagger}$.

Equation (2.7) on differentiation becomes

$\dfrac{d\ln k}{dT} = \dfrac{E_a}{RT^2}$ $\qquad \ldots(2.8)$

From equation (2.2) we obtain

$\ln k = \ln\left(\dfrac{k}{h}\right) + \ln T + \ln K^{\ddagger}$ $\qquad \ldots(2.9)$

which on differentiation becomes

$\dfrac{d\ln k}{dT} = \dfrac{1}{T} + \dfrac{d\ln K^{\ddagger}}{dT}$ $\qquad \ldots(2.10)$

As $\dfrac{d\ln K^{\ddagger}}{dT} = \dfrac{\Delta H^{\ddagger}}{RT^2}$ $\qquad \ldots(2.11)$

then substitution of (2.11) into (2.10) gives

$\dfrac{d\ln k}{dT} = \dfrac{1}{T} + \dfrac{\Delta H^{\ddagger}}{RT^2}$ $\qquad \ldots(2.12)$

Equating equations (2.8) and (2.12)

$E_a = RT + \Delta H^{\ddagger}$ $\qquad \ldots(2.13)$

By using equation (2.13) $\Delta H^{\ddagger}$ at 298K can be found.

$\Delta G^{\ddagger}_{293}$ can be found by rearranging equation (2.4) to give

$$\Delta G^{\ddagger} = RT\ln\left(\frac{k_B T}{h}\right) - RT\ln k \qquad \qquad ...(2.14)$$

$\Delta S^{\ddagger}_{293}$ can be found by re-arranging equation (2.5) to give

$$\Delta S^{\ddagger} = \frac{\Delta G^{\ddagger} - \Delta H^{\ddagger}}{T} \qquad \qquad ...(2.15)$$

2.3 Intramolecular Exchange

This section on intramolecular exchange is a brief overview of the early theoretical models that were developed to explain exchange phenomena.

2.3.1 Chemical Exchange

NMR is an important tool in the study of rates of reaction under equilibrium conditions. The total numbers of nuclei in each environment remain constant, but each individual nucleus changes between different environments.

The effect of this exchange process on the NMR spectrum depends on the rate at which it occurs. If, on the NMR time scale, the nucleus is exchanging very slowly between two sites, the slow exchange limit, the spectrum is a superposition of the spectra of the various species. If, however, the rate of exchange is very fast, the spectrum depends only on the mean magnetic environment of the nuclei, fast exchange limit. A rate that lies between these two extremes gives a broad-line spectrum, intermediate exchange. As will be discussed in subsequent sections, the rate of exchange can be determined from the NMR spectra obtained in this intermediate region.

2.3.2 Underlined Two-site case

The development of a theory of spectra observed from intermediate exchange rates was first accomplished by Gutowsky, McCall and Slichter[19] in 1953. Further extensions were made by Gutowsky and Saika[20] in 1953 and Gutowsky and Holm[18] in 1956.

Gutowsky and Holm[18] showed that for intermediate rates of exchange the absorption mode line-shape is given by the equation

$$v = \frac{\nu_0 M_0 \left[(1 + \frac{\tau}{T_2})P + QR \right]}{P^2 + Q^2} \qquad \ldots(2.16)$$

where

$$P = \tau \left\{ T_2^{-2} - \left[\tfrac{1}{2}(\omega_A + \omega_B) - \right]^2 + \tfrac{1}{4}(\omega_A - \omega_B)^2 \right\} + T_2^{-1}$$

$$Q = \tau \left[\tfrac{1}{2}(\omega_A + \omega_B) - \omega - \tfrac{1}{2}(P_A - P_B)(\omega_A - \omega_B) \right]$$

$$R = \tau \left[\tfrac{1}{2}(\omega_A + \omega_B) - \omega \right](1 + 2\tau T_2^{-1}) + \tfrac{1}{2}(P_A - P_B)(\omega_A - \omega_B)$$

$$\tau = \frac{\tau_A \tau_B}{\tau_A + \tau_B}$$

ω_A = angular resonance frequency of A

ω_B = angular resonance frequency of B

τ_A = lifetime of proton at site A in terms of angular frequency

τ_B = lifetime of proton at site B in terms of angular frequency

The case Gutowsky and Holm considered, was a liquid in which there is negligible dipolar broadening of proton resonance because of motional narrowing, but in which there are sites with different local fields giving a resonance with two components A and B shifted by $+\delta\omega/2$ and $-\delta\omega/2$ from their average angular

frequency.   The relative intensities of these components are directly proportional to the proton fractions p_A and p_B contributing to each component.

Experimentally one measures the separation between two absorption lines, and from it, calculates τ .   The positions of the two components and their dependence on τ are given by the maxima of the Gutowsky-Holm equation.

When $p_A = p_B$, $\tau_A = \tau_B = 2\tau$, and by differentiating v (equation 2.16) with respect to $\frac{1}{2}(\omega_A + \omega_B) - \omega$ the following equation is obtained.

$$\tau^4 T_2^{-1} \left[\tfrac{1}{2}(\omega_A + \omega_B) - \omega\right]^5 + 2\tau^2 S(1 + \tau T_2^{-1}) +$$
$$\left[\tfrac{1}{2}(\omega_A + \omega_B) - \omega\right]^3 + \left\{(1 + \tau T_2^{-1})(1 + 2\tau T_2^{-1})^2 - \right.$$
$$\left. \tau S(2 + 3\tau T_2^{-1})\right\} S \left[\tfrac{1}{2}(\omega_A + \omega_B) - \omega\right] = 0 \qquad \ldots (2.17)$$

where $S = \dfrac{1}{T_2} + \dfrac{\tau}{T_2^2} + \tau\left(\dfrac{\delta\omega}{2}\right)^2$

One solution of the above equation is when
$\tfrac{1}{2}(\omega_A + \omega_B) - \omega = 0$
i.e. the radio-frequency has a value mid-way between the absorption lines at A and B.   This solution corresponds to a minimum (two separate lines) when τ is large, and a maximum (a single line), where τ is small.

If the line-widths at half-height, given by $\dfrac{1}{T_2}$, are small compared to the separation $\delta\omega$, the experimentally observed separation is given by
$$\delta\omega_e = (\omega_A + \omega_B) - 2\omega = \left[1 - \tfrac{1}{2}\tau^{-2}(\omega_A - \omega_B)^2\right]^{\tfrac{1}{2}} \tfrac{1}{2}(\omega_A - \omega_B)$$

The general non-zero solution of the derived Gutowsky and Holm equation which includes the effects of overlap is

$$\Delta\omega_e = \pm \left(-S\left(\frac{1}{\tau} + \frac{T_2}{\tau^2}\right) \pm S^{\frac{1}{2}}\left(\frac{\delta\omega}{2} \quad \frac{T_2^2}{\tau^3} + \frac{4T_2}{\tau^2} + \frac{4}{\tau}\right)^{\frac{1}{2}}\right)^{\frac{1}{2}} \quad \ldots(2.18)$$

The dependence of $\delta\omega_e$ on τ and T_2 has been computed.[21]

Gutowsky and Holm's analysis assumed that the exchange rate did not influence T_2. However, they did report that the line-widths in the absence of exchange effects were most likely due to magnetic field inhomogeneties, and concluded that temperature dependence of the effective T_2 was slight. With their small value of $\delta\omega$, errors in their final result were fairly large (E_a for dimethylformamide was 7 ± 3 kcal mol^{-1}).[13] Over a temperature range 236 K to 269 K, the experimentally observed separation $\delta\omega_e$ only ranged from 20.1 to 11.9 rad s^{-1}. Results reported for the uncoupled 2-site case using equation (2.17) are exact only for equal populations and for equal transverse relaxation rates.[22]

2.3.3 Chemical Exchange Considering Coupling

This section considers absorption lines which consist of spin multiplets. At slow exchange conditions the components of spin multiplets are clearly observable. As the rate of exchange is increased these are broadened, until finally the multiplet is a single line. Exchange processes which replace the interacting nucleus with others of random orientation lead to mixing of the spin

states and to collapse of the multiplets.   To obtain
the useful equations the chemical shift must be
larger than the spin-spin interaction.

Takida and Stejskal[23] have systematised the
effect of chemical exchange on a doublet originating
from spin coupling.   They used as a starting point
the total complex moment, G evaluated by Gutowsky,
McCall and Slichter.[19]

$$G = \frac{-\omega_1 M_o \tau\left[2 + (T_2^{-1} - i\Delta\omega)\tau\right]}{\left\{1 + \tau\left[T_2^{-1} - i(\Delta\omega + \tfrac{1}{2}J)\right]\right\} \left\{1 + \tau\left[T_2^{-1} - i(\Delta\omega - \tfrac{1}{2}J)\right]\right\}}$$
$$\dots(2.19)$$

to give for v

$$v = \omega_1 M_o J^{-1} \frac{Q\left\{z^2 + (2t^{-1} + Q^{-1})\left[(2t^{-1} + Q^{-1}) + Q\right]\right\}}{Q^2 z^4 + Q^2 z^2\left[(\tfrac{2}{t} + Q^{-1})^2 + Q^{-2} - \tfrac{1}{2}\right] + \left[(\tfrac{2}{t} + Q^{-1}) + \tfrac{1}{4}Q\right]^2}$$
$$\dots(2.20)$$

$$Q = T_2 J$$

$$t = \tau J$$

$$z = \Delta\omega/J$$

By differentiating the above equation with respect
to z and putting the differential equal to zero the
result is

$$\frac{\delta_{obs}}{J} = \left\{\left[4Q(2t^{-1} + Q^{-1})^3 + (Q^2 + 8)(2t^{-1} + Q^{-1})^2 + (Q^2 + 2) + (2t^{-1} + Q^{-1}) + 1\right]^{\frac{1}{2}} - 4(2t^{-1} + Q^{-1})^2 - (2t^{-1} + Q^{-1})Q\right\}^{\frac{1}{2}}$$
$$\dots(2.21)$$

where δ_{obs} is the separation between the maxima of the
absorption lines.

The above expressions were cumbersome to apply,
hence Takeda and Stejskal used graphical methods
similar to those of previous investigators.

Tables of exchange broadened doublets, triplets, and quartets have been compiled.[24]

2.4   The use of Approximate Equations

In earlier work published by workers who did not have access to high speed computers, semi-classical theory for exchange between two uncoupled sites was applied to situations where the theory did not apply. Although the simple semi-classical model can be valid for more complicated systems, it is necessary to compare results obtained using such a model with the results obtained from the truly applicable equations. In general, the further one goes from the region of validity the further the systematic error will be increased.

Complicated coupling patterns can also be simplified by selective deuteration.   Difficulties in chemical syntheses then replace difficulties in mathematical analyses.   However, even for exchange between two uncoupled sites the line-shape equation is sufficiently complicated to require the use of a computer to complete the necessary calculations in reasonable time.

It is useful to have approximate equations which relate some readily measured characteristic of the spectrum to the exchange rate.   The accuracy of the approximations made to derive the approximate equations depends upon the relative value of the exchange rate, as compared to the chemical shifts $\delta\nu$, the coupling constants J, and the natural line-

widths $1/\pi T_2^0$ in the absence of exchange.
Neglecting this dependence can lead to appreciable
systematic errors.

The most widely used approximations are those
which relate a single characteristic to the
exchange rate between two equally populated
uncoupled sites, A and B.

These equations result if

$$\frac{1}{\tau} \quad \text{and} \quad \delta\nu \gg \frac{1}{T_2''} \qquad \qquad ...(2.22)$$

$$\frac{1}{T_2''} = \frac{1}{T_2^0} + \frac{1}{T_2'} \qquad \qquad ...(2.23)$$

$\frac{1}{T_2'}$ represents the inhomogeneity, instability
and other instrumental contributions to the effective
line-width in the absence of exchange. $\delta\nu$, the
chemical shift, can only be controlled by solvent
effects and the magnetic field. For very small
chemical shifts, the approximate equations are not
valid.

For exchange rates less than those determined
at the coalescence point for the AB system, the
experimentally observed peak separation $\delta\nu_e$, and the
maximum to central minimum intensity ratio r, have
been used in the following equations.[25]

$$\frac{1}{2\tau} = \frac{\pi}{\sqrt{2}} \left(\delta\nu^2 - \delta\nu_e^2 \right)^{\frac{1}{2}} \qquad \qquad ...(2.24)$$

$$\frac{1}{2\tau} = \frac{\pi \delta\nu}{\sqrt{2}} \left[r + (r^2 - r)^{\frac{1}{2}} \right]^{-\frac{1}{2}} \qquad \qquad ...(2.25)$$

Allerhand et al[26] have checked the above
equations and have shown that they give, in all cases,
an apparent rate which is larger than the true rate.

For exchange rates just above coalescence, where only a single line is observed for the AB case, the spectral parameter utilized is the observed line-width, where the line-width is the resultant of the line-widths caused by exchange and the natural line-width (no exchange).

$$\frac{1}{\pi T_2^*} = \left(\frac{1}{\pi T_2}\right) \text{exchange} + \left(\frac{1}{\pi T_2''}\right) \text{no exchange}$$

$$...(2.26)$$

For two uncoupled sites with fractional populations P_A and P_B the following equation has been derived for very fast exchange.[27] This is the region where if the temperature is lowered, the sharp single line obtained in the fast exchange limit begins to broaden.

$$\frac{1}{2\tau} = 2\pi P_A P_B (\delta\nu)^2 \left\{\frac{1}{\pi T_2^*} - \frac{1}{\pi T_2''}\right\}^{-1} ...(2.27)$$

The fast exchange condition is

$$\tau^{-1} \gg 2\pi\delta\nu$$

This equation for $\frac{1}{2\tau}$ has been used close to coalescence when the fast-exchange condition is not valid.

At coalescence[18], the exchange rate is

$$\frac{1}{2\tau} = \frac{\pi\delta\nu}{\sqrt{2}}$$

$$...(2.28)$$

Rates obtained by using equation (2.28) have been shown to be too low[26], the error decreasing with increasing rate and thus making $\Delta H^{\ddagger}$ too large.

Using the equation at coalescence a single value of the rate has been obtained, namely that at T_c. Many papers use $\Delta G_c^{\ddagger}$ values for comparative studies.
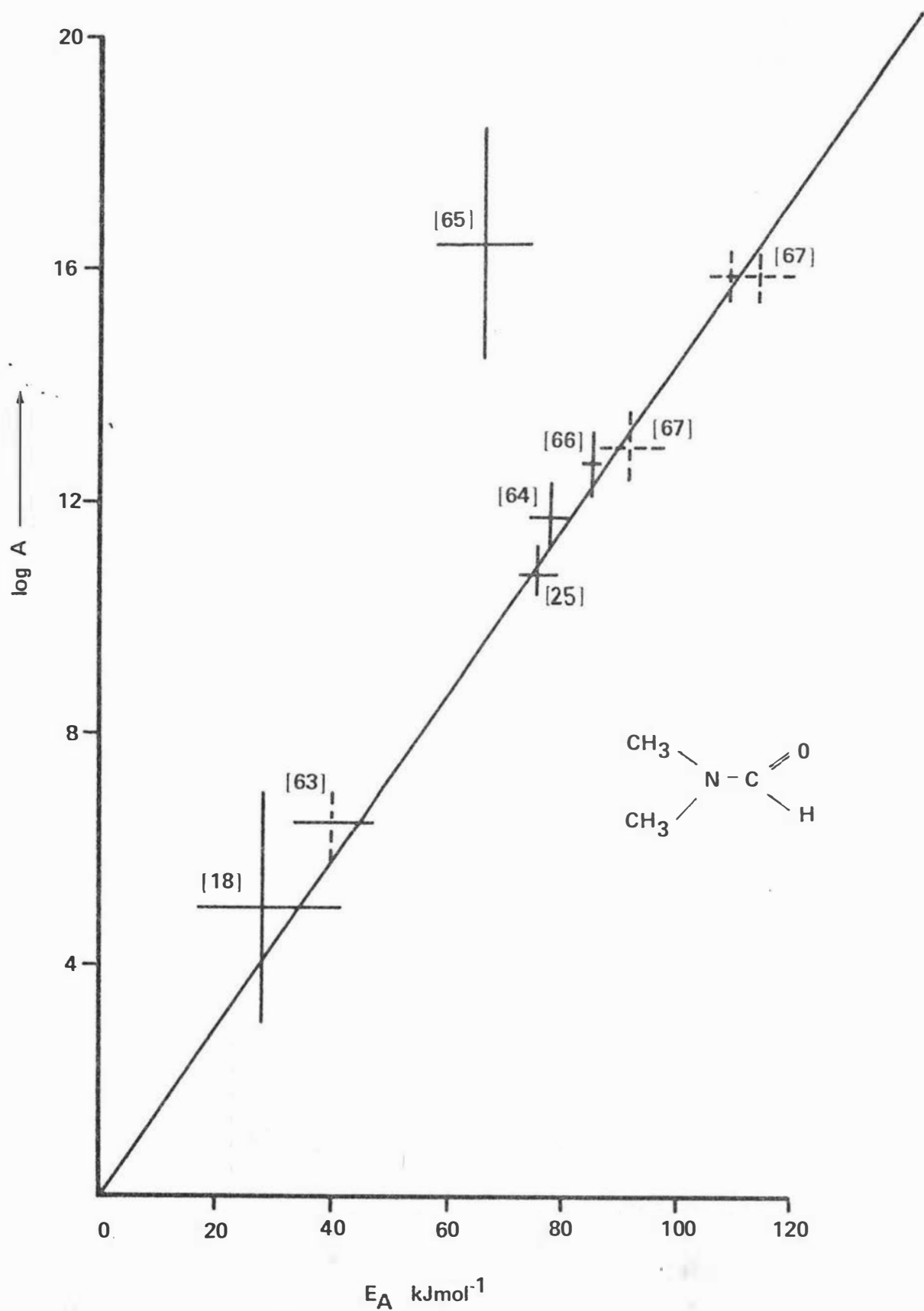
Figure 2.2 Experimental data for the rotation about the C-N bond in neat DMF. The numbers [ ] are literature references.

The error in T_c (usually about ± 2 to 5^oC) largely determines the error in the $\Delta G^{\ddagger}_c$ values ($\pm$ 0.5 to 4%).[14]

2.5   "Approximate" Exchange Studies

The following two sets of results illustrate the unreliability of some of the data that have so far been obtained using approximate equations.

2.5.1   Internal Rotation in N,N -dimethyl formamide

One of the most intensively studied exchange processes is the hindered internal rotation of N,N-dimethylformamide.   The literature however contains E_a values ranging from 29.26 to 117 kJ mol^{-1} and log A values from 7 to 17 and the true values are still uncertain.[14] The reason for this is to be found in the k_r (rotational rate) values, errors in which increase with increasing distance from the coalescence temperature.   A limiting factor is the relatively small temperature range available for the evaluation.   The gradient of the Arrhenius line, which is a measure of the activation energy E_a, hence also its intercept on the ordinate (log A), are very much influenced by small uncertainties in the k_r values;   high E_a values go with high log A values and _vice versa_.

Thus, for dimethylformamide, a plot of the E_a values from the literature against the corresponding log A values, has all but one of the points on a straight line which passes through the origin (see Figure 2.2).

2.5.2 <u>Ring Inversion of Cyclohexane</u>.

Cyclohexane holds a central position in the theory of conformational analysis.[28] All the experimental data which has been obtained about the chair-chair interconversion came from nuclear magnetic resonance studies on cyclohexane or cyclohexane-d_{11}. Table 2.1 shows general agreement about the order of magnitude of the Gibbs free energy of activation, but the situation for $\Delta H^{\ddagger}$, $\Delta S^{\ddagger}$ is quite different.

<div align="center">

Table 2.1

<u>Thermodynamic parameters of cyclohexane obtained</u>
<u>by different techniques</u>

</div>

Compound	Temp.Range °C	$\Delta G^{\ddagger}$ (-67°C)	$\Delta H^{\ddagger}$	$\Delta S^{\ddagger}$
C_6H_{12} [a]	...	42.2	43.1 $\pm$ 8.4	0.020
C_6H_{12} [b]	-70 to -20	43.1	37.6 $\pm$ .8	-0.027 $\pm$ .004
C_6H_{12} [c]	-	44.7	43.1	0.020
C_6HD_{11} [d]	-94 to -32	43.1	45.6 $\pm$ 2.5	0.012 $\pm$ .009
C_6HD_{11} [e]	-75 to -47	42.6	43.9 $\pm$ 2.1	0.006 $\pm$ .004
C_6H_{12} [f]	-60 to -25	43.1	38.0 $\pm$ 2.1	-0.024 $\pm$ .010
C_6HD_{11} [g]	-98 to +25	43.1	38.0 $\pm$ 0.4	-0.024 $\pm$ .002
C_6HD_{11} [h]	-117 to -27	42.7	45.1 $\pm$ 3.3	0.012

The units of $\Delta G^{\ddagger}$, $\Delta H^{\ddagger}$, $\Delta S^{\ddagger}$ kJ mol^{-1}

(a) [29] The method used was the line separation equation (Gutowsky and Holm) in the temperature range immediately below the coalescence temperature. The temperature interval was only 6°. The authors

commented that it was improbable that sufficiently
accurate temperature and rate measurements could
be made over such a small temperature interval,
using currently available methods, to give a
reliable enthalpy of activation.

(b) [30] The line-width method of Piette and Anderson
was used with the fast exchange approximation
equation

$$\log (\pi \Delta T_2^{-1}) = \log (2V_o/T_2) + E_a/2.303RT$$

The line-width was measured directly whenever
practicable; at higher temperatures, when the width
was very small, the exponential decay of the line at
fast passage was measured instead.

(c) [31] S. Meiboom - Private Communication

(d) [32] Gutowsky-Holm line-separation method
Fast-exchange line-width method

(e) [33] The authors reported that previous studies
by NMR of the rate of conformational isomerisation
of cyclohexane had yielded fairly concordant
results for $\Delta G^{\ddagger}$, but the results for $\Delta S^{\ddagger}$ had been
less than satisfactory, reflecting the fact that it
was not easy to measure this rate accurately over a
wide temperature range. At temperatures well above
"coalescence", the resonance line is narrow, and
accurate measurement of its width is difficult.
Near coalescence, there is spurious broadening
caused by coupling of axial and equatorial protons.
Below the coalescence temperature, the spectrum
becomes very complex, representing the envelope of

many thousands of lines of a 12-spin system, and is
not really well represented as an AB quartet, still
less as a doublet.

Rate constants were calculated by comparison
of observed line-widths and (below coalescence)
peak-to-valley ratios, to those of plots of the
line-shape function of Gutowsky and Holm.

(f) and (g) [34] spin-echo measurements

In comparing the ranges accessible to the spin-
echo and high resolution methods, their measurements
were carried out at a relatively low frequency of
26.85 MHz.   The range of rates obtained covered 5
orders of magnitude.   The authors commented that
instrumental improvements leading to more accurate
values of T_2 would extend the range of accessible
rates.

(h) [28] In a review of cyclohexane-d_{11} Anet and
Bourn regarded this system as particularly favourable
for the study of rates by both spin-echo and high
resolution methods because of the simplicity of the
spectra obtained.   Their explicit aim was to obtain
more accurate data over a wider temperature range
than had been possible with previous instrumentation
and techniques.   Approximate equations[35] were used,
supported by a computer program describing the line-
shape.

For the fast exchange region

$$k = \frac{\pi \nu_{AB}^2}{2 \delta\nu}$$

For the slow exchange region

$$k = \pi \delta\nu$$

where ν_{AB} is the chemical shift for a proton exchanging between axial and equatorial sites. $\delta\nu$ is the line-width at half-height when all broadenings other than that resulting from ring inversion are zero.

When Anet and Bourn compared their results with those of Allerhand, Chen and Gutowsky[g] they hinted at the possibility of systematic errors in Allerhand, Chen, and Gutowsky's data.

As shown in the previous specific examples a growing awareness of the possible seriousness of the systematic errors which can occur developed. These sources of systematic errors arose from different mathematical approaches as previously discussed, and limitations in experimental conditions.

2.6 Experimental Problems in Exchange

Besides the problems that have arisen in selecting the correct theoretical model for a particular system, the rate data can also be subject to experimental problems.

Experimental problems arise in general from instrumental instabilities, calibration errors and from spectral distortion due to causes other than instabilities. These problems, and their relative importance, vary greatly, depending upon which particular NMR technique is used, such as steady state, fast passage, double resonance, and spin echo.

In steady state work, temperature drifts, frequency changes, magnetic field drifts and variations in sample spinning rate are all examples of instrumental instabilities. A 1 K temperature difference is possible between spinning and non-spinning samples. The most important temperature effect is the loss of resolution produced by changing the temperature of the sample. Factors that contribute are changes in the sample position produced by thermal expansion and changes in the bulk magnetic susceptibility. A loss in resolution has a lesser effect upon peak separation than line-shapes. In the intensity-ratio method of Rogers and Woodbrey[25,12] it causes the ratio of peak maximum to central minimum to be too small. The area under a peak is independent of the inhomogeneity broadening, so, as the line-width increases, the peak height decreases, the minimum increases, and the apparent exchange rate is too high. Therefore the resolution must be "peaked-up" at each temperature, with the resolution the same at each temperature. This requires care, because, accompanying reversible resolution changes produced by changes in the sample temperature, there is a gradual deterioration in resolution, caused by fluctuations in room temperature, magnet cooling water and line voltage over the period of a day.

Another source of experimental error is in the measurement of sample temperature. A thermocouple can be inserted into the probe so that

it measures the temperature at the coil or placed
somewhere in the flow of gas used to control the
temperature.   The problem associated with
thermocouple measurement is that the thermocouple
must be calibrated, and this has the disadvantage
that constancy of calibration is poor.   Usually,
a secondary standard with a highly temperature-
dependent shift, is employed such as methanol for
lower temperatures and ethylene glycol for higher
temperatures.

Spectral distortions arise from inhomogeneties
in B_o, improper adjustment of sweep rate,
instrumental response times, and saturation effects
from a too intense radio-frequency field.

To avoid spectral distortions associated with
recording conditions, the filter band width and
sweep rate have to be adjusted accordingly.
Theoretical line-shapes, and the single parameter
equations are calculated for steady state conditions
and no saturation.   Neither of these two conditions
is met in an actual experiment.   Non-steady state
passage tends to reduce the saturation effects at
the expense of line-shape distortion by relaxation
transients.

CHAPTER THREE

The Density Matrix Method

Applied to a Four-Spin System

Dahlquist and Forsen[58] have demonstrated the applic-
ability of density matrix theory to intramolecular
exchange in four-spin systems. This chapter describes
the density matrix theory and examines briefly the
setting up of the computer program that was derived from
this theory. The program was used to enable a study
of the p-substituted nitrosobenzenes.

3.1 <u>Line Shape Calculations by the Density Matrix Method</u>[36,37,38]

The allowed energies and wave functions for molecules
and atoms are found by solving the Schroedinger equation
which may be written as:

$$\mathscr{H}\psi = E\psi \tag{3.1}$$

Different quantum mechanical systems in different
states can be described by any one of a number of different
state functions, each one belonging to a different rep-
resentation of the system. The Dirac formulism of quantum
mechanics renders the form of the analysis of any part-
icular problem independent of the particular representation
chosen.

In quantum mechanics the wave function represented
by ψ defines the properties of a system.

The equation which gives the energy states associated
with the wavefunction is defined as

$$E = \int \psi^* \mathscr{H} \psi d\tau = \langle \psi^* | \hat{\mathscr{H}} | \psi \rangle \tag{3.2}$$

Observable properties are represented by the equation

$$Q = \langle \psi | Q | \psi \rangle \tag{3.3}$$

The aim of quantum mechanics is to find a suitable wave
function $\psi(x_1, x_2, \ldots x_n)$. $(x_1, x_2, \ldots$ are position
coordinates).

3.2 Density Matrix

In the density matrix method a basis set of orthogonal and normalized wave functions is assumed[39] $(\emptyset_1, \emptyset_2, \ldots \emptyset_n)$.

The wave function is defined as

$$\psi = c_1\emptyset_1 + c_2\emptyset_2 + c_3\emptyset_3 + \cdots c_n\emptyset_n \tag{3.4}$$

where c_1, c_2, $\ldots c_n$ are constants which determine the amount of contribution of each of the functions in the basis set.

Starting from a given set, the problem in the density matrix treatment is finding the values of the constants.

The density matrix is defined as[40]

$$M = \begin{bmatrix} \rho_{11} & \rho_{12} & \rho_{13} & \cdots & \rho_{1n} \\ \rho_{21} & \rho_{22} & \rho_{23} & \cdots & \rho_{2n} \\ \rho_{31} & \rho_{32} & \rho_{33} & \cdots & \rho_{3n} \\ \cdot & \cdot & \cdot & \cdots & \cdot \\ \cdot & \cdot & \cdot & \cdots & \cdot \\ \cdot & \cdot & \cdot & \cdots & \cdot \\ \rho_{n1} & \rho_{n2} & \rho_{n3} & \cdots & \rho_{nn} \end{bmatrix}$$

where $\rho_{ij} = c_i c^*_j = c^*_j c_i = \rho_{ji}$

3.3 Single Spin System

This definition can be illustrated by considering a single spin $\frac{1}{2}$ nucleus.

The basis states chosen are

$$\emptyset_1 = \alpha \quad I_z = +\tfrac{1}{2}$$
$$\emptyset_2 = \beta \quad I_z = -\tfrac{1}{2}$$

There $\psi = c_1\alpha + c_2\beta$

As α and β are the solution functions of the Hamiltonian there are only two solutions to be considered.

(1) $\psi_1 = \alpha$ $(c_1 = 1, c_2 = 0)$

The density matrix for this is written as

$$M_1 = \begin{bmatrix} c_1 c_1^* & c_1 c_2^* \\ c_2 c_1^* & c_2 c_2^* \end{bmatrix} = \begin{bmatrix} 1 & 0 \\ 0 & 0 \end{bmatrix}$$

(2) $\psi_2 = \beta$ $(c_1' = 0, c_2' = 1)$

$$M_2 = \begin{bmatrix} 0 & 0 \\ 0 & 1 \end{bmatrix}$$

If a different set of basis functions were chosen which are not eigenfunctions of the Hamiltonian, then different density matrices would result.

If $\emptyset_1 = \varphi$ $(I_y = \tfrac{1}{2})$

$\emptyset_2 = \varphi$ $(I_y = -\tfrac{1}{2})$ are chosen as the basis set

then $\psi_1 = c_1 \emptyset_1 + c_2 \emptyset_2$

$\psi_2 = c_1' \emptyset_1 + c_2' \emptyset_2$

but since $\int \psi_1^* \psi_1 d\tau = 1$

and $c_1 = c_2$

then $\int c_1 (\emptyset_1^* + \emptyset_2^*) c_1 (\emptyset_1 + \emptyset_2) d\tau = 1$

$c_1^2 [\int \emptyset_1^* \emptyset_1 d\tau + \int \emptyset_1^* \emptyset_2 d\tau + \int \emptyset_2^* \emptyset_1 d\tau + \int \emptyset_2^* \emptyset_2 d\tau] = 1$

$c_1^2 (1 + 0 + 0 + 1) = 1$

$\therefore c_1 = \sqrt{\dfrac{1}{2}}$

The density matrix for ψ_1 is then

$$\begin{bmatrix} \dfrac{1}{\sqrt{2}} & \dfrac{1}{\sqrt{2}} & \dfrac{1}{\sqrt{2}} & \dfrac{1}{\sqrt{2}} \\ \dfrac{1}{\sqrt{2}} & \dfrac{1}{\sqrt{2}} & \dfrac{1}{\sqrt{2}} & \dfrac{1}{\sqrt{2}} \end{bmatrix} = \begin{bmatrix} \tfrac{1}{2} & \tfrac{1}{2} \\ \tfrac{1}{2} & \tfrac{1}{2} \end{bmatrix} = M_1$$

3.4 Usefulness of the Density Matrix Definition

If $\bar{Q}$ is equivalent to the mean value for the operator of a system with wave function ψ

$$\bar{Q} = \int \psi^* \hat{Q} \psi d\tau \tag{3.5}$$

$\bar{Q}$ corresponds to an observable property of the system.

If ψ is expanded in terms of a basis set $(\emptyset_1, \emptyset_2, \ldots \emptyset_n)$, and using equation (3.4), then

$$\bar{Q} = \int (c_1^* \emptyset_1^* + c_2^* \emptyset_2^* + \ldots c_n^* \emptyset_n^*) \hat{Q} (c_1 \emptyset_1 + c_2 \emptyset_2 + \ldots c_n \emptyset_n) d\tau$$

$$= \int c_1^* \emptyset_1^* \hat{Q} (c_1 \emptyset_1 + c_2 \emptyset_2 + \ldots c_n \emptyset_n) d\tau + \int c_2^* \emptyset_2^* \hat{Q} (c_1 \emptyset_1 + c_2 \emptyset_2 \ldots$$

$$+ \ldots \int c_n^* \emptyset_n^* \hat{Q} (c_1 \emptyset_1 + c_2 \emptyset_2 \ldots c_n \emptyset_n) d\tau \tag{3.6}$$

The basis set is orthonormal.

$$\int \emptyset_i^* \emptyset_i d\tau = 1$$

Q_{ij} is defined as $\int \emptyset_i^* \hat{Q} \emptyset_j d\tau$

Thus equation (3.6) becomes

$$\bar{Q} = c_1^* c_1 Q_{11} + c_1^* c_2 Q_{12} + \ldots c_1^* c_n Q_{1n}$$

$$+ c_2^* c_1 Q_{21} + c_2^* c_2 Q_{22} + \ldots c_2^* c_n Q_{2n}$$

$$+ \ldots + c_n^* c_1 Q_{n1} + c_n^* c_2 Q_{n2} + \ldots c_n^* c_n Q_{nn}$$

which can be written as

$$\bar{Q} = \sum_{i=1, j=1}^{i=n, j=n} c_i^* c_j Q_{ij}$$

as $\quad c_i c_j^* = c_j^* c_i = \rho_{ij}$

then $\quad \bar{Q} = \sum_{ij} \rho_{ji} Q_{ij} \tag{3.7}$

The observable property $(\bar{Q})$ is given by the trace of ρQ which is equivalent to the trace of $Q \rho$. This can be demonstrated as follows:

The matrix representation of the operator Q is

$$
\begin{bmatrix}
\langle \emptyset_1|\hat{Q}|\emptyset_1\rangle & \langle \emptyset_1|\hat{Q}|\emptyset_2\rangle & \cdots & \langle \emptyset_1|\hat{Q}|\emptyset_n\rangle \\
\vdots & & & \vdots \\
\langle \emptyset_n|\hat{Q}_1|\emptyset_1\rangle & & & \langle \emptyset_n|\hat{Q}|\emptyset_n\rangle
\end{bmatrix}
$$

$$
= \begin{bmatrix}
Q_{11} & Q_{12} & Q_{13} & \cdots & Q_{1n} \\
Q_{21} & Q_{22} & Q_{23} & \cdots & Q_{2n} \\
Q_{31} & Q_{32} & Q_{33} & \cdots & Q_{3n} \\
\vdots & \vdots & \vdots & \cdots & \vdots \\
Q_{n1} & Q_{n2} & Q_{n3} & & Q_{nn}
\end{bmatrix}
$$

$$
\therefore \ \rho Q = \begin{bmatrix}
\rho_{11} & \rho_{12} & \cdots & \rho_{1n} \\
\rho_{21} & \rho_{22} & \cdots & \rho_{2n} \\
\vdots & \vdots & \cdots & \vdots \\
\rho_{n1} & \rho_{n2} & & \rho_{nn}
\end{bmatrix}
\begin{bmatrix}
Q_{11} & Q_{12} & \cdots & Q_{1n} \\
Q_{21} & Q_{22} & \cdots & Q_{2n} \\
\vdots & \vdots & \cdots & \vdots \\
Q_{n1} & Q_{n2} & \cdots & Q_{nn}
\end{bmatrix}
$$

$$
= \begin{bmatrix}
\rho_{11}Q_{11} + \rho_{12}Q_{21} + \cdots \rho_{1n}Q_{n1} & \rho_{11}Q_{12} + \rho_{12}Q_{22} + \cdots \rho_{1n}Q_{n2} \\
\rho_{21}Q_{11} + \rho_{22}Q_{21} + \cdots \rho_{2n}Q_{n2} & \rho_{21}Q_{12} + \rho_{22}Q_{32} + \cdots \rho_{2n}Q_{n2} \\
& \cdots
\end{bmatrix}
$$

trace $\rho Q = \ \rho_{11}Q_{11} + \rho_{12}Q_{21} + \cdots \rho_{1n}Q_{n1}$

$\quad + \rho_{21}Q_{12} + \rho_{22}Q_{22} + \cdots \rho_{2n}Q_{n1}$

$\quad \cdots$

$\quad + \rho_{n1}Q_{1n} + \rho_{n2}Q_{n2} + \cdots \rho_{nn}Q_{nn} \qquad = \bar{Q}$

A similar proof would show that

$$\bar{Q} = \text{trace } \rho Q = \text{trace } Q\rho \qquad (3.8)$$

Thus for a given basis set, if the density matrix elements can be calculated, then any observable property of the system can be calculated.

3.5 Wave Functions and the Density Matrix

A wave function can be defined in terms of different basis sets. (1) $\emptyset_1, \emptyset_2, \emptyset_3, \ldots \emptyset_n$ leads to the density matrix $\rho^{\emptyset}$

(2) $x_1, x_2, \ldots x_n$ leads to the density matrix ρ^{x}

The two density matrices will not be the same, as the basis sets are not the same.

As a density matrix can be written for the $\emptyset$ basis set and for the x basis set, there must be a relationship between x and $\emptyset$.

Thus

$$x_1 = c_{11}\emptyset_1 + c_{12}\emptyset_2 + \ldots c_{1n}\emptyset_n$$
$$x_2 = c_{21}\emptyset_1 + c_{22}\emptyset_2 + \ldots c_{2n}\emptyset_n$$
$$\vdots \quad \ldots \quad \ldots \quad \ldots \quad \ldots$$
$$x_n = c_{n1}\emptyset_1 + c_{n2}\emptyset_2 + \ldots c_{nn}\emptyset_n$$

In matrix notation

$$
\begin{bmatrix} x_1 \\ x_2 \\ \vdots \\ x_n \end{bmatrix} =
\begin{bmatrix} c_{11} & c_{12} & \cdots & c_{1n} \\ c_{21} & c_{22} & \cdots & c_{2n} \\ \vdots & & & \\ c_{n1} & & \cdots & c_{nn} \end{bmatrix}
\begin{bmatrix} \emptyset_1 \\ \emptyset_2 \\ \vdots \\ \emptyset_n \end{bmatrix}
$$

The two density matrices can be related by a similarity transform[41]

$$\rho^{x} = c^{-1}\rho^{\emptyset}c \qquad (3.9)$$

A density matrix operator $\hat{\rho}$ can be defined which will generate the density matrix. A basis set can be chosen such that the matrix generated will be <u>diagonal</u>.

Suppose χ_1, χ_2, $\cdots \chi_n$ are the basis state functions which will give a diagonal density matrix then

$$\hat{\rho} = \sum_i |\chi_k> P_k <\chi_k|$$

(3.10)

in general $\quad \rho_{ij}^{\emptyset} = \sum_k <\emptyset_i|\chi_k> P_k <\chi_k|\emptyset_j>$

unless i=j this expression is zero, generating only diagonal elements.

To obtain the equation of motion of ρ we need to differentiate equation (3.10).

$$\frac{d\hat{\rho}_{ij}}{dt} = \sum_k \frac{d}{dt} |\chi_k> P_k <\chi_k|$$

(3.11)

and from quantum mechanics[42]

$$\frac{d<\chi_k|}{dt} = -\frac{1}{i\hbar} <\chi_k|\mathcal{H}$$

$$\frac{d|\chi_k|>}{dt} = \frac{\mathcal{H}}{i\hbar} |\chi_k>$$

substituting in (3.11)

$$\frac{d\hat{\rho}}{dt} = \sum_k ([\frac{d}{dt}|\chi_k>](P_k <\chi_k|) + |\chi_k> P_k \frac{d}{dt} <\chi_k|$$

$$= \sum_k (\frac{\mathcal{H}}{i\hbar} |\chi_k> P_k <\chi_k| - |\chi_k> P_k \frac{1}{i\hbar} <\chi_k|\mathcal{H})$$

$$i\hbar \frac{d\hat{\rho}}{dt} = \mathcal{H}\hat{\rho} - \hat{\rho}\mathcal{H}$$

In matrix notation[43]

$$i\hbar \frac{d\hat{\rho}}{dt} = \mathcal{H}\hat{\rho} - \hat{\rho}\mathcal{H}$$

(3.12)

3.6 Single Spin $\frac{1}{2}$ Nucleus

The nucleus is in a strong magnetic field B_o and an oscillating magnetic field $B_1\cos\omega_1 t$ is at right angles to B_o. B_1 is much smaller than B_o.

The Hamiltonian for such a system is

$$= -\gamma B_o(1-\sigma)I_z - \gamma B_1\cos(\omega_1 t)I_x \qquad (3.13)$$

where $\omega_o = \gamma B_o(1-\sigma)$

The oscillating field can be split into two components; an in-phase and an out-of-phase component. The Hamiltonian thus becomes

$$\mathcal{H}_o = -\omega_o I_z - \frac{\gamma B_1}{2}\cos(\omega_1 t)I_x - \frac{\gamma B_1}{2}\sin(\omega_1 t)I_y$$

$$\mathcal{H}_I = -\omega_o I_z - \frac{\gamma B_1}{2}\cos(\omega_1 t)I_x + \frac{\gamma B_1}{2}\sin(\omega_1 t)I_y$$

Considering only the in-phase component $\mathcal{H}_I$

The basis set functions considered are α and β ($I_z = +\frac{1}{2}$ and $I_z = -\frac{1}{2}$)

The effect of the various spin operators on the basis set are:[44]

$$\hat{I}_z\alpha = \tfrac{1}{2}\alpha$$

$$\hat{I}_z\beta = -\tfrac{1}{2}\alpha$$

$$\hat{I}_x\alpha = \tfrac{1}{2}\beta$$

$$\hat{I}_x\beta = \tfrac{1}{2}\alpha$$

$$\hat{I}_y\alpha = \tfrac{1}{2}i\beta$$

$$\hat{I}_y\beta = -\tfrac{1}{2}i\beta$$

Matrix representations of these operators are as follows:

$$\hat{I}_z = \begin{bmatrix} \tfrac{1}{2} & 0 \\ 0 & -\tfrac{1}{2} \end{bmatrix} \qquad \hat{I}_x = \begin{bmatrix} 0 & \tfrac{1}{2} \\ \tfrac{1}{2} & 0 \end{bmatrix} \qquad \hat{I}_y = \begin{bmatrix} 0 & -\tfrac{1}{2}i \\ \tfrac{1}{2}i & 0 \end{bmatrix}$$

These representations are known as the Pauli spin matrices.

The matrix representation for the in-phase components is

$$\mathcal{H}_I = -\omega_1 \begin{bmatrix} \frac{1}{2} & 0 \\ 0 & -\frac{1}{2} \end{bmatrix} - \frac{\gamma B_1}{2} \cos\omega t \begin{bmatrix} 0 & \frac{1}{2} \\ \frac{1}{2} & 0 \end{bmatrix} + \frac{\gamma B_1}{2} \sin\omega t \begin{bmatrix} 0 & -\frac{1}{2}i \\ \frac{1}{2}i & 0 \end{bmatrix}$$

$$= \begin{bmatrix} -\frac{1}{2}\omega_o & \frac{-\gamma B_1}{4}(\cos\omega t + i\sin\omega t) \\ \frac{-\gamma B_1}{4}(\cos\omega t - i\sin\omega t) & \frac{1}{2}\omega_o \end{bmatrix}$$

and as $\sin\omega t = (e^{i\omega t} - e^{-i\omega t})/2i$

$$\cos\omega t = (e^{i\omega t} + e^{-i\omega t})/2$$

$\mathcal{H}_I$ becomes

$$\begin{bmatrix} -\frac{1}{2}\omega_o & \frac{-\gamma B_1}{4}e^{i\omega t} \\ \frac{-\gamma B_1}{4}e^{-i\omega t} & \frac{1}{2}\omega_o \end{bmatrix}$$

using the density matrix equation of motion equation (3.12)

$$\rho = \begin{bmatrix} \rho_{11} & \rho_{12} \\ \rho_{21} & \rho_{22} \end{bmatrix}$$

$$\begin{bmatrix} i\frac{d\rho_{11}}{dt} & i\frac{d\rho_{12}}{dt} \\ i\frac{d\rho_{21}}{dt} & i\frac{d\rho_{22}}{dt} \end{bmatrix} = \begin{bmatrix} -\frac{1}{2}\omega_o & -De^{i\omega t} \\ -De^{-i\omega t} & \frac{1}{2}\omega_o \end{bmatrix} \begin{bmatrix} \rho_{11} & \rho_{12} \\ \rho_{21} & \rho_{22} \end{bmatrix}$$

$$- \begin{bmatrix} \rho_{11} & \rho_{12} \\ \rho_{21} & \rho_{22} \end{bmatrix} \begin{bmatrix} -\frac{1}{2}\omega_o & -De^{-\omega t} \\ -De^{-i\omega t} & \frac{1}{2}\omega_o \end{bmatrix}$$

where $D = \frac{\gamma B_1}{4}$

$$i\frac{d\rho_{11}}{dt} = -\frac{1}{2}\omega_o\rho_{11} - De^{i\omega t}\rho_{21} + \frac{1}{2}\omega_o\rho_{11} + \rho_{12}De^{-i\omega t}$$

$$= D(\rho_{12}e^{-i\omega t} - \rho_{21}e^{i\omega t})$$

$$i\frac{d\rho_{12}}{dt} = -\frac{1}{2}\omega_o\rho_{12} - De^{i\omega t}\rho_{22} + De^{i\omega t}\rho_{11} - \frac{1}{2}\rho_{12}\omega_o$$

$$= -\omega_o\rho_{12} + De^{i\omega t}(\rho_{11} - \rho_{22})$$

$$i \frac{d\rho_{21}}{dt} = -\rho_{11}De^{-i\omega t} + \tfrac{1}{2}\omega_o\rho_{21} + \tfrac{1}{2}\omega_o\rho_{21} + \rho_{22}De^{-i\omega t}$$

$$= \omega_o\rho_{21} + De^{-i\omega t}(\rho_{22} - \rho_{11})$$

$$i \frac{d\rho_{22}}{dt} = -\rho_{12}De^{-i\omega t} + \tfrac{1}{2}\omega_o\rho_{22} + \rho_{21}De^{i\omega t} - \tfrac{1}{2}\omega_o\rho_{22}$$

$$= D(\rho_{21}e^{i\omega t} - \rho_{12}e^{-i\omega t})$$

So far there have been no relaxation terms involved in the treatment. The diagonal terms of the matrix involve a return to equilibrium of the magnetization component in the z-direction. The off diagonal terms of the matrix involve a return to equilibrium of the magnetization component in the x-direction.

The relaxation terms are:

$$\frac{d\rho_{ij}}{dt} = \frac{-\rho_{ij}}{T_2}$$

$$\frac{d\rho_{ii}}{dt} = (\rho_{ii} - \rho_{ii}^o)/T_1$$

ρ_{ii}^o is the equilibrium value when the radiofrequency field is switched off.

The previous equations now become

$$i \frac{d\rho_{11}}{dt} = D(\rho_{12}e^{-i\omega t} - \rho_{21}e^{i\omega t}) - i(\rho_{11} - \rho_{11}^o)/T_1$$

$$i \frac{d\rho_{12}}{dt} = -\omega_o\rho_{12} + De^{i\omega t}(\rho_{11} - \rho_{22}) - i\rho_{12}/T_2$$

$$i \frac{d\rho_{21}}{dt} = \omega_o\rho_{21} - De^{-i\omega t}(\rho_{11} - \rho_{22}) - i\rho_{21}/T_2$$

$$i \, d\rho_{22} = D(\rho_{21}e^{i\omega t} - \rho_{12}e^{-i\omega t}) - i(\rho_{22} - \rho_{22}^o)/T_1$$

These equations can be regarded as a set of simult-
aneous equations with the density matrix elements as
unknowns. The observable quantities are the magnetization
of the sample in the x, y, and z directions. These
quantities are proportional to the expectation values of
the operators representing the projections of the angular
momentum along the x, y, and z directions respectively.

$$<M_x> \quad \alpha \quad <I_x>$$

$$<M_y> \quad \alpha \quad <I_y>$$

$$<M_z> \quad \alpha \quad <I_z>$$

As $\quad <Q> \quad = \quad \text{trace } Q\rho \quad = \quad \text{trace } \rho Q$

$$<M_x> \quad = \quad k \quad \text{trace } \rho I_x$$

$$<M_y> \quad = \quad k \quad \text{trace } \rho I_y$$

$$<M_z> \quad = \quad k \quad \text{trace } \rho I_z$$

where k is a proportionality constant.

$$\rho I_x = \begin{bmatrix} \rho_{11} & \rho_{12} \\ \rho_{21} & \rho_{22} \end{bmatrix} \begin{bmatrix} 0 & \frac{1}{2} \\ \frac{1}{2} & 0 \end{bmatrix} = \begin{bmatrix} \frac{\rho_{12}}{2} & \frac{\rho_{11}}{2} \\ \frac{\rho_{22}}{2} & \frac{\rho_{21}}{2} \end{bmatrix}$$

$$\therefore \quad \frac{<M_x>}{k} = \tfrac{1}{2}(\rho_{12} + \rho_{21}) = \text{trace } \rho I_x \tag{3.14}$$

$$\text{and} \quad \frac{<M_y>}{k} = \tfrac{1}{2}i(\rho_{12} - \rho_{21}) = \text{trace } \rho I_y \tag{3.15}$$

$$\frac{<M_z>}{k} = \tfrac{1}{2}(\rho_{11} - \rho_{22}) = \text{trace } \rho I_z \tag{3.16}$$

Differentiating the above equations with respect to
time, and substituting for, first the time dependence of
the density matrix elements in terms of $<M_x>$, $<M_y>$, and $<M_z>$,
the Bloch equations are obtained.

$$\langle \dot{M}_x \rangle = + \omega_o \langle M_y \rangle + \gamma B_1 \sin\omega t \langle M_z \rangle - \frac{\langle M_x \rangle}{T_2} \tag{3.17}$$

$$\langle \dot{M}_y \rangle = - \omega_o \langle M_x \rangle + \gamma B_1 \cos\omega t \langle M_z \rangle - \frac{\langle M_y \rangle}{T_2} \tag{3.18}$$

$$\langle \dot{M}_z \rangle = - \gamma B_1 \cos\omega t \langle M_y \rangle - \gamma B_1 \sin\omega t \langle M_x \rangle - \frac{\langle M_z \rangle - \langle M_z \rangle^o}{T_1} \tag{3.19}$$

3.7 Intramolecular Exchange

To study the effects of intramolecular exchange the effects of exchanging magnetic nuclei in the same molecule must be included in the equation of motion. If magnetic nuclei exchange environments then the iniyial spin ket of the molecule $|\psi\rangle$ is changed to $R|\psi\rangle$. (R is the exchange operator).

If τ is the mean life-time of the nucleus in each environment then the rate of change of ρ caused by exchange is $\dfrac{R\rho R - \rho}{\tau}$.

The equation of motion of the density matrix including the radio frequency probing field and the effects of intramolecular exchange is[45]

$$\frac{d\rho}{dt} = \frac{R\rho R - \rho}{\tau} + i[\rho, \mathcal{H}] + \frac{\rho^o \text{ diagonal} - \rho \text{ diagonal}}{T_1} - \frac{\rho \text{ off diagonal}}{T_2} \tag{3.20}$$

This equation can be written in component form as[46]

$$\frac{d\rho_{kl}}{dt} = \frac{1}{\tau}[\sum_{n,m} R_{kn}\rho_{nm} R_{ml} - \rho_{kl}] - \rho_{kl}/T_2$$

$$- i\rho_{kl}(\sum_i (\omega_{oi}-\omega)[(I_{zi})_{kk}-(I_{zi})_{ll}] + h\sum_{i<j} J_{ij}[(I_{zi}I_{zj})_{kk}-(I_{zi}I_{zj})_{ll}])$$

$$+ \frac{i}{2} h\sum_{i<j} J_{ij}[\rho, I_i^+ I_j^- + I_i^- I_j^+]_{kl} + i\omega_r (\rho_{kk} - \rho_{ll}) \sum_i (I_{xi})_{kl}$$

$$\tag{3.21}$$

There are simplifications which are usually applied to these equations.

(a) The NMR experiment is performed under "slow passage" steady state conditions.[46] $\therefore \frac{d\rho}{dt} = 0$

(b) $B_1 << B_0$. The significant transitions are thus governed by the selection rule $\Delta m_z = \pm 1$. This means that those density matrix elements linking energy levels between forbidden radiative transitions may be neglected.

(c) The last term in equation (3.21) may be simplified. The diagonal elements of the density matrix are proportional to the probability of finding a molecule of the system in the appropriate energy level. The differences between the energy levels in the NMR experiment are so small relative to the Boltzmann energy kT, that the differences between the diagonal elements of the density matrix may be all equal to a constant times Δm_z.

3.8 AB Spin System Undergoing Internal Rotation

The basis set chosen is the simple product kets formed from α and β, where $\alpha = \begin{bmatrix} 1 \\ 0 \end{bmatrix}$ and $\beta = \begin{bmatrix} 0 \\ 1 \end{bmatrix}$

Hence the basis set is (with the quantum number given on the right)

$$|\psi_1> = \alpha\alpha = \begin{bmatrix} 1 \\ 0 \end{bmatrix} \otimes \begin{bmatrix} 1 \\ 0 \end{bmatrix} = \begin{bmatrix} 1 \\ 0 \\ 0 \\ 0 \end{bmatrix} \qquad m_z = 1$$

$$|\psi_2> = \alpha\beta = \begin{bmatrix} 1 \\ 0 \end{bmatrix} \otimes \begin{bmatrix} 0 \\ 1 \end{bmatrix} = \begin{bmatrix} 0 \\ 1 \\ 0 \\ 0 \end{bmatrix} \qquad m_z = 0$$

$$|\psi_3> = \beta\alpha = \begin{bmatrix} 0 \\ 1 \end{bmatrix} \otimes \begin{bmatrix} 1 \\ 0 \end{bmatrix} = \begin{bmatrix} 0 \\ 0 \\ 1 \\ 0 \end{bmatrix} \qquad m_z = 0$$

$$|\psi_4> = \beta\beta = \begin{bmatrix} 0 \\ 1 \end{bmatrix} \otimes \begin{bmatrix} 0 \\ 1 \end{bmatrix} = \begin{bmatrix} 0 \\ 0 \\ 0 \\ 1 \end{bmatrix} \qquad m_z = 1$$

Under exchange conditions, nucleus A exchanges magnetic environment with nucleus B. Before rotation the basis set is formed by writing nucleus A first, after rotation the basis set is formed by writing nucleus B first.

	Before rotation	After rotation
(i)	$|\psi_1> = \alpha\alpha$	$|\psi_1> = \alpha\alpha$
(ii)	$|\psi_2> = \alpha\beta$	$|\psi_3> = \beta\alpha$
(iii)	$|\psi_3> = \beta\alpha$	$|\psi_2> = \alpha\beta$
(iv)	$|\psi_4> = \beta\beta$	$|\psi_4> = \beta\beta$

Using the exchange operator R, the rotation can be represented in matrix notation as

(i) $\begin{bmatrix} 1 \\ 0 \\ 0 \\ 0 \end{bmatrix}$ becomes $\begin{bmatrix} 1 \\ 0 \\ 0 \\ 0 \end{bmatrix}$ $\therefore R \begin{bmatrix} 1 \\ 0 \\ 0 \\ 0 \end{bmatrix} = \begin{bmatrix} 1 \\ 0 \\ 0 \\ 0 \end{bmatrix}$ $\therefore R_{11} = 1$

(ii) $\begin{bmatrix} 0 \\ 1 \\ 0 \\ 0 \end{bmatrix}$ becomes $\begin{bmatrix} 0 \\ 0 \\ 1 \\ 0 \end{bmatrix}$ $\therefore R \begin{bmatrix} 0 \\ 1 \\ 0 \\ 0 \end{bmatrix} = \begin{bmatrix} 0 \\ 0 \\ 1 \\ 0 \end{bmatrix}$ $\therefore R_{32} = 1$

(iii) $\begin{bmatrix} 0 \\ 0 \\ 1 \\ 0 \end{bmatrix}$ becomes $\begin{bmatrix} 0 \\ 1 \\ 0 \\ 0 \end{bmatrix}$ $\therefore R \begin{bmatrix} 0 \\ 0 \\ 1 \\ 0 \end{bmatrix} = \begin{bmatrix} 0 \\ 1 \\ 0 \\ 0 \end{bmatrix}$ $\therefore R_{23} = 1$

(iv) $\begin{bmatrix} 0 \\ 0 \\ 0 \\ 1 \end{bmatrix}$ becomes $\begin{bmatrix} 0 \\ 0 \\ 0 \\ 1 \end{bmatrix}$ $\therefore R \begin{bmatrix} 0 \\ 0 \\ 0 \\ 1 \end{bmatrix} = \begin{bmatrix} 0 \\ 0 \\ 0 \\ 1 \end{bmatrix}$ $\therefore R_{44} = 1$

The exchange operator R is thus a 4 x 4 matrix

$$R = \begin{bmatrix} 1 & 0 & 0 & 0 \\ 0 & 0 & 1 & 0 \\ 0 & 1 & 0 & 0 \\ 0 & 0 & 0 & 1 \end{bmatrix}$$

By knowing the initial and final forms of the molecular spin kets the elements of the transformation matrix are easily identified.

The pre-exchange density matrix, ρ, becomes $R\rho R$ on exchange where

$$R\rho R = \begin{bmatrix} 1 & 0 & 0 & 0 \\ 0 & 0 & 1 & 0 \\ 0 & 1 & 0 & 0 \\ 0 & 0 & 0 & 1 \end{bmatrix} \begin{bmatrix} \rho_{11} & \rho_{12} & \rho_{13} & \rho_{14} \\ \rho_{21} & \rho_{22} & \rho_{23} & \rho_{24} \\ \rho_{31} & \rho_{32} & \rho_{33} & \rho_{34} \\ \rho_{41} & \rho_{42} & \rho_{43} & \rho_{44} \end{bmatrix} \begin{bmatrix} 1 & 0 & 0 & 0 \\ 0 & 0 & 1 & 0 \\ 0 & 1 & 0 & 0 \\ 0 & 0 & 0 & 1 \end{bmatrix}$$

$$= \begin{bmatrix} \rho_{11} & \rho_{13} & \rho_{12} & \rho_{14} \\ \rho_{31} & \rho_{33} & \rho_{32} & \rho_{34} \\ \rho_{21} & \rho_{23} & \rho_{22} & \rho_{24} \\ \rho_{41} & \rho_{43} & \rho_{42} & \rho_{44} \end{bmatrix}$$

Therefore on exchange ρ_{12} becomes ρ_{13}, ρ_{42} becomes ρ_{43} and so on.

The Hamiltonian for a two spin $\frac{1}{2}$ system undergoing intramolecular exchange reduces to

$$\mathcal{H} = -\omega(I_{zA} + I_{zB}) + \omega_{oA}I_{zA} + \omega_{oB}I_{zB} + \gamma_1 B_1(I_{xA} + I_{xB})$$
$$+ J'_{AB}hI_{zA}I_{zB} + \tfrac{1}{2}J'_{AB}h(I_A^+ I_B^- + I_A^- I_B^+) \tag{3.22}$$

where $\mathcal{H}$ is in rad s^{-1}. However $\mathcal{H}$ is usually written in terms of linear frequency.

$$\mathcal{H} = -\nu(I_{zA} + I_{zB}) + \nu_{oA}I_{zA} + \nu_{oB}I_{zB} + \frac{\gamma B_1}{2\pi}(I_{xA} + I_{xB})$$
$$+ J_{AB}I_{zA}I_{zB} + \tfrac{1}{2}J_{AB}(I_A^+ I_B^- + I_A^- I_B^+) \tag{3.23}$$

where $\omega = 2\pi\nu$ and $J_{AB} = hJ'_{AB}/2\pi$

$\mathcal{H}$ as now written differs from that of equation (3.22) by a factor of $1/2\pi$. Substituting for values of I_{zA}, I_{yA} etc., the following matrix representations for the terms in equation (3.23) are obtained

$$I_{zA} = \begin{bmatrix} \tfrac{1}{2} & 0 \\ 0 & -\tfrac{1}{2} \end{bmatrix} \otimes \begin{bmatrix} 1 & 0 \\ 0 & 1 \end{bmatrix} = \begin{bmatrix} \tfrac{1}{2} & 0 & 0 & 0 \\ 0 & \tfrac{1}{2} & 0 & 0 \\ 0 & 0 & -\tfrac{1}{2} & 0 \\ 0 & 0 & 0 & -\tfrac{1}{2} \end{bmatrix}$$

$$I_{zB} = \begin{bmatrix} 1 & 0 \\ 0 & 1 \end{bmatrix} \otimes \begin{bmatrix} \frac{1}{2} & 0 \\ 0 & -\frac{1}{2} \end{bmatrix} = \begin{bmatrix} \frac{1}{2} & 0 & 0 & 0 \\ 0 & -\frac{1}{2} & 0 & 0 \\ 0 & 0 & \frac{1}{2} & 0 \\ 0 & 0 & 0 & -\frac{1}{2} \end{bmatrix}$$

$$I_{zA}\,I_{zB} = \begin{bmatrix} \frac{1}{4} & 0 & 0 & 0 \\ 0 & -\frac{1}{4} & 0 & 0 \\ 0 & 0 & -\frac{1}{4} & 0 \\ 0 & 0 & 0 & \frac{1}{4} \end{bmatrix}$$

$$I_A^+ I_B^- + I_A^- I_B^+ = \begin{bmatrix} 0 & 0 & 0 & 0 \\ 0 & 0 & 1 & 0 \\ 0 & 1 & 0 & 0 \\ 0 & 0 & 0 & 0 \end{bmatrix} \quad \text{and so on.}$$

Therefore the matrix representation of the Hamiltonian given in equation (3.23) is

$$= \begin{bmatrix} \Delta\nu + J/4 & f & f & 0 \\ f & \delta\nu - J/4 & J/2 & f \\ f & J/2 & -\delta\nu - J/4 & f \\ 0 & f & f & -\Delta\nu + J/4 \end{bmatrix}$$

where $J = J_{AB}$, $f = \dfrac{\gamma B_1}{4\pi}$, $\Delta\nu = \frac{1}{2}(\nu_{oA} + \nu_{oA}) - \nu$ and $\delta\nu = \frac{1}{2}(\nu_{oA} - \nu_{oB})$

The NMR absorption mode spectrum line shape is proportional to the expectation value of the spin angular momentum in the y direction and hence $\langle I_y \rangle$

$$\langle I_{yT} \rangle = \mathrm{Tr}\,(\rho I_{yT}) \tag{3.24}$$

where $\langle I_{yT} \rangle$ is the total angular momentum in the y direction.

$$I_{yT} = \sum_{i=1}^{2} I_{yi} = \begin{bmatrix} 0 & -\frac{i}{2} \\ \frac{i}{2} & 0 \end{bmatrix} \otimes \begin{bmatrix} 1 & 0 \\ 0 & 1 \end{bmatrix} + \begin{bmatrix} 1 & 0 \\ 0 & 1 \end{bmatrix} \otimes \begin{bmatrix} 0 & -\frac{i}{2} \\ \frac{i}{2} & 0 \end{bmatrix}$$

$$= \frac{i}{2} \begin{bmatrix} 0 & -1 & -1 & 0 \\ 1 & 0 & 0 & -1 \\ 1 & 0 & 0 & 1 \\ 0 & 1 & 1 & 0 \end{bmatrix}$$

$$\therefore \mathrm{Tr}\,I_{yT} = \frac{1}{2}i(\rho_{12} + \rho_{13} + \rho_{24} + \rho_{34} - \rho_{21} - \rho_{31} - \rho_{42} - \rho_{43})$$

$$= \mathrm{Im}\,(\rho_{21} + \rho_{31} + \rho_{42} + \rho_{43}) \quad \text{as } \rho \text{ is hermitian}$$

$$\text{i.e. } \mathrm{Tr}\,I_{yT} = -\mathrm{Im}\,(\rho_{12} + \rho_{13} + \rho_{24} + \rho_{34}) \tag{3.25}$$

The sign is irrelevant since the constant f is set arbitrarily.

The Hamiltonian matrix representation of equation (3.23) may now be used in equation (3.20), and the appropriate simplification made to obtain the following equations relating the required elements of the density matrix.

$$i(f\rho_{11} + (\delta\nu - \frac{J}{4})\rho_{12} + \frac{J}{2}\rho_{13} - (\Delta\nu + \frac{J}{4})\rho_{12} - f\rho_{22}) - \frac{\rho_{12}}{T_2'} + \frac{\rho_{13} - \rho_{12}}{\tau'} = 0$$

$$i(f\rho_{11} - (\delta\nu + \frac{J}{4})\rho_{13} + \frac{J}{2}\rho_{12} - (\Delta\nu + \frac{J}{4})\rho_{13} - f\rho_{33}) - \frac{\rho_{13}}{T_2'} + \frac{\rho_{12} - \rho_{13}}{\tau'} = 0$$

$$i(f\rho_{22} - (\delta\nu - \frac{J}{4})\rho_{24} - \frac{J}{2}\rho_{34} + (-\Delta\nu + \frac{J}{4})\rho_{24} - f\rho_{44}) - \frac{\rho_{24}}{T_2'} + \frac{\rho_{34} - \rho_{24}}{\tau'} = 0$$

$$i(f\rho_{33} + (\delta\nu + \frac{J}{4})\rho_{34} - \frac{J}{2}\rho_{24} + (-\Delta\nu + \frac{J}{4})\rho_{34} - f\rho_{44}) - \frac{\rho_{34}}{T_2'} + \frac{\rho_{24} - \rho_{34}}{\tau'} = 0$$

$$(3.26)$$

These equations can be solved to obtain the required density matrix elements. Substitution of these elements into equation (3.25) gives $<I_{yT}>$. A graph of $<I_{yT}>$ against ν is the observed "absorption mode" NMR spectrum.

3.9 Detailed Solution of the AB System: Intramolecular Exchange

The absorption mode spectrum line shape for such a system is given by the equation (3.25).

i.e. $<I_{yT}>$ = $Tr\rho I_{yT}$ = $-Im(\rho_{12} + \rho_{13} + \rho_{24} + \rho_{34})$

and that the essential density matrix elements can be obtained from solutions of equations (3.26). In general, these density matrix elements are complex numbers.

i.e. $\rho_{nm} = R_{nm} + iI_{nm}$

where R_{nm} and I_{nm} are real numbers.

Furthermore, because the density matrix is hermitian (i.e.

$\rho_{nm} = \rho^{*}_{mn}$) the diagonal elements must be real numbers

i.e. $\rho_{nn} = R_{nn}$

Making use of these relationships, equation (3.25) becomes

$$\langle I_{yT} \rangle = I_{12} + I_{13} + I_{24} + I_{34}$$

and equations (3.26) become

$$i(fR_{11} + (\delta\nu - \tfrac{J}{4})(R_{12} + iI_{12}) + \tfrac{J}{2}(R_{13} + iI_{13}) - (\Delta\nu + \tfrac{J}{4})(R_{12} + iI_{12} - fR_{22})$$

$$\frac{-(R_{12} + iI_{12})}{T_2'} + \frac{(R_{13} + iI_{13}) - (R_{12} + iI_{12})}{\tau'} = 0$$

$$i(fR_{11} - (\delta\nu + \tfrac{J}{4})(R_{13} + iI_{13}) + \tfrac{J}{2}(R_{12} + iI_{12}) - (\Delta\nu + \tfrac{J}{4})(R_{13} + iI_{13}) - fR_{33})$$

$$\frac{-(R_{13} + iI_{13})}{T_2'} + \frac{(R_{12} + iI_{12}) - (R_{13} + iI_{13})}{\tau'} = 0$$

$$i(fR_{22} - (\delta\nu - \tfrac{J}{4})(R_{24} - iI_{24} - \tfrac{J}{2}(R_{34} + iI_{34}) - (\Delta\nu - \tfrac{J}{4})(R_{24} + iI_{24} - fR_{44})$$

$$\frac{-(R_{24} + iI_{24})}{T_2'} + \frac{(R_{34} + iI_{34}) - (R_{24} + iI_{24})}{\tau'} = 0$$

$$i(fR_{33} + (\delta\nu + \tfrac{J}{4})(R_{34} + iI_{34}) - \tfrac{J}{2}(R_{24} + iI_{24}) - (\Delta\nu - \tfrac{J}{4})(R_{34} + iI_{34}) - fR_{44})$$

$$\frac{(R_{34} + iI_{34})}{T_2'} + \frac{(R_{24} + iI_{24}) - (R_{34} + iI_{34})}{\tau'} = 0$$

Each of the above equations can be divided into two separate equations by equating all the real terms and then separately all the imaginary terms to obtain the following equations:

$$-(\delta\nu - \frac{J}{4})I_{12} - \frac{J}{2}I_{13} + (\Delta\nu + \frac{J}{4})I_{12} - \frac{R_{12}}{T_2'} + \frac{R_{13} - R_{12}}{\tau'} = 0$$

$$(\delta\nu - \frac{J}{4})R_{12} + \frac{J}{2}R_{13} - (\Delta\nu + \frac{J}{4})R_{12} - \frac{I_{12}}{T_2'} + \frac{I_{13} - I_{12}}{\tau'} = f\,(R_{22} - R_{11})$$

$$(\delta\nu + \frac{J}{4})I_{13} - \frac{J}{2}I_{12} + (\Delta\nu + \frac{J}{4})I_{13} - \frac{R_{13}}{T_2'} + \frac{R_{12} - R_{13}}{\tau'} = 0$$

$$-(\delta\nu + \frac{J}{4})R_{13} + \frac{J}{2}R_{12} - (\Delta\nu + \frac{J}{4})R_{13} - \frac{I_{13}}{T_2'} + \frac{I_{12} - I_{13}}{\tau'} = f(R_{33} - R_{11})$$

$$(\delta\nu - \frac{J}{4})I_{24} + \frac{J}{2}I_{34} + (\Delta\nu - \frac{J}{4})I_{24} - \frac{R_{24}}{T_2'} + \frac{R_{34} - R_{24}}{\tau'} = 0$$

$$-(\delta\nu - \frac{J}{4})R_{24} - \frac{J}{2}R_{34} - (\Delta\nu - \frac{J}{4})R_{24} - \frac{I_{24}}{T_2'} + \frac{I_{34} - I_{24}}{\tau'} = f(R_{44} - R_{22})$$

$$-(\delta\nu + \frac{J}{4})I_{34} + \frac{J}{2}I_{24} + (\Delta\nu - \frac{J}{4})I_{34} - \frac{R_{34}}{T_2'} + \frac{R_{24} - R_{34}}{\tau'} = 0$$

$$(\delta\nu + \frac{J}{4})R_{34} - \frac{J}{2}R_{24} - (\Delta\nu - \frac{J}{4})R_{34} - \frac{I_{34}}{T_2'} + \frac{I_{24} - I_{34}}{\tau'} = f(R_{44} - R_{33})$$

$$(3.27)$$

There are two sets of coupled equations. The first four involve terms from ρ_{12} and ρ_{13} and can be solved to obtain I_{12} and I_{13} while the second four involve terms from ρ_{24} and ρ_{34} and will yield I_{24} and I_{34}. It is possible to solve these equations algebraically but very time consuming since in order to produce a theoretical spectrum covering 10 Hz at 0.1 Hz intervals it would be necessary to calculate a hundred values of $<I_{yT}>$. The only practical method is to use a computer. The equations are arranged in matrix form and solved by a matrix inversion program.

Equations (3.27) in matrix form become

$$\begin{bmatrix} -\frac{1}{T_2} - \frac{1}{\tau} & \Delta\nu - \delta\nu + \frac{J}{2} & \frac{1}{\tau} & -\frac{J}{2} \\[2mm] -\Delta\nu + \delta\nu - \frac{J}{2} & \frac{-1}{T_2} - \frac{1}{\tau} & \frac{J}{2} & \frac{1}{\tau} \\[2mm] \frac{1}{\tau} & -\frac{J}{2} & -\frac{1}{T_2} - \frac{1}{\tau} & \Delta\nu + \delta\nu + \frac{J}{2} \\[2mm] \frac{J}{2} & \frac{1}{\tau} & -\Delta\nu - \delta\nu - \frac{J}{2} & -\frac{1}{T_2} - \frac{1}{\tau} \end{bmatrix} \begin{bmatrix} R_{12} \\[2mm] I_{12} \\[2mm] R_{13} \\[2mm] I_{13} \end{bmatrix} = \begin{bmatrix} 0 \\[2mm] 1 \\[2mm] 0 \\[2mm] 1 \end{bmatrix}$$

and

$$\begin{bmatrix} -\frac{1}{T_2} - \frac{1}{\tau} & \Delta\nu + \delta\nu - \frac{J}{2} & \frac{1}{\tau} & \frac{J}{2} \\[2mm] -\Delta\nu - \delta\nu + \frac{J}{2} & \frac{1}{T_2} - \frac{1}{\tau} & -\frac{J}{2} & \frac{1}{\tau} \\[2mm] \frac{1}{\tau} & \frac{J}{2} & -\frac{1}{T_2} - \frac{1}{\tau} & \Delta\nu - \delta\nu - \frac{J}{2} \\[2mm] -\frac{J}{2} & \frac{1}{\tau} & -\Delta\nu + \delta\nu + \frac{J}{2} & -\frac{1}{T_2} - \frac{1}{\tau} \end{bmatrix} \begin{bmatrix} R_{24} \\[2mm] I_{24} \\[2mm] R_{34} \\[2mm] I_{34} \end{bmatrix} = \begin{bmatrix} 0 \\[2mm] 1 \\[2mm] 0 \\[2mm] 1 \end{bmatrix}$$

The terms $f(R_{ii} - R_{jj})$ have been set equal to one. This is a scaling factor for the intensity.

These matrices can be represented by

$$AX = B$$

The computer program for the four spin system uses the same representation.

Matrix inversion involves the multiplication of both sides by the inverse of A.

$$A^{-1} A X = A^{-1} B$$

or $\quad X = A^{-1} B$

The right hand side of this equation involves purely numerical quantities and the four unknowns needed to obtain $\langle I_{yT} \rangle$ can be determined.

3.10 Strongly-coupled Four-site Exchange System

In the equation of motion (3.12) both $\mathcal{H}$ and ρ are now 16 x 16 matrices. Corresponding elements in the array are equated and equations of the form shown by equation (3.21) are obtained.

When real and imaginary parts are separately equated, 112 simultaneous equations are obtained, but because of symmetry, these equations reduce to two sets of 48 simult-aneous equations and two sets of 8 equations which are independent of each other. These equations must be solved to obtain the imaginary parts of the density matrix elements required for calculating the line shape.

The mathematical manipulations are precisely the same as the AB case. For the four-spin system there are sixteen product functions which are used as the basis set.

	1 2 3 4		1 2 3 4			
ψ_1	α α α α	$\xrightarrow[\text{rotation}]{\text{on}}$	α α α α	$\lvert\psi_1\rangle \to \lvert\psi_1\rangle$	R_{11}	$= 1$
ψ_2	α α α β	$\longrightarrow$	α α β α	$\lvert\psi_2\rangle \to \lvert\psi_3\rangle$	R_{32}	$= 1$
ψ_3	α α β α	$\longrightarrow$	α α α β	$\lvert\psi_3\rangle \to \lvert\psi_2\rangle$	R_{23}	$= 1$
ψ_4	α α β β	$\longrightarrow$	α α β β	$\lvert\psi_4\rangle \to \lvert\psi_4\rangle$	R_{44}	$= 1$
ψ_5	α β α α	$\longrightarrow$	β α α α	$\lvert\psi_5\rangle \to \lvert\psi_9\rangle$	R_{95}	$= 1$
ψ_6	α β α β	$\longrightarrow$	β α β α	$\lvert\psi_6\rangle \to \lvert\psi_{11}\rangle$	$R_{11\ 6}$	$= 1$
ψ_7	α β β α	$\longrightarrow$	β α α β	$\lvert\psi_7\rangle \to \lvert\psi_{10}\rangle$	$R_{10\ 7}$	$= 1$
ψ_8	α β β β	$\longrightarrow$	β α β β	$\lvert\psi_8\rangle \to \lvert\psi_{12}\rangle$	$R_{12\ 8}$	$= 1$
ψ_9	β α α α	$\longrightarrow$	α β α α	$\lvert\psi_9\rangle \to \lvert\psi_{15}\rangle$	$R_{15\ 9}$	$= 1$
ψ_{10}	β α α β	$\longrightarrow$	α β β α	$\lvert\psi_{10}\rangle \to \lvert\psi_7\rangle$	$R_{7\ 10}$	$= 1$
ψ_{11}	β α β α	$\longrightarrow$	α β α β	$\lvert\psi_{11}\rangle \to \lvert\psi_6\rangle$	$R_{6\ 11}$	$= 1$
ψ_{12}	β α β β	$\longrightarrow$	α β β β	$\lvert\psi_{12}\rangle \to \lvert\psi_8\rangle$	$R_{8\ 12}$	$= 1$
ψ_{13}	β β α α	$\longrightarrow$	β β α α	$\lvert\psi_{13}\rangle \to \lvert\psi_{13}\rangle$	$R_{13\ 13}$	$= 1$
ψ_{14}	β β α β	$\longrightarrow$	β β β α	$\lvert\psi_{14}\rangle \to \lvert\psi_{15}\rangle$	$R_{15\ 14}$	$= 1$
ψ_{15}	β β β α	$\longrightarrow$	β β α β	$\lvert\psi_{15}\rangle \to \lvert\psi_{14}\rangle$	$R_{14\ 15}$	$= 1$
ψ_{16}	β β β β	$\longrightarrow$	β β β β	$\lvert\psi_{16}\rangle \to \lvert\psi_{16}\rangle$	$R_{16\ 16}$	$= 1$

For the four site case used in this investigation, the observed quantity $Tr(\rho I_{yT})$ contains thirty two density matrix elements. The density matrix, the Hamiltonian matrix, and the exchange matrix are all 16 x 16. By using the same procedures as in the AB case an expression for $<I_{yT}>$ is obtained.

$$<I_{yT}> = \rho_{1\,2} + \rho_{1\,3} + \rho_{1\,5} + \rho_{1\,9} + \rho_{2\,4} + \rho_{2\,6} + \rho_{2\,10} + \rho_{3\,4} +$$

$$\rho_{3\,7} + \rho_{3\,11} + \rho_{4\,8} + \rho_{4\,12} + \rho_{5\,6} + \rho_{5\,7} + \rho_{5\,13} + \rho_{6\,8} +$$

$$\rho_{6\,14} + \rho_{7\,3} + \rho_{7\,15} + \rho_{8\,16} + \rho_{9\,10} + \rho_{9\,11} + \rho_{9\,13} + \rho_{1012} +$$

$$\rho_{10\,14} + \rho_{11\,12} + \rho_{11\,15} + \rho_{12\,16} + \rho_{13\,14} + \rho_{13\,15} + \rho_{1\,16} + \rho_{15\,1\iota}$$

The program in Appendix One shows the setting up of the required matrices. It was developed by Paul Buckley and Neil Pinder over the first year of this project. The program will solve any four spin system of the form

2 ⌐   ⌐ 1
3 ⌐Y⌐ 4
X
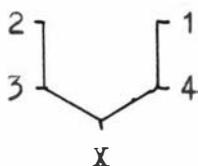
It should be noted that the numbering shown above is that used in the program and the normal numbering convention for the aromatic systems will be used throughout this thesis.

The data required for the program were the coupling constants, the chemical shifts and the spin-spin relaxation rate. The rotational rate combined with the lower and upper limits of the frequency range was also required.

To check the program's reliability, the work of Dahlquist and Forsen[58] on N-acetylpyrrole was repeated. Identical results were obtained. However this preliminary investigation revealed a number of errors[47] in Dahlquist and

Forsen's paper. The value 0.65 sec which they had reported as the transverse relaxation time was in fact found to be the inverse of the relaxation time T_2. Additionally, the error in τ was found to be out by a factor of 2π. This can arise from not converting angular frequencies to frequencies, or vice versa. Through this preliminary investigation, there developed an awareness of the time which would be involved in a full investigation of a four-spin system.

CHAPTER FOUR

Intramolecular Exchange

In the p-Substituted Nitrosobenzenes

The two systems investigated by means of the density matrix program were the p-nitrosoanilines and the p-nitrosophenols. In this chapter the results of these investigations are presented.

4.1 The N,N-dialkyl-p-nitrosoanilines

In 1968 it was reported that the most sophisticated studies of rate processes deriving enthalpy and entropy of activation were exemplified by an investigation of hindered rotation about the aryl-nitroso bond in N,N-dimethyl-p-nitrosoaniline.[48]

The starting point in this investigation was from a comprehensive paper[49] studying the NMR spectra of p-substituted nitrosobenzenes. The authors, Calder and Garratt, showed that the nitrosoanilines were particularly suitable for a detailed line shape study. Spectra had been obtained in acetone-d_6 over a temperature range of 70 K (223 K-293 K). Sample spectra shown in their paper pointed to the possibility of obtaining the slow exchange spectral parameters that were necessary for the density matrix program.

In checking their references to previous work it was noted that there was a disparity in the thermodynamic parameters between MacNicol et al's[50] results for N,N-dimethyl-p-nitrosoaniline and Korver et al's[51] results for the same compound. Korver et al, unable to explain their results, suggested that further experiments were necessary to

establish whether there was a significant correlation between rotational barriers and the nature of the solvent.   This was because two different solvents, chloroform-d_1 and acetone-d_6, had been used by each group.

These previous investigators had left the question of whether the solvent affected the barrier to rotation unanswered, and if there was no solvent effect, which value for the thermodynamic parameters was correct.

The study outlined here was the first attempt at a detailed study of the nitrosoanilines in a range of solvents.

4.1.1 Properties of the N, N-dialkyl-p-nitrosoanilines

The canonical forms of the two nitrosoanilines that were studied are listed below

(I)   (II)   R = Me, Et
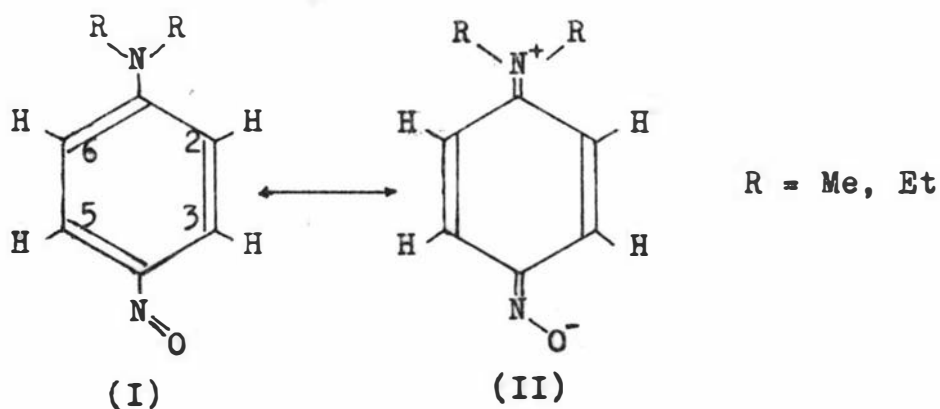
There exists in the p-nitrosoanilines a rotational energy barrier reflecting the contribution of structure (II) which has been inferred from dipole moment,[52] infrared,[53] and ultraviolet measurements.[54]   In these compounds, the main contributor to the barrier is assumed to be the

conjugative interaction between π electrons on both sides of the single bond that exhibits restricted rotation. These compounds are monomeric in the solid state[54] and in solution[55] so that no complications arise out of their dimerization. Their green colour in the solid state and in solution is a further indicator of their monomeric state.[55]

4.1.2 <u>Preparation of Compounds</u>

<u>Preparation of N,N-dimethyl-p-nitrosoaniline.</u>[56]

30 g of dimethylaniline (May and Baker) was dissolved in 105 cm^3 of concentrated hydrochloric acid contained in a 600 cm^3 beaker. Finely crushed ice was added until the temperature fell below 5°C. While maintaining the temperature of the reaction mixture below 8°C by the addition of ice, a solution of 18 g of sodium nitrite in 30 cm^3 of water was slowly added from a separatory funnel. After the nitrite solution had been added, the mixture was allowed to stand for one hour. The yellow crystalline product of N,N-dimethyl-p-nitrosoaniline hydrochloride was filtered, washed with 40 cm^3 of dilute hydrochloric acid (1:1), and then finally washed with a little alcohol.

30 g of the hydrochloride was transferred to a 500 cm^3 separatory funnel and 100 cm^3 of water was added. Cold aqueous sodium hydroxide solution (10% w/v) was added, with shaking, until the whole mass became bright green. (This is the colour of

the free base). The free base was extracted by shaking with 3 x 60 cm^3 portions of benzene. The combined benzene extracts were dried with anhydrous potassium carbonate. The potassium carbonate was filtered off and the benzene solution reduced by distillation to half its volume. The residual hot benzene solution was poured into a beaker. On cooling, crystals of N,N-dimethyl-p-nitrosoaniline formed. These were filtered and air-dried. The yield of product was almost quantitative. Melting point 86°C. (lit. value Vogel 85°C)

Preparation of N,N-diethyl-p-nitrosoaniline.

250 cm^3 of commercial grade diethylaniline (May and Baker) and 107 cm^3 of acetic anhydride were refluxed for six hours. On distilling, the pure diethylaniline was collected at 215°C as a clear pale yellow liquid.

Using the same basic procedure as for the preparation of N,N-dimethyl-p-nitrosoaniline, 19.6 g of purified diethylaniline and 8.6 g of sodium nitrite were used. The solution turned dark red with no precipitate on the addition of the sodium nitrite. The subsequent addition of an excess of a cold aqueous sodium hydroxide solution (10% w/v) caused a colour change from red to green with the formation of a precipitate. The free base was extracted with benzene which, after drying with potassium carbonate, filtering, and distilling gave green crystals of melting point 84°C.

Checks on Purity

The NMR spectra of both these compounds showed that they were free from impurities. Analyses by the mass spectrometer also verified that if impurities were present they were insignificant.

An interesting point on the melting points of both compounds was that the literature values for both compounds varied. Values reported for N,N-dimethyl-p-nitrosoaniline were 93°C,[57] 87-88°C,[57] and 85°C[56] quoted by Vogel. Values for N,N-diethyl-p-nitrosoaniline were 87-88°C[57] and 84°C.[56]

The use of the calibrated Reichert melting point apparatus gave greater reliability to the values obtained in this study as did the support of the NMR spectra obtained on these compounds which were not available to previous investigators.

4.1.3 Preparation of the Samples.

The samples were made up individually in 2 cm^3 flasks and then transferred into NMR tubes (4mm i.d. and 5mm o.d.) equipped with B17 quickfit male joint heads.

To ensure there was no dissolved oxygen in the samples each sample was made up in a dry box in an atmosphere of nitrogen. The required nitrosoaniline was transferred to the 2 cm^3 volumetric flask, stoppered, and transferred out of the dry box and weighed. This process was repeated until the correct mass of p-nitrosoaniline was added.

With the flask still in the dry box the flask was made up to the mark with the required solvent.

All the solvents used contained 1% v/v tetramethylsilane.

With the quick vaporization of tetramethylsilane (TMS) it was found easier to add the TMS to the stock bottle of solvent. As the stock supply of both acetone-d_6 and toluene-d_8 only amounted to 10 cm^3 this did not require much TMS. To ensure the correct amount of TMS was added, a standard sample of ethyl benzene containing 1% TMS was run on external lock and the spectrum of the TMS signal was recorded. TMS was added to the stock solution of solvent and a sample was taken every few drops and compared with the previously run TMS signal. When the signal heights of standard sample and TMS from the stock solvent matched this meant the amount of TMS added was suitable for an adequate lock signal. This method provided a good way of ensuring a standard amount of TMS was added to each sample.

To complete making up the samples, approximately 0.5 cm^3 of each sample was transferred to an NMR tube with a borosilicate glass extension which had a constriction for sealing. The extension was then attached by means of its quickfit joint to a vacuum line.

On the vacuum line the sample was first frozen by being inserted into a flask of liquid air. The reservoir above the NMR tube was evacuated of air and the vacuum pump was sealed off by a valve and the sample was allowed to thaw. Bubbles of dissolved gas were seen to evolve rapidly on the first thaw each

Table 4.1

Solvents and solute solubility

Solvent	Temperature Range* (^{o}C) of Solvent			Solubility of Solute at low temperatures
acetic acid-d$_4$	16.7	-	118.0 U	...
acetone-d$_6$	-94.0	-	56.5 S	soluble
benzene-d$_6$	5.5	-	80.1 U	...
carbon tetrachloride	-23.0	-	76.8 U	...
chloroform-d$_1$	-63.5	-	61.5 S	soluble
carbon disulphide	-111.6	-	46.5 S	reacts with solute
dimethylsulphoxide-d$_6$	-18.45	-	189 U	...
ethanol-d$_6$	-130	-	78.5 S	insoluble
methanol-d$_4$	-97.8	-	64.7 S	insoluble
methylene chloride-d$_4$	-96.8	-	39.95 S	soluble
nitrobenzene-d$_5$	6	-	210 U	...
nitromethane-d$_3$	-29	-	101.2 U	...
pyridine-d$_5$	-42	-	115 U	...
toluene-d$_8$	-95	-	110.6 S	soluble
trichlorofluoromethane	-111	-	23.7 S	insoluble

*   U = unsuitability because of temperature range

    S = suitability because of temperature range

time a solvent (sample) was placed on the vacuum line.

This process was repeated three times to ensure no dissolved gases remained in solution. At the end of this process, with the sample tube still remaining enclosed by the liquid air, the NMR tube was sealed off using an oxy-natural gas flame.

4.1.4 Solvents used for the N,N-dialkyl-p-nitrosoanilines

Three solvents were used in the investigation: acetone-d_6, chloroform-d_1, and toluene-d_8. The acetone-d_6, and chloroform-d_1, were obtained from British Drug Houses, and the toluene-d_8 from Stohler Isotope Chemicals.

Though the nitrosoanilines have reasonable solubility in a number of solvents not all of these solvents were suitable because of the need to work at temperatures of about 223 K. Table (4.1) lists a range of deuterated and non-proton containing solvents that were examined in the course of this work. The requirement of a suitable temperature range, considerably reduced the range of solvents that were suitable.

This same table (4.1) shows the solubility of the nitrosoanilines at low temperatures. Calder and Garratt[49] report being able to use a 5% w/v solution of N,N-dimethyl-p-nitrosoaniline in their studies. In this investigation it was found that for temperatures of 233 K and lower, a 5% w/v nitrosoaniline solution precipitated. The dimethyl-p-nitrosoaniline precipitated from the toluene at all concentrations below 253 K. However, this compound had considerable solubility in chloroform, which enabled Korver et al[50]

to use a 15% w/w solution.

The concentration that was used for N,N-dimethyl-p-nitrosoaniline in both chloroform-d$_1$ and acetone-d$_6$ was $2\frac{1}{2}$% w/v.

The N,N-diethyl-p-nitrosoaniline was considerably more soluble in all solvents at temperatures of 223 K. At this temperature it precipitated only slowly in toluene-d$_8$ and allowed sufficient time for a spectrum to be run. The concentration used for the three solvents for N,N-diethyl-p-nitrosoaniline was a 4% w/v solution.

Both nitrosoanilines gave an intense green colour in solution. The N,N-dimethyl-p-nitrosoaniline gave a light green solution in contrast to the very dark green of the N,N-diethyl-p-nitrosoaniline.

4.1.5 Experimental Conditions

As was mentioned in Chapter Two, optimum experimental conditions are needed to eliminate or reduce errors from this source. This section is concerned with detailing the minor and major difficulties that beset the obtaining of spectra. The method or technique that was used in this study relied entirely on optimum experimental conditions from the spectrometer and its associated hardware for up to eight hours continuous running.

The Instrument

The spectrometer used in the experimental investigation was a JEOL JNM-C-60HL high resolution NMR instrument equipped with a variable temperature unit and detector used in conjunction with a JES-VT-3

temperature controller.

A visit by the Japanese engineer from JEOL in the second year of this study had the spectrometer operating at its best performance level. The ease of obtaining spectra decreased gradually over the remaining years of the project. As the spectrometer uses valves, this was probably a reflection of the slowly changing characteristics of the valves. One problem in the latter phases of the project was the spiking of spectra. This occasional fault occurred when a spectrum was being run at slow scan. The recording pen would suddenly give two or more abrupt jerks introducing spikes into a supposedly smooth lorentzian curve.

Another problem associated with the spectrometer was the variable frequency selector that was used to obtain internal lock. Instead of producing a single locking signal of 4 kHz the selector also gave a broad band of leaked radiofrequency radiation at a lower level. This was suitable for samples containing high concentrations of protons, but with dilute solutions any moderate to high power through the lock channel completely saturated any recordable spectral signal. This meant that all spectra had to be recorded with a very low power lock signal to avoid saturation.

Resolution

As a non-uniform magnetic field gives rise to broad-line NMR spectra, an important factor was to obtain high resolution spectra for the determination

of coupling constants and chemical shifts. The spectrometer was equipped with four shim controls which controlled the uniformity of the local magnetic fields in the detector. With careful adjustment and patience these shim controls could be adjusted to give the optimum lock signal. In this investigation the lock signal was observed as a straight line on a oscilloscope. Maximum resolution was always found when this line was at its maximum for the lowest possible power output from the variable frequency lock channel. However, it was not possible to leave the lock signal shim controls at one setting as the signal deteriorated within ten minutes or less. In running spectra, continual attention had to be paid to keeping the lock signal "peaked up" by use of these shim controls.

Spinning The Sample Tube

One factor that affects resolution and the appearance of spectra is the spinning of the sample tube. A non-spinning tube will always result in broad-line spectra.

The sample tube inserted into the teflon turbine must be perfectly balanced to spin in the probe. As most sample tubes are not perfectly balanced they have to be readjusted in the turbine to ensure satisfactory spinning. Vigorous spinning can give rise to side-bands in the spectra but this effect was not observed at any time.

Before the sample tube was placed in the probe, it was cleaned thoroughly with tissue moistened in

ligroin, and dried. The detector head was also cleaned with ligroin.

With six or seven hour continuous usage it was found that the spinner had to be cleaned thoroughly for maximum performance. The spinner rotated on a bearing made of Teflon from which a thin film of resin could adhere to the bottom of the sample tube. This was compounded by dust settling on the bearing. When this occurred, the rotating spinner often slowed down or completely halted. This problem was reduced by lightly smearing the bottom of the sample tube with silicon grease thus reducing the friction.

Dust building up in the air supply to the spinner also caused great problems. On occasions the detector head and probe had to be completely removed and cleaned to eliminate the accumulation of dust particles and grease. An accidental use of dirty tubing for the air supply created havoc with the spinning of the sample. Fine pieces of rubber tubing passing through the air jets of the spinner gave problems over a three month period. On some days it was found impossible to obtain a minimum of one hour's operation. Continual operation of the spectrometer for very long periods also caused this contamination build-up. This would never have occurred in the routine use of the spectrometer.

The spinning of a sample tube utilized air from an air compressor. However at temperatures below 283 K, water vapour from the air would have condensed as ice round the detector head. To eliminate this
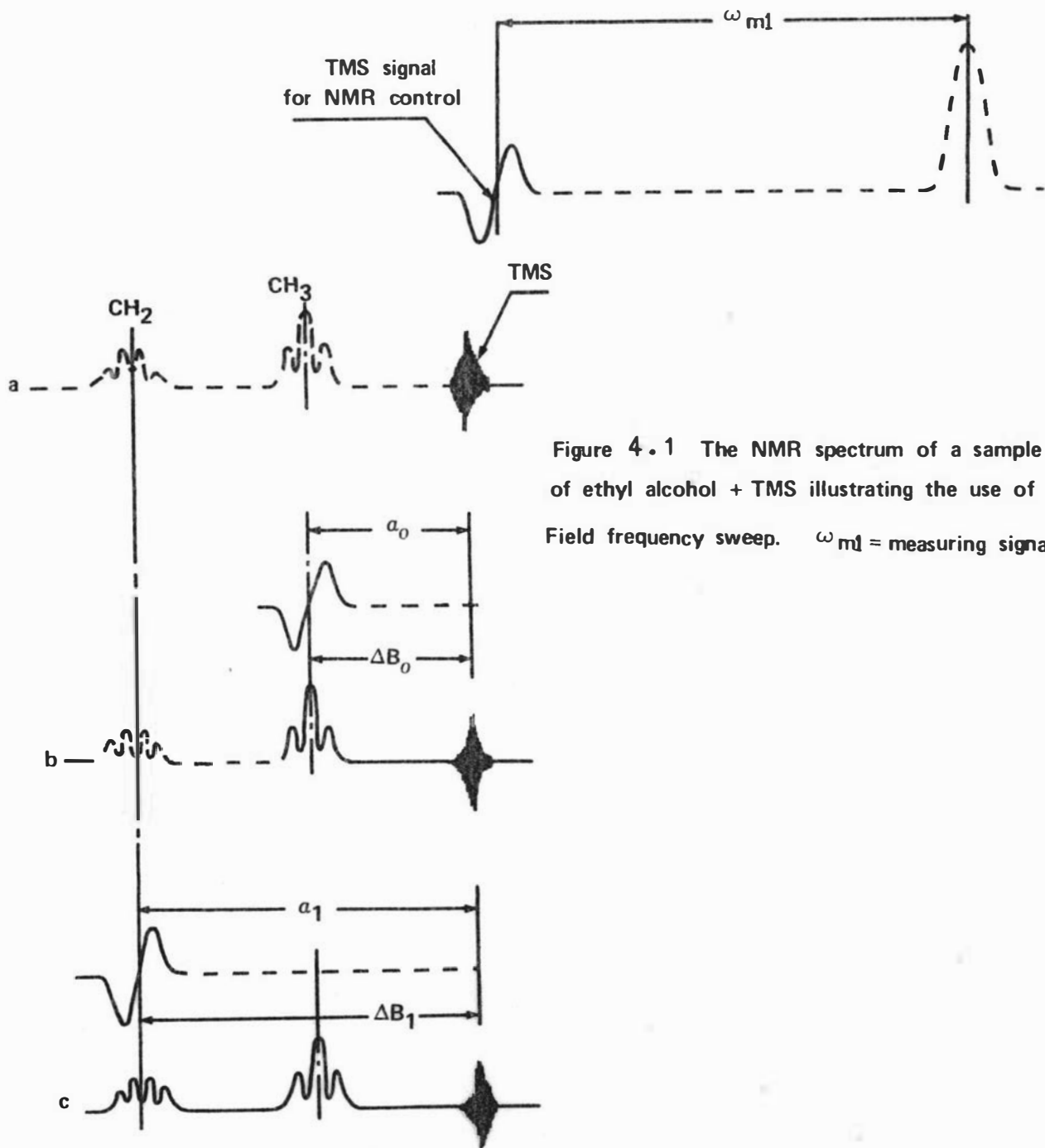
Figure 4.1 The NMR spectrum of a sample of ethyl alcohol + TMS illustrating the use of Field frequency sweep. ω_{ml} = measuring signal.

undesirable problem a dry-ice ethanol trap was
installed to condense any water-vapour.   On a
damp day up to 60 cm^3 of water was obtained from
five hours operation.   An effect of the trap was
the freezing out of carbon dioxide in the air.
This meant the trap gradually filled up with ice
and solid carbon dioxide over a period of five or
six hours.   The result of this was that the air
supply to the spinner was blocked which caused
spinning to cease.

4.1.6 Measuring Procedures

There are two methods of NMR lock :

(i) The external lock system

(ii) The internal lock system

All spectra in this study were obtained using
the internal lock system under field/frequency
sweep.

Field/frequency Sweep

The use of field/frequency sweep can be
illustrated from Fig. 4.1.   Initially, the measuring
and control signals are super-imposed.   That is
$\omega_{m1} = \omega_{m2}$.   The measuring signal takes the form of a
beat pattern as shown in Figure 4.1(a).

If $\omega_{m2} = \omega_{m1} + \alpha_0$, the magnetic field is shifted
to match it to the resonance condition of the TMS
control signal.   Only the magnetic field applied to
the measuring signals is charged by ΔB_0 and the CH_3
signal is observed as in Figure 4.1(b).

When $\omega_{m2} = \omega_{m1} + \alpha_1$ as in Figure 4.1 (c) the
magnetic field is shifted by ΔB_1 and the CH_2 signal
is measured.
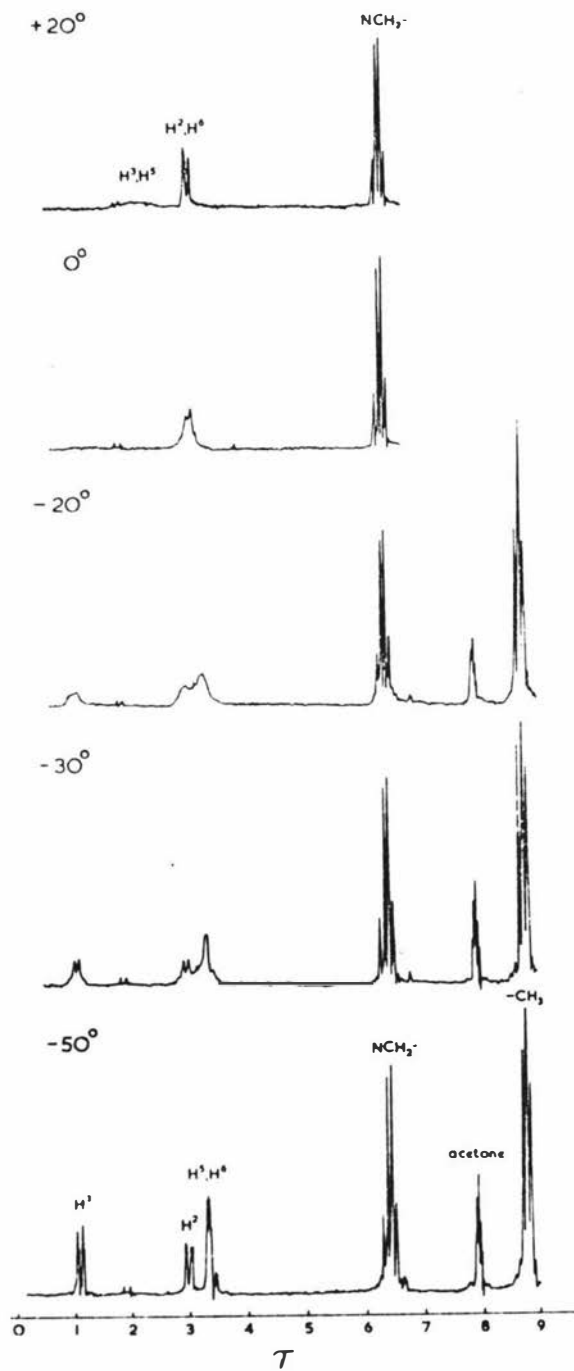
Fig. 4.2   NMR spectrum of N,N-diethyl-p-nitrosoaniline
as a 5% w/v solution in acetone-d$_6$, taken at various
temperatures at 100 MHz.

4.1.7 Temperature effects on the NMR spectra of the N,N-dialkyl-p-nitrosoanilines.

Having examined the experimental conditions under which the samples were studied, this section looks at the overall changes that occur in the nitrosoanilines. Figure (4.2) from Calder and Garratt's paper[49] demonstrates the effects of temperature on N,N-diethyl-p-nitrosoaniline in acetone. This pattern of change was similar for both nitrosoanilines in acetone-d_6 and chloroform-d_1.

The ring protons of the nitrosoanilines in the slow exchange region, exhibit an ABKX pattern in acetone-d_6 and chloroform-d_1. Examples of these spectra can be seen in Figures 4.3 and 4.4. The H3 resonance occurs between 530 and 540 Hz from TMS while the H2, H5, and H6 resonances occur between 380 and 430 Hz. As the temperature is increased spin splitting is eliminated. The H2, H5 and H6 protons then coalesce into a broad band which sharpens as the temperature increases. The coalescence of the H3 and H5 protons is characterized by a very broad band. This coalescence occurs at a higher temperature than the coalescence for the H2 and H6 protons.

In toluene-d_8 an ABMX pattern is exhibited in the slow exchange region (see Figure 4.4).

Both nitrosoanilines in the fast exchange region for all three solvents, show typical AA'XX' patterns. Internal rotation of the NR_2 group has no effect on either chemical shifts or coupling constants and leaves no mark on the spectra.

B

t= -56°C

541   531   521   430   420   410   400   390

Hz from TMS
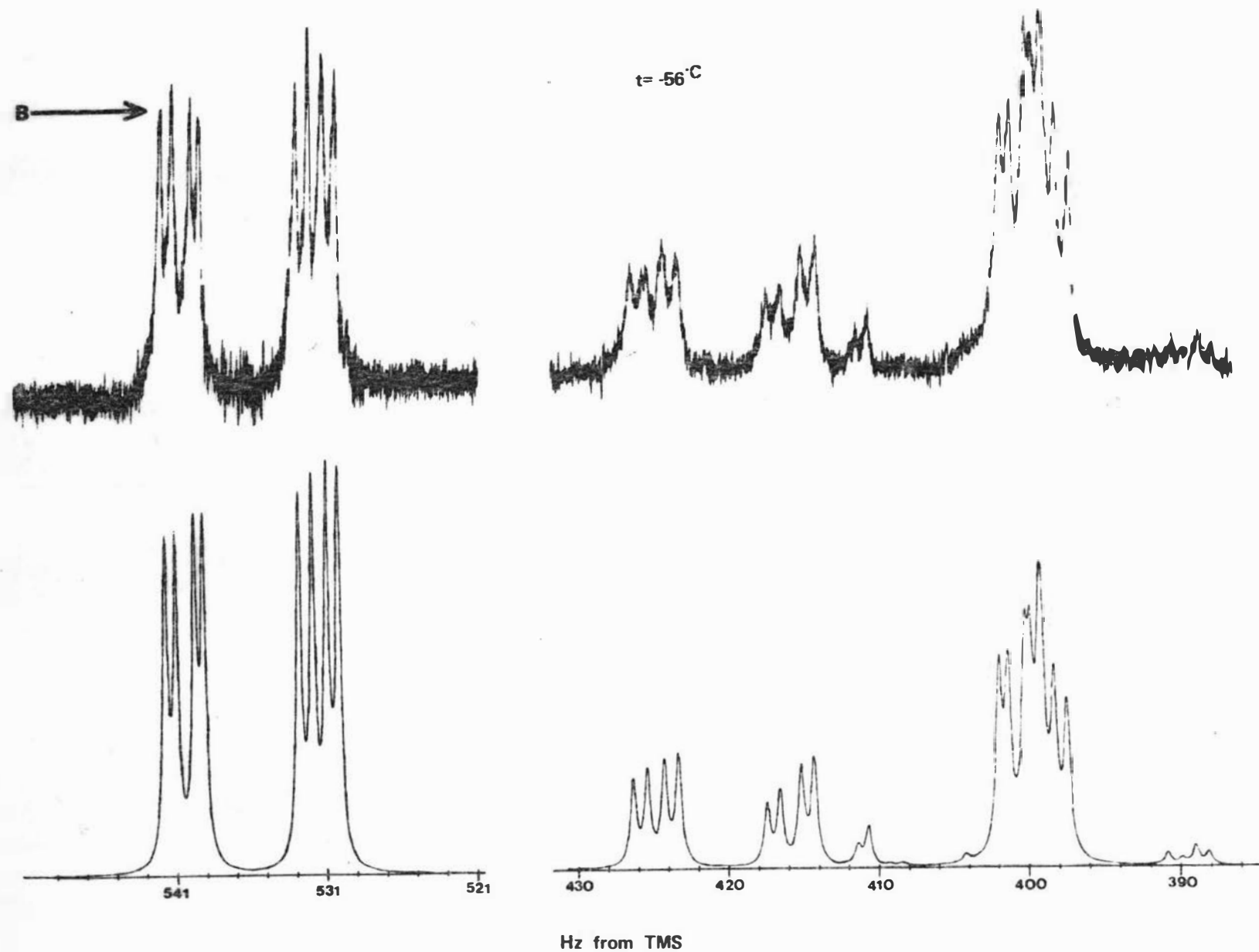
Figure 4.3 The spectrum of N,N-dimethyl-p-nitrosoaniline in the slow exchange region. The theoretical spectrum shown is that calculated from LAOCON 3. The solvent is acetone-d₆.

4.1.8 <u>Temperature Measurements</u>.

In studying temperature effects on spectra, an obvious need is for accurate temperature measurement.

The JES-VT-3 temperature controller was used to vary and maintain temperatures at high or low temperatures. The required temperature was obtained by passing either pressure regulated hot air or cold nitrogen gas in the vicinity of the sample.

For temperatures over 303 K air from an air compressor at a preset pressure was passed through a heat blasting pipe. In the temperature range 273 K to 303 K, nitrogen gas driven off from a liquid air dewar was heated to the required temperature by passing through the heat blasting pipe. Any change in temperature was detected by a thermocouple placed in the air flow and stabilized by a feed-back system to the heater.

To obtain low temperatures (below 273 K) cold nitrogen gas from the liquid air dewar was passed round the sample site.

The stability of the temperature controller claimed in the manufacturers specifications at the sample site is ±0.5 K. Measurements were always found to be well within this limit.

To obtain accurate temperature measurements, use was made of a methanol NMR thermometer. This consisted of a sealed capillary tube of "super-dry"[56] methanol, which was centred in an NMR tube containing the same solvent as the sample being studied. The solvent contained 1% tetramethylsilane.
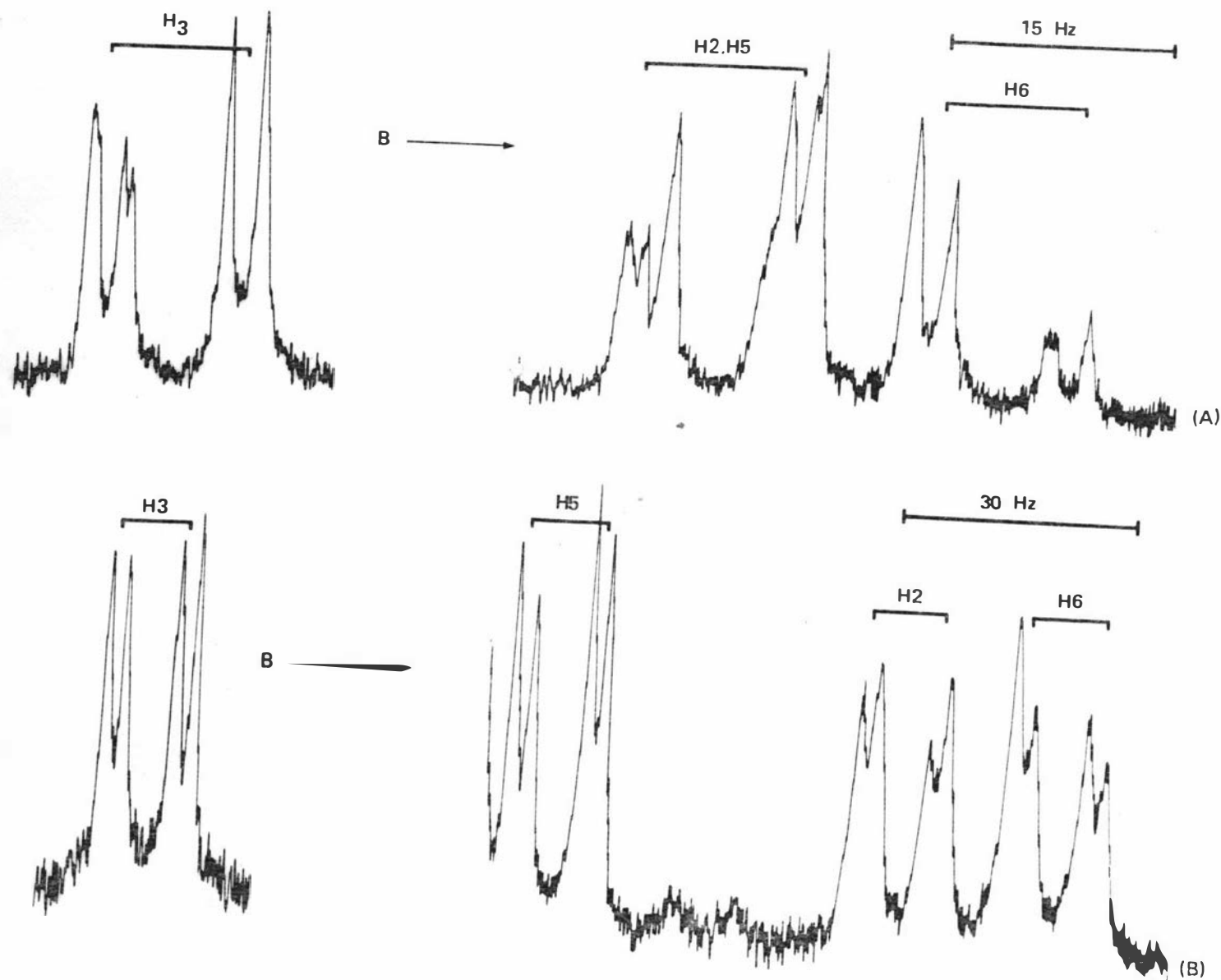
Figure 4.4   The slow exchange spectra of N,N-diethyl-p-nitrosoaniline in
chloroform-d$_1$(A), and toluene-d$_8$(B).

The spectrometer was locked to the TMS signal with the recorder centred on the CH_3 and OH resonances in turn. The chemical shifts were read from the frequency counter. Using the difference in chemical shifts converted into ppm, the temperature was obtained from a JEOL calibration chart.

All measurements made in the study of the N,N-dialkyl-p-nitrosoanilines used the JEOL calibration chart. Temperatures at any particular setting of the temperature controller were completely reproducible. Measurements were made to within 0.5 K.

Temperatures over 273 K, measured by a calibrated thermometer, showed no detectable difference compared with the JEOL chart measurements.

Errors in temperature measurement arise from the frequency measurements ($\pm$ 0.1 Hz), pen recorder position on the resonance peak ($\pm$ 0.1 Hz), and temperature gradients in the NMR tube. At the lowest temperature used in this investigation, gradients of at least 0.5 K cm^{-1} were measured. As the thermocouple was in a spinning NMR tube this result represented the lower limit of error. A realistic estimated error in temperature readings was 1 K.

4.1.9 Frequency Measurements.

Frequency measurements were made using a Marconi TF 2414 counter timer. At any particular pen position the stability of the frequency was $\pm$ 0.1 Hz.

For the N,N-dialkyl-p-nitrosoanilines, the chemical shift positions were measured in Hz from tetramethylsilane.

For the slow exchange spectra of all the systems studied, frequency measurements were made by placing vertical frequency markers at intervals across the spectrum. Thus peak positions were measured by interpolation between the frequency markers. This process was repeated for the intermediate and fast exchange regions.

4.1.10 Analyses of the Slow Exchange Spectra.

To generate theoretical spectra the density-matrix program requires the chemical shifts of the H2, H3, H5 and H6 nuclei with their associated coupling constants and the spin-spin relaxation time T_2. This information was obtained from the slow exchange spectrum. Kessler[14] has an interesting comment in regard to "slow" exchange. "Slow" can be regarded as a statistical-kinetic description. A slow rotation is one in which only a small fraction of the molecules can overcome the energy barrier in unit time. The actual rotation of the individual molecule, however, is very fast owing to the small moment of inertia.

The slow exchange region for the aromatic protons occurs about 223 K. For the nitrosoanilines, the lowest temperature needed to observe the slow exchange spectrum occurred in acetone-d_6. This was for N,N-dimethyl-p-nitrosoaniline. As can be imagined the solubility of compounds at these temperatures was very limited, in the case of the compound mentioned $2\frac{1}{2}$% w/v.

The quality of the experimental spectrum obtained at this temperature is shown in Figure 4.3. Spectra

obtained for the nitrosoanilines in acetone-d_6 exhibited fine structure that was not present in spectra recorded in chloroform and toluene.

To analyse a spectrum such as shown in Figure 4.3, the peak positions were measured by interpolation between frequency markers placed at intervals across the spectrum.

The sweep-width of the spectrometer was set at 27 Hz and the recording speed of the pen was 0.02 Hz s^{-1}. The slow exchange spectrum as shown in Figure 4.3 was measured at least three times to ensure the reliability of the assigned experimental frequencies.

To obtain useful experimental spectra at this temperature involved a considerable amount of skill, time, and patience.

The slow exchange spectra were analysed using the LAOCON3 program of Bothner-By and Castellano.[58] The best value parameters and a brief description of the capabilities of LAOCON3 are given in Appendix II.

To obtain data for LAOCON3, the assigning of chemical shifts and coupling constants was done by assuming first-order interactions in parts of the spectrum. In all cases the H3 proton was easily assigned to the low-field group of peaks. Both nitrosoanilines show only a very small variation (less than 7 Hz) for the chemical shift of this proton. For the nitrosoanilines in acetone-d_6 the shifts of the H5 and H6 nuclei were assigned unambiguously in each case, since only with H5 to high fields of H6 was a good fit obtained.

Table 4.2

Chemical shifts and coupling constants for the ring protons of (1) and (2)

in the slow exchange region

Compound	Solvent	Chemical Shifts (Hz from Si Me$_4$)				Coupling Constants (Hz)					
		H2	H3	H5	H6	J_{23}	J_{25}	J_{26}	J_{35}	J_{36}	J_{56}
(1)	$(CD_3)_2CO$	420.4	535.8	397.1	402.7	9.0	0.2	2.8	2.5	0.0	9.5
(1)	$CDCl_3$	409.3	534.4	407.1	391.6	8.9	0	2.6	2.4	0	9.6
(2)	$(CD_3)_2CO$	424.0	533.6	399.6	406.3	9.1	0.1	2.9	2.5	0.0	9.4
(2)	$CDCl_3$	409.7	531.8	410.5	392.3	9.0	0	2.5	2.4	0	9.5
(2)	$C_6D_5CD_3$	360.4	537.5	404.3	340.4	9.0	0	2.7	2.4	0	9.5

Compound (1) = N,N-dimethyl-p-nitrosoaniline

Compound (2) = N,N-diethyl-p-nitrosoaniline

Obtaining a trial spectrum was not just a case of running an experimental spectrum, measuring the peak positions and then assigning the chemical shift positions through LAOCON3. Good estimates of the chemical shifts had to be made first and the protons assigned correctly.

In chloroform-d$_1$ a considerable amount of difficulty was experienced in assigning the chemical shift positions. The experimental spectrum in this solvent kept changing until about -52°C. (This was assumed to be the slow exchange limit). In comparing the experimental spectrum obtained at this temperature with the trial LAOCON spectra there was found to be no correlation between peaks and intensities in the 380-430 Hz region.

At first the order of chemical shifts was assigned the same as in acetone. This proved to be of no use because the trial LAOCON3 spectra bore no resemblance to the experimental spectrum. The H3 chemical shift was assumed to be correct and was kept constant while the H2, H5 and H6 chemical shifts were interchanged to see what effects these would have on the theoretical LAOCON spectra.

As can be seen from Table 4.2 the shifts for the H2, H3, H5 and H6 nuclei were found to be 409, 534, 407 and 392 Hz respectively. When LAOCON3 did not seem to be giving the correct solution i.e. a spectrum that matched the experimental, the experimental spectrum for N,N-dimethyl-p-nitrosoaniline was repeated, to check the peak position measurements.

The re-run experimental spectrum obtained was the same as had been obtained previously.

As the nitrosoaniline spectrum in chloroform contained less fine detail than the spectrum in acetone this lack of detail was thought to be a source of error. Different values were assigned to the coupling constants to see how much effect they had on the trial LAOCON spectra. The trial spectra thus generated had different peak height and peak positions and were still different from the experimental spectrum. After a number of weeks all that had been obtained was a series of different trial LAOCON spectra which did not correlate with the experimental spectrum although two or three approximated to it. At this stage, it was felt better to continue the line-shape study with the approximate values that had been obtained.

Spectral changes were observed at 10 K intervals to see how rapidly the effects due to exchange took place. The experimental spectrum run at 233 K was seen to have a marked similarity to one of the many trial spectra generated by the computer. The experimental spectrum was re-run, peak positions measured and in the iterative calculation by LAOCON3 a best fit was obtained after three iterations.

In comparison with acetone the H5 and H6 positions had interchanged in chloroform solution (see Table 4.2). Though the assigning of the chemical shift positions had taken a long time, considerable confidence could be placed in them as they were assigned by two methods.

Firstly, by the predictive use of LAOCON3 and secondly by the spectral changes in that region which could be assigned to solvent viscosity effects. The latter appeared to be playing a significant role at temperatures below -40°C.

The assignment of the chemical shifts in toluene proceeded very smoothly in contrast to the problems experienced with assigning the shifts in chloroform. A feature of the spectrum in toluene (see Figure 4.4(b)), is the relatively large chemical difference for the two ortho protons. This difference, which can be seen more clearly in Table 4.2, has been attributed to the solvent effect of the toluene[59] and results in four clearly defined chemical shifts.

The spin-spin relaxation time, T_2, was obtained by measuring the line-width at half-height of the low-field peaks (H3) in the slow exchange region. This T_2 value was used in the LAOCON3 trial plots and was also used in the density matrix program.

4.1.11 The Exchange Rate (τ)

In using the density matrix method the standard technique is to generate experimental spectra over the temperature range to be studied. A theoretical spectrum that matches a particular experimental spectrum is generated from the density matrix program by changing the exchange rate τ, until matching occurs. This method involves the minimum use of spectrometer time and the maximum use of computer time. Even with a high speed computer the computation time can occupy a considerable period of time.

The computers that were used in this investigation were an IBM 1130 with a Calcomp plotter type 565 and a Burroughs 6700 computer with no plotting or card-punching facilities. The IBM 1130 was used in the initial months of this work because of the delayed arrival (nine months) of the Burroughs 6700 at Massey University.

Calculation time for a single point on the theoretical spectrum took four minutes for the IBM 1130 and eight seconds for the B6700. With the limitation of core storage in the IBM 1130, the matrix inversion was done in four steps. Two 8x8 matrices, and two 48x48 matrices. Thus at each frequency, the calculated intensity was obtained by the addition of the four six figure numbers generated by the program.

This very slow computation rate, especially on the IBM 1130, meant a new method had to be used. This method was the reverse of the standard technique. The method involved calculating the theoretical spectra first (knowing the exchange rate), then finding the temperatures at which theoretical spectra matched the experimental spectra.

To know which τ values to feed into the program, a trial temperature study had to be done on each compound. The regions which gave broad featureless bands were chosen as this reduced computation time. The upper and lower limits of their frequency range were noted. This upper and lower limit was needed as input for the density matrix program. The four-spin systems have two coalescence points, and, by using the
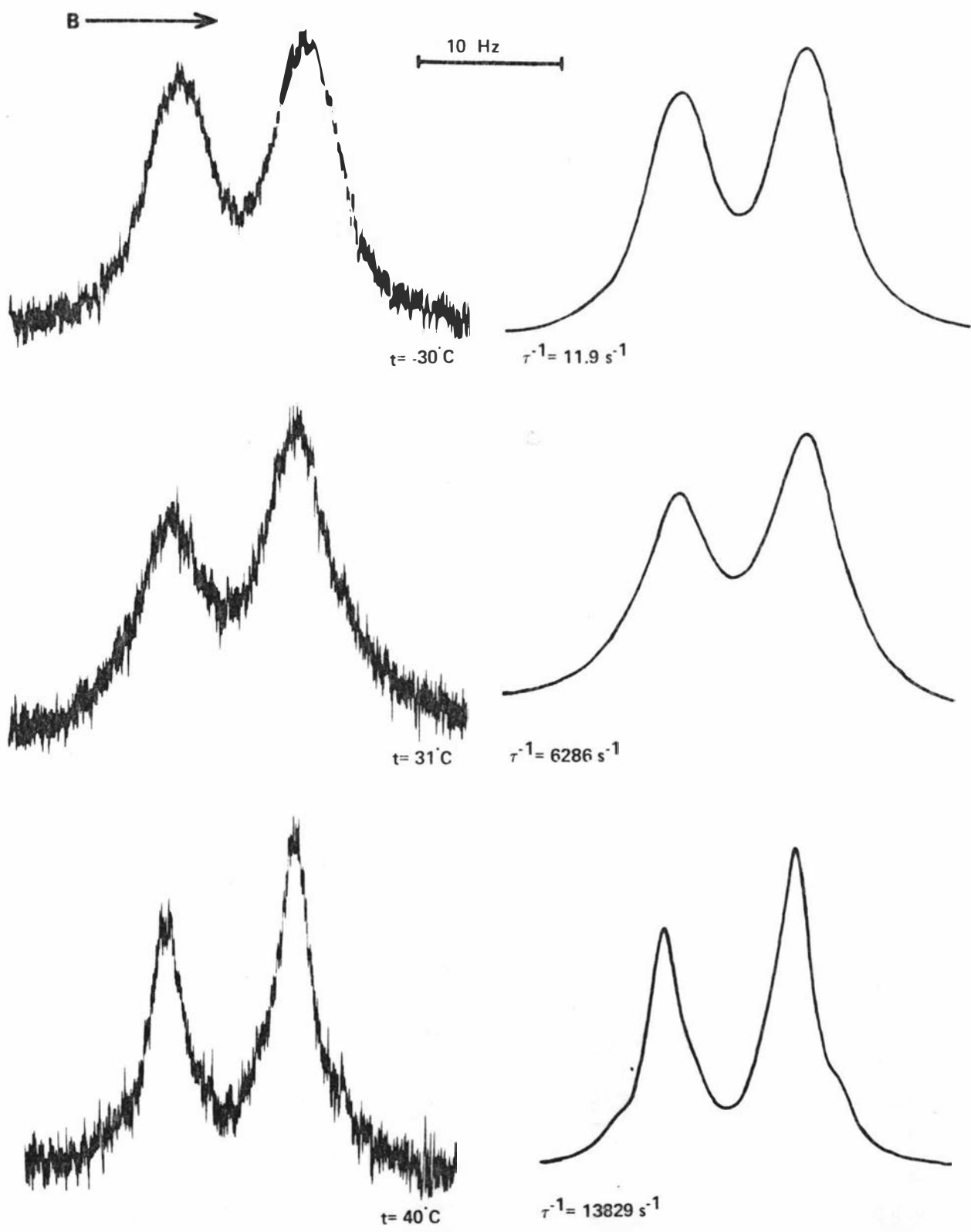
Figure 4.5 Examples of experimental and theoretical spectra for the H_3H_5 nuclei of N,N-dimethyl-p-nitrosoaniline in acetone-d_6.

Gutowsky-Holm equation for the rate at the coalescence temperature, two approximate values of   were obtained at two temperatures.   A plot of $\log \tau^{-1}$ versus T^{-1} gives approximate values of τ for the whole temperature range.   With the information from the trial temperature study, a suitable range of spectra was obtained for the line-shape study.

As mentioned previously, selecting broad featureless bands reduced computation time.   Fifty to sixty points were needed to generate a theoretical spectrum, giving a total computation time of about 200 minutes for the IBM 1130.   It took that time again to add the intensities, punch cards bearing the frequencies and intensities, and plot the theoretical spectra with appropriate scaling.   The arrival of the B6700 removed the factors of computation time and hand addition of the intensities, and left only punching cards and plotting.   The total computation time for N,N-dimethyl-p-nitrosoaniline in acetone was over 30 hours using the IBM 1130.

This type of approach has been termed "unorthodox",[60] but as this thesis shows, it proves useful when one is limited by computing facilities.

4.1.12   Experimental Matching of the Density Matrix
Spectra.

To generate an Arrhenius plot, the corresponding temperature was required for each τ value, and to find the value of this temperature, the experimental spectrum was matched exactly with the theoretical one.

If the experimental spectra obtained matched the
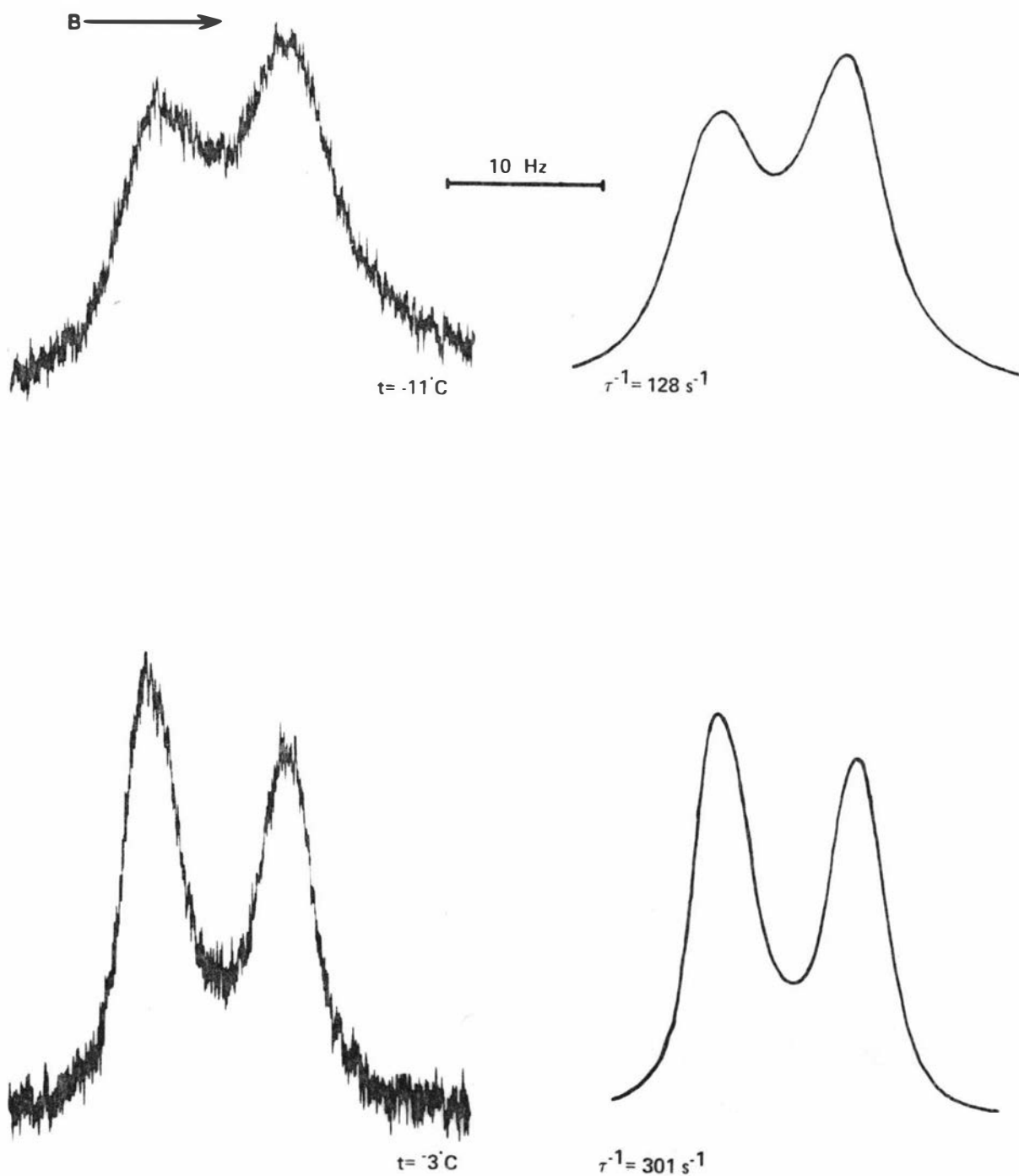
Figure 4.6 Examples of experimental and theoretical spectra for the H_2,H_6 nuclei of N,N-dimethyl-p-nitrosoaniline in acetone-d_6.

theoretical spectra generated by the density matrix
program, and the temperatures which gave good fits
to the computed spectra resulted in a straight line
Arrhenius plot, then the criteria for the success of
the method had been met.

The first compound that this method was used with
was N,N-dimethyl-p-nitrosoaniline in acetone-d_6.
The lengthy computation times on the computer have
already been mentioned but this tended to limit the
amount of base-line used for the theoretical spectra.
The first attempts at matching experimental and
theoretical spectra resulted in a non-linear Arrhenius
plot. At first, it was thought that the program was
wrong or the data from the slow exchange region supplied
was not valid over a larger temperature range. However,
it was decided to increase the base lines of the
theoretical spectra even though this involved an extra
hour of computer time for each spectrum. On repeating
the matching process, a good linear Arrhenius plot was
obtained.

The matching process for the spectra was carried
out by directly overlaying the theoretical spectrum
onto the experimental spectrum.

The paper on which the theoretical spectrum had
been plotted was transparent enough to facilitate a
direct comparison. The experimental spectrum's peak
heights were increased by using the field frequency
modulation and amplitude controls. Basically the
whole process was a combination of peak height
adjustment and temperature adjustment until matching
occurred.

Table 4.3

Rotational rates as a function of temperature
for Compound (1) and Compound (2) in acetone-d_6

Compound (1)[a]

T (K)	τ^{-1} (rad s^{-1})	10^{-3} T^{-1} (K^{-1})	$\log_{10}\tau^{-1}$
242.0	11.9	4.132	1.0755
252.0	39.6	3.968	1.5977
262.0	128.2	3.817	2.1079
270.0	301.0	3.704	2.4786
285.5	1256.6	3.503	3.0993
304.0	6283.2	3.289	3.7982
314.0	13823.0	3.185	4.1405

Compound (2)[b]

T (K)	τ^{-1} (rad s^{-1})	10^{-3} T^{-1} (K^{-1})	$\log_{10}\tau^{-1}$
250.0	12.6	4.000	1.1004
257.0	31.4	3.891	1.4969
270.0	128.2	3.704	2.1079
280.0	314.2	3.571	2.4972
294.0	1256.6	3.401	3.0993
314.0	6283.2	3.185	3.7982

[a]Compound (1) = N,N-dimethyl-p-nitrosoaniline

[b]Compound (2) = N,N-diethyl-p-nitrosoaniline

Using a scan speed of 0.18 Hz s^{-1}, experimental spectra were generated in conjunction with small adjustments to the temperature. This process of temperature change, spectral scan, and then overlay comparison of theoretical and experimental spectra was done until matching occurred. The scan speed was adjusted to .09 Hz s^{-1} and the experimental spectrum rerun. This was done twice to check that the temperature had completely stabilized.

The sample tube was then replaced by an NMR thermometer and the temperature was measured as described earlier. The NMR thermometer spent at least twenty minutes in the probe to ensure temperature equilibration and on removal was replaced by the sample tube. The experimental spectrum was then rerun as a final check for temperature drift and resolution loss.

The resolution was continuously "peaked up" for maximum resolution. A full readjustment of the resolution was made every hour to ensure optimum conditions. With the changing temperature the phasing of the experimental spectrum had to be continuously readjusted.

Figure 4.5 shows the theoretical and experimental spectra for the H3, H5 nuclei of N,N-dimethyl-p-nitrosoaniline. The method was sensitive enough that a change in temperature of 1 K produced a considerable deterioration in fit, with the valley height between the peaks of the spectra increasing or decreasing. This was combined with broadening effects on the spectra.

Table 4.4

Rotational rates as a function of temperature for
Compound (1) and Compound (2) in chloroform-d_1

Compound (1)[a]

T (K)	τ^{-1} (rads s^{-1})	10^{-3} T^{-1} (K^{-1})	$\log_{10}\tau^{-1}$
247.0	12.6	4.049	1.1004
252.5	25.1	3.960	1.3997
254.0	37.7	3.937	1.5763
267.0	125.7	3.745	2.0993
272.0	219.9	3.676	2.3422
275.5	314.2	3.630	2.4972
284.0	754.0	3.521	2.8774
289.5	1256.6	3.454	3.0993
305.5	5026.5	3.273	3.7013
309.0	6283.2	3.236	3.7982
314.5	9425.0	3.180	3.9743
318.0	12566.0	3.145	4.0993

Compound (2)[b]

T (K)	τ^{-1} (rads s^{-1})	10^{-3} T^{-1} (K^{-1})	$\log_{10}\tau^{-1}$
254.5	12.6	3.929	1.1004
260.5	25.1	3.839	1.3997
276.0	125.7	3.623	2.0993
282.0	219.9	3.546	2.3422
285.5	314.2	3.503	2.4972
297.5	942.5	3.361	2.9743
315.5	4398.0	3.170	3.6433
320.0	6283.0	3.125	3.7982
325.5	9425.0	3.072	3.9743

The spectrum at $-30^{\circ}C$ (Figure 4.5) involved 4 hours of computing time plus 3 hours adding and plotting the intensities. To find the experimental spectrum took one entire week in the first stages of this project. Figures (4.5), (4.6) and Table 4.3 represent the results of seven weeks' work. But the confidence and experience gained in the method from this study helped reduce the analysis of other systems. However, an analysis of a four-spin system using this technique does mean at least a minimum of one month's work.

Table 4.3 shows the two nitrosoanilines that were studied using the IBM 1130. Only thirteen data points are recorded here but they represent approximately thirteen weeks' work. The method was given a boost by the arrival of the B6700. Table 4.4 for compound (1) shows 12 data points. These were generated over a period of only 10 days using the B6700. Although lack of punching facilities meant that nearly 3000 computer cards had to be punched for plotting the theoretical spectra.

Tables 4.3-4.5 show that for the temperature range studied, (70 K), the rate varies by a factor of a thousand. As can be seen by the spectra presented in this chapter, only broad line spectra were studied. There were two reasons why this type of spectra was studied. The first and most important reason was that it saved computation time. The second reason was to ensure that spectral regions were chosen that were not influenced by T_2 because the method that was being used, necessitated the use of the slow exchange

Table 4.5

Rotational rates as a function of temperature for

Compound (2) in toluene-d$_8$

Compound (2)[b]

T (K)	τ^{-1} (rad s^{-1})	$10^{-3}T^{-1}$ (K^{-1})	$\log_{10}\tau^{-1}$
244.0	12.6	4.098	1.1004
249.5	25.1	4.008	1.3997
262.5	125.7	3.810	2.0993
269.5	314.2	3.711	2.4972
278.0	628.3	3.597	2.7982
297.5	4398.0	3.361	3.6433
301.5	6283.0	3.317	3.7982
305.5	9425.0	3.273	3.9743
310.5	12566.0	3.221	4.0993

parameters over the whole temperature range.

Looking at Table 4.5 it can be seen that the temperature measurements are measured to only even and half degree values with no in-between values. The JEOL calibration chart for temperature measurement only enabled measurement to within 0.5 K. A guess estimate could have been to say 0.2 K or 0.8 K, but with a probable real error of 1 K these figures were rounded off. The graphical method was not useful in giving an absolute idea of temperature in the probe but as commented earlier in the Chapter, actual temperature gradients are of the order of 0.5 K cm^{-1}.

It was found that a 0.5 K variation of temperature as recorded by the JEOL calibration chart produced a very real and significant change in the line-shape. The sensitivity of the method was to within 0.5 K especially in the areas of slow and intermediate exchange. To ensure confidence in the temperature measurements, spectral measurements were repeated at least two or three times several days apart.

In the initial stages of this project the first spectra, represented by Figures (4.5) and (4.6) were repeated on at least five separate occasions. This meant some spectra had at least fifteen hours NMR spectrometer time. Running a spectrum at a particular temperature to check the line-shape took 10 minutes. It was found to be a waste of time running the same spectrum at a faster speed.

B ⟶

10Hz

τ^{-1} 9425s^{-1} 305.5 K

τ^{-1} 25.1s^{-1} 249.5 K
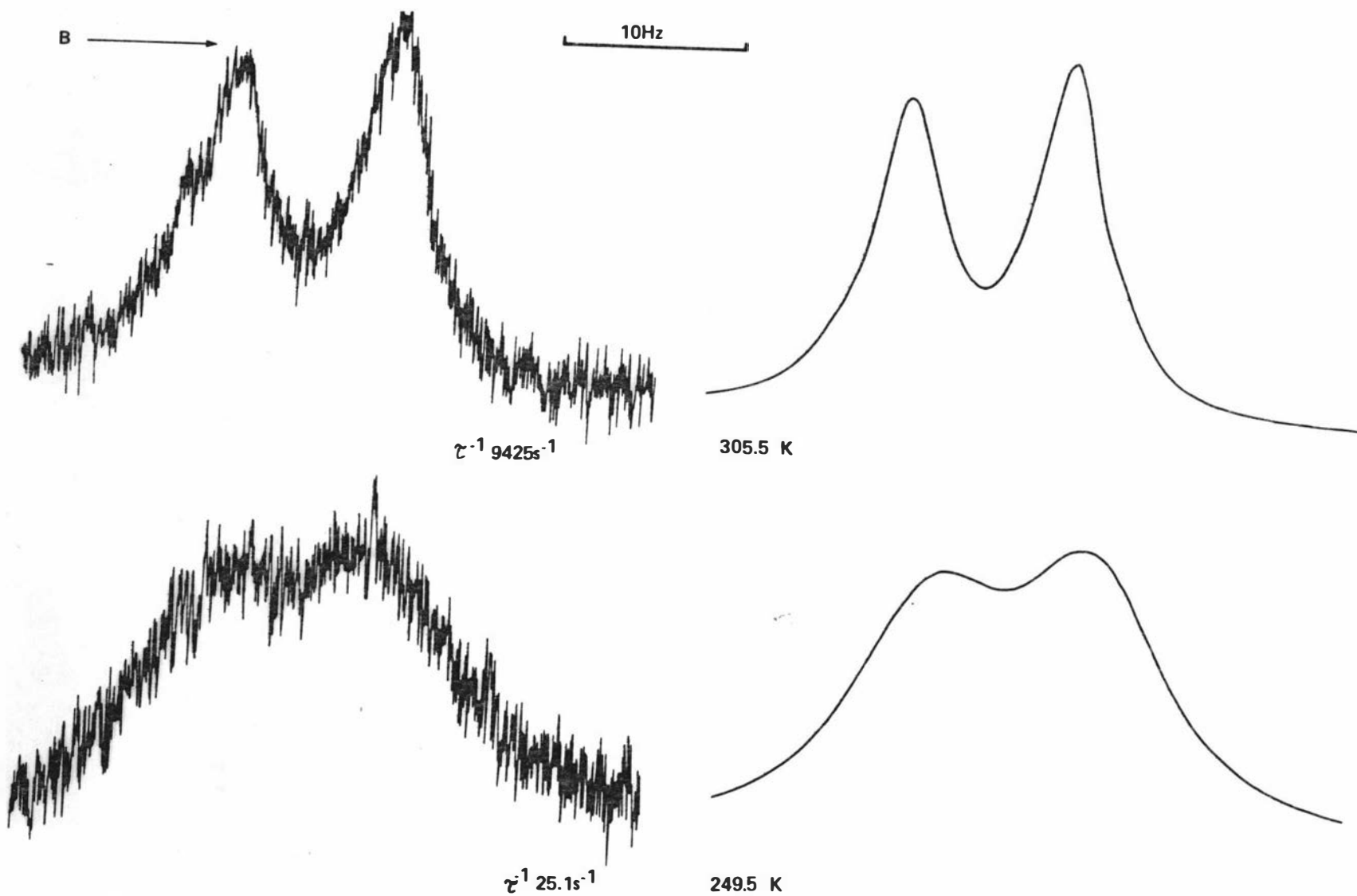
Figure 4.7 Examples of experimental and theoretical spectra for the H3,H5 nuclei of N,N-diethyl-p-nitrosoaniline in toluene-d$_8$.

The noise filter had to be reduced and this made the noise level so large a comparison of peaks and valleys of the experimental and theoretical spectra proved meaningless.

Spectra were simulated using the same rotational rates for most spectra. This was found to facilitate an easier comparison of temperature values, as can be seen in Table 4.4 where direct comparison of compounds (1) and (2) at an exchange rate of 314.2 rads s^{-1} shows a 10 K difference. This does not however tell us anything about the barrier to rotation.

4.1.13 <u>The Barrier to rotation.</u>

Arrhenius plots of log τ^{-1} versus T^{-1} for the nitrosoanilines can be seen in Figures 4.9 and 4.10.

Visually the slopes of all five plots are very similar. A more exact comparison can be made by looking at the activation energies of these systems. Table 4.6 shows a difference of only 1.7 kJ mol^{-1} for N,N-dimethyl-p-nitrosoanilines in acetone (61.9 kJ mol^{-1}) and chloroform (63.6 kJ mol^{-1}). For N,N-diethyl-p-nitrosoaniline the range of values for E_a is only 3 kJ mol^{-1}.

Comparing compounds (1) and (2) in the same solvent, the difference is found to be about 1 kJ mol^{-1} for both acetone and chloroform. Again it is unfortunate that data could not be obtained on compound (1) in toluene due to solubility problems at low temperatures.
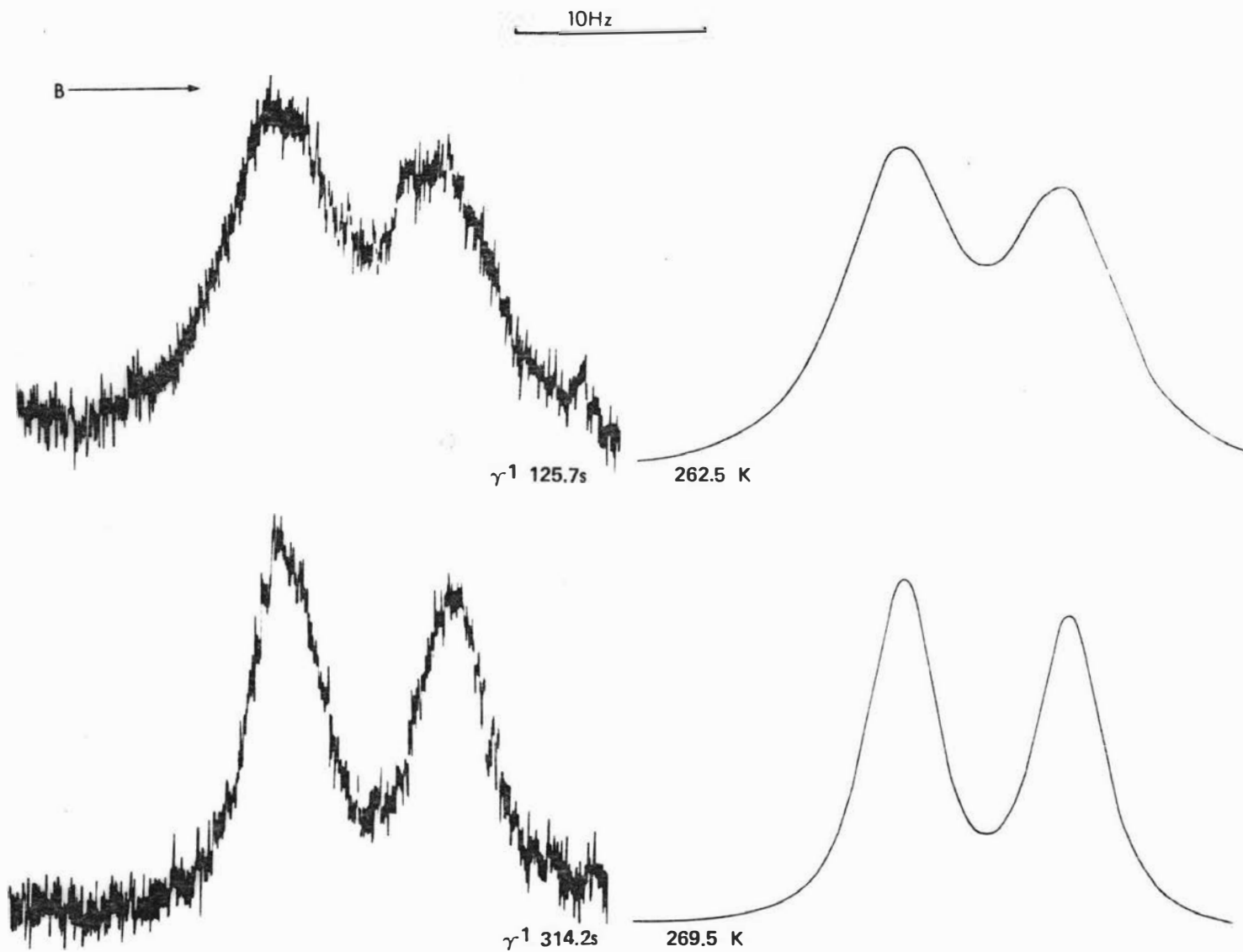
Figure 4.8 Examples of experimental and theoretical spectra for the H2,H6 nuclei of N,N-diethyl-p-nitrosoaniline in toluene-d$_8$.

Though the slopes of each system are similar, the intercepts of each graph are certainly not. This can be seen from the values of $\Delta S^{\ddagger}$ shown in Table 4.6.

The frequency factor A or the intercept is related to the actual rotation of the individual molecule. The rotation of an individual molecule is very fast owing to the small amount of inertia. In the author's opinion, A perhaps reflects slight changes to the inertia of the molecule either by changing the p-substituent or the environment (that is the solvent).

One of the obvious questions that needs to be answered is: How do these values for the barrier to rotation compare with previous studies?

Four different methods have been used by previous investigators. These will each be examined briefly. The only compound that has been studied by all groups is N,N-dimethyl-p-nitrosoaniline.

The first reported study of internal rotation in N,N-dimethyl-p-nitrosoaniline was in 1964.[50] Using the method of Piette and Anderson,[27] rate constants were obtained in the regions of slight exchange broadening and motional narrowing. Rate constants were not obtained at intermediate temperatures by these investigators through difficulties of analysis.

The activation parameters derived are shown below.

Figure 4.9 Arrhenius plots for rotation about the Ar-NO bond of N,N-dimethyl-p-nitrosoaniline in chloroform-d_1 and acetone-d_6 (dotted line).

$\log \tau^{-1}$

$10^{-3}T^{-1}(K^{-1})$
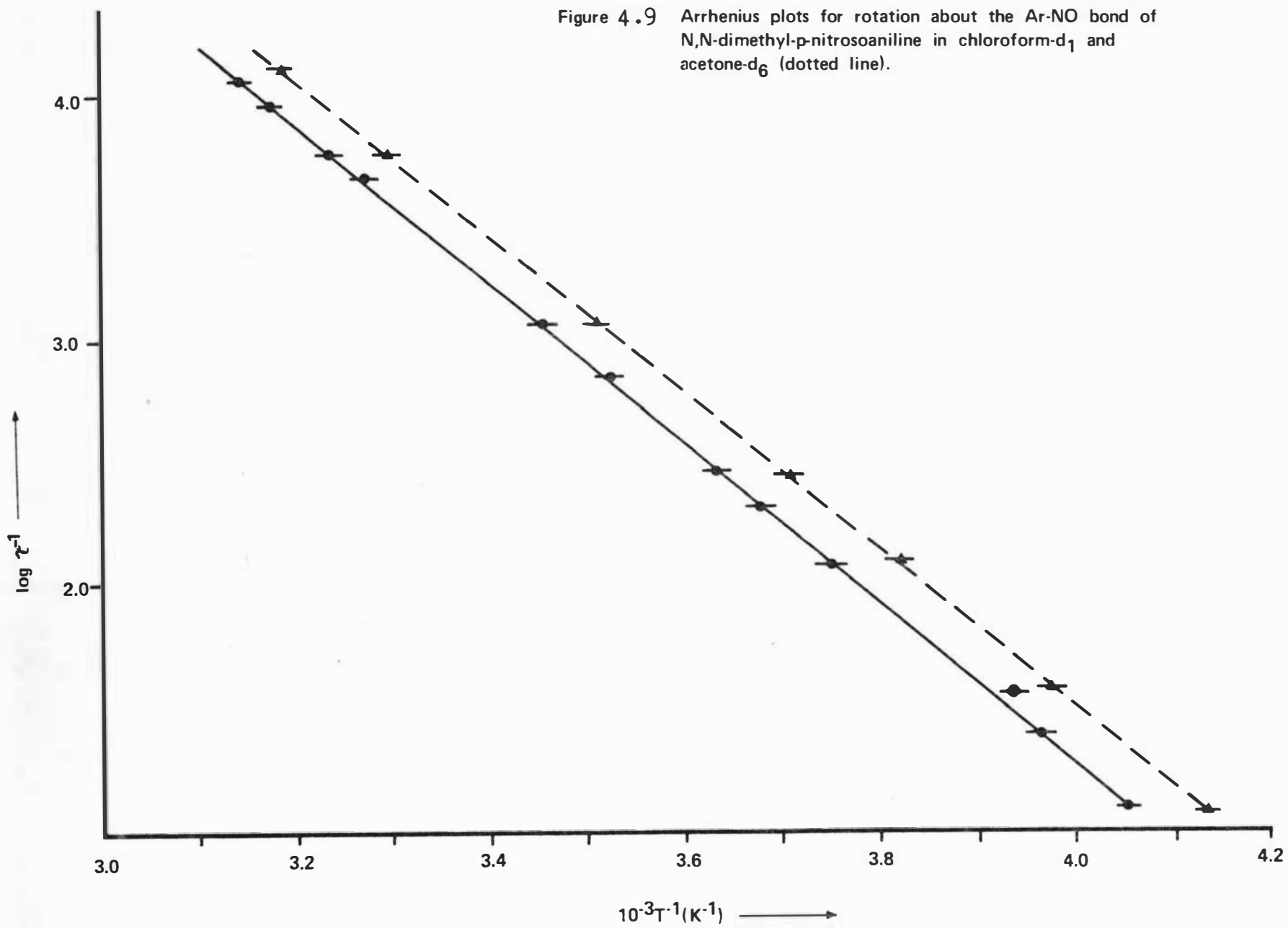
	$\Delta G^{\ddagger}_{298}$	$\Delta H^{\ddagger}$	$\Delta S^{\ddagger}$
motional narrowing	50.6 ± 2.1	46.8 ± 4.6	$-0.012 \pm .020$
exchange broadening	49.3 ± 2.1		

units : $kJ \ mol^{-1}$

The solvent used was acetone.

The values obtained by the use of the density matrix method are shown in Table 4.6 with $\Delta G^{\ddagger}_{298}$ = 52.5 kJ mole^{-1} and $\Delta H^{\ddagger}$ = 59.4 kJ mole^{-1}. This value for $\Delta H^{\ddagger}$ lies well outside the experimental error shown in MacNicol et al's[50] figures. Piette and Anderson[27] had made a number of simplifications in their study of the alkyl nitrites. The mathematical models utilised by MacNicol et al were the simplifications of Piette and Anderson. These approximate equations ignore not only the relative value of the exchange rate as compared to the chemical shifts and coupling constants, but also instrumental contributions to the effective line-width in the absence of exchange.

Piette and Anderson estimated their line-width measurements as accurate to within 20%, giving an overall experimental error of 20% in E_a. In contrast, MacNicol et al's experimental error in $\Delta H^{\ddagger}$ is claimed to be only $\pm$ 10%.

A second group of investigators, Korver et al,[51] used two independent methods to derive activation parameters for N,N-dimethyl-p-nitrosoaniline in chloroform. They simplified the aromatic spin pattern by selective deuteration at the ortho positions to enable easier analysis.

One method they used was that developed by Woodbrey

Table 4.6

Activation parameters for (1) and (2)

Compound	Solvent	E_a (kJ mol^{-1})	$\Delta H^{\ddagger}$ (kJ mol^{-1})	$\Delta G^{\ddagger}$ (kJ mol^{-1})[A]	$\Delta S^{\ddagger}$ (kJ mol^{-1}K^{-1})
(1)	$(CD_3)_2CO$	61.9	59.4	52.5	0.023
(1)	$CDCl_3$	63.6	61.1	53.6	0.025
(2)	$(CD_3)_2CO$	63.0	60.5	54.5	0.020
(2)	$CDCl_3$	64.4	61.9	55.8	0.020
(2)	$C_6D_5CD_3$	66.0	63.5	52.1	0.038

[A] $\Delta G^{\ddagger}$ calculated at 298 K

Errors : $\pm$ 1.6 kJ mol^{-1} in E_a and $\Delta H^{\ddagger}$

$\pm$ 0.2 kJ mol^{-1} in $\Delta G^{\ddagger}$

$\pm$ 0.006 kJ mol^{-1} K^{-1} in $\Delta S^{\ddagger}$

(1) = N,N-dimethyl-p-nitrosoaniline

(2) = N,N-diethyl-p-nitrosoaniline

and Rogers.[25]   This was to record the resonances
caused by the aromatic protons in the meta-positions
at temperatures below the coalescence temperature
and measure the maximum (I_{max}) and central (I_{min}) v-
mode intensities for the H3, H5 doublet.   Equation
(2.25) is utilized thereafter to find the rotational
rate k.

In this case the theoretical model is adequate,
as equation (2.25) only applies for the uncoupled
two-site case.   However, the effect of a systematic
error is somewhat reduced by the large chemical shift
difference between the H3 and H5 protons.

In contrast to the density matrix method the
chief disadvantage is the limited temperature range
which can be covered using Rogers and Woodbrey's
method.   For Korver et al[51] the temperature range
covered was only 10 K.   The rate parameters thus
derived are very dependent on precise temperature
measurements for which they claim an accuracy of 0.1 K.
The experimental constraints suggest that these results
are not reliable.   Harris and Sheppard[61] comment that
published errors in $\Delta H^{\ddagger}$ obtained by the high-resolution
NMR method should be interpreted liberally, particularly
when taken over a small temperature range.

Values obtained for $\Delta H^{\ddagger}$ and $\Delta S^{\ddagger}$ using Rogers and
Woodbrey's method are shown below.   The results for
N,N-dimethyl-nitrosoaniline in chloroform obtained by
the density matrix method are in parentheses.

$$\Delta H^{\ddagger} = 61.0 \pm 4.2 \text{ kJ mol}^{-1} \quad (61.1 \pm 1.6 \text{ kJ mol}^{-1})$$
$$\Delta S^{\ddagger} = 0.005 \pm 0.015 \text{ kJ mol}^{-1} \quad (0.025 \pm .006 \text{ kJ mol}^{-1})$$

Figure 4.10 Arrhenius plots for rotation about the Ar-NO bond of N,N-diethyl-p-nitrosoaniline in chloroform-d(1), acetone-d_6(2), toluene-d_8(3).
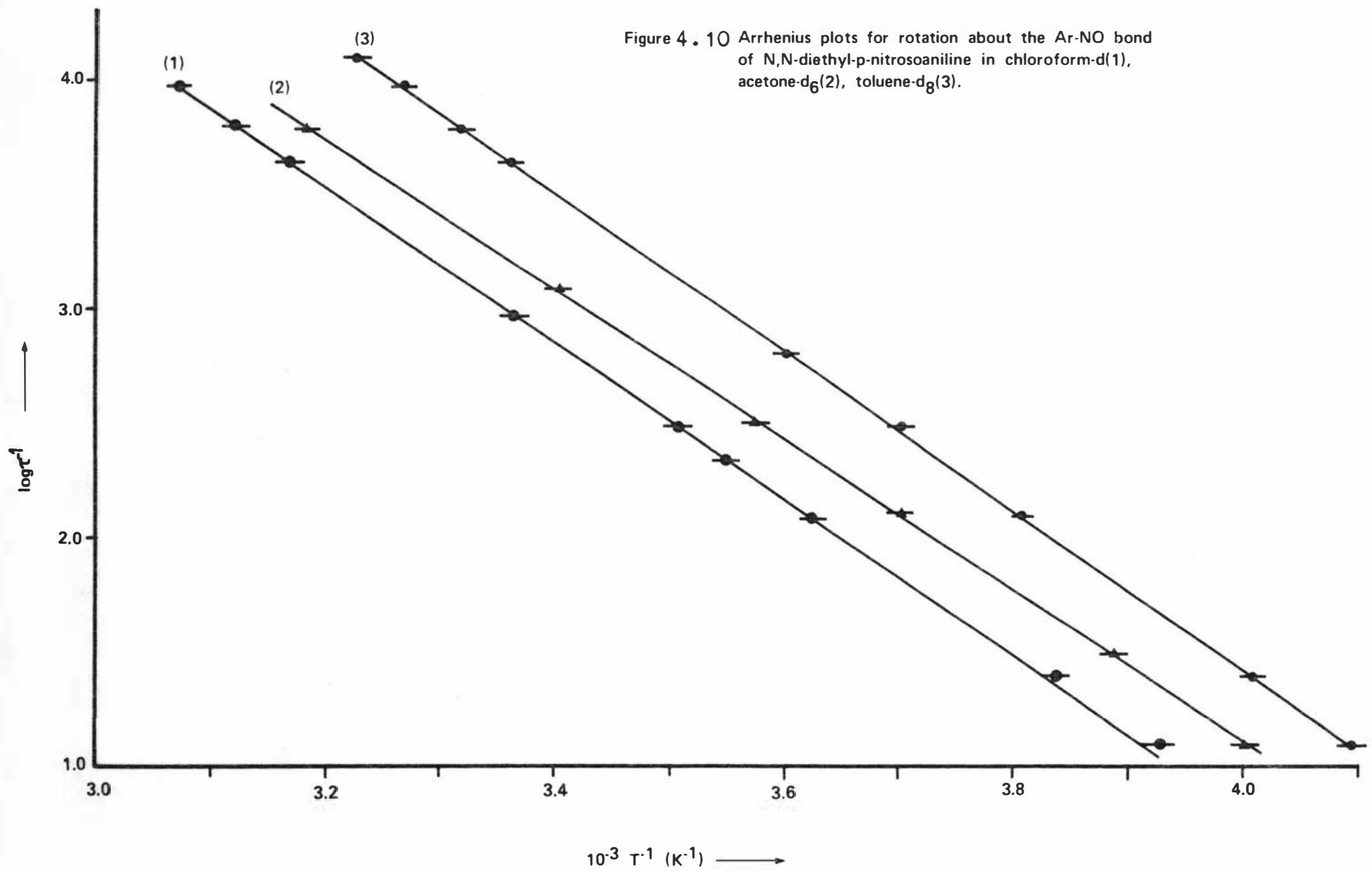
The second method used by Korver et al, was developed by Alexander[22] and involves exchange narrowing of the absorption band at temperatures above coalescence. The height of the absorption band (A) at a certain temperature relative to the height (A_o) at "infinite" temperature is related to in a very complex equation which can be simplified to give :

$$k = \frac{1}{2\tau} = \frac{T_2 \delta \nu^2}{4\left(\frac{A_o}{A}\right) - 1}$$

...(4.1)

The values obtained for the activation parameters $\Delta H^{\ddagger}$ and $\Delta S^{\ddagger}$ using the second method are :

$$\Delta H^{\ddagger} = 62.3 \pm 0.4 \text{ kJ mol}^{-1}$$
$$\Delta S^{\ddagger} = 0.020 \pm 0.001 \text{ kJ mol}^{-1}$$

Again these values lie very close to those obtained using the density matrix approach. Figure (4.11) shows an Arrhenius plot of the combined results of Korver et al[51] in comparison with the plot obtained using the density matrix treatment.

The only other study on p-substituted nitrosobenzenes was accomplished by Calder and Garratt.[49] These investigators obtained a series of values for $\Delta G^{\ddagger}$ at the coalescence temperature. The approximate method used was the Gutowsky-Holm equation which was originally intended for the uncoupled two-site case but does give reasonable values for $\Delta G^{\ddagger}$ at the coalescence temperature.

4.1.14 Errors in the Activation Parameters

In a study of this type where an objective is to critically examine a previous investigator's results

Figure 4.11

A comparison of Korver et al's data, with this investigation's data for rotation about the Ar-NO bond of N,N-dimethyl-p-nitrosoaniline in chloroform-d.
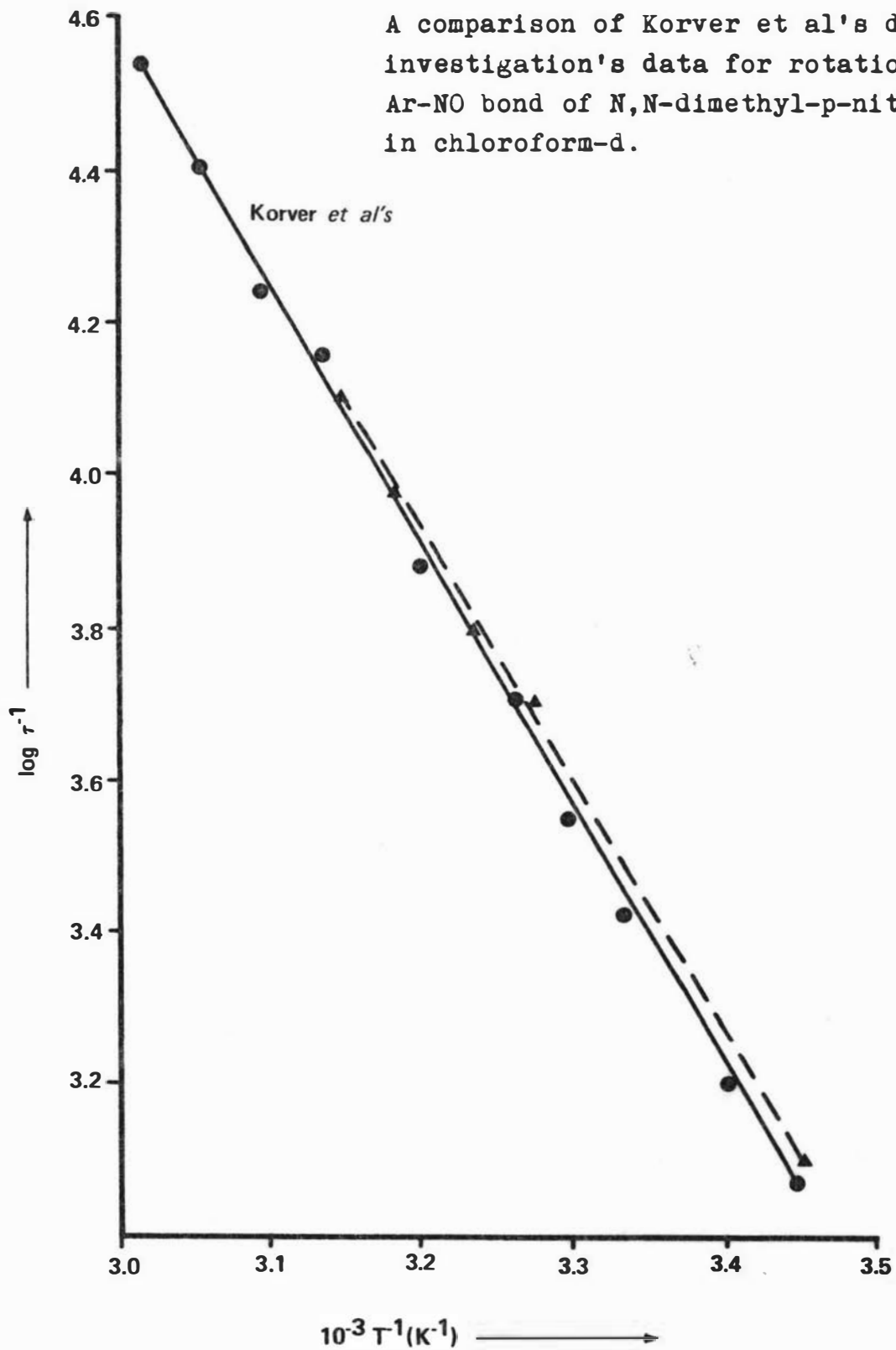
● Korver et al's
▲ This investigation's

there must be an awareness of the strengths and
weakness's of a new approach. This section
suggests what the magnitude of the errors involved
in the activation parameters are and looks at some
of the physical problems in using the spectrometer
that contribute to errors in the kinetic parameters.
The magnitude of the errors involved in the
activation parameters can best be studied by
considering temperature measurements and the exchange
rate.

Errors were calculated using an uncertainty in
the temperature of $\pm$ 1 K although as discussed in
the previous section, Korver et al[51] claimed an error
of $\pm$ 0.1 K. Temperature measurements (see Chapter
Two) are a source of considerable error in line-shape
analyses and much controversy has gone on over the
accuracy of temperature measurements at the sample
site. With the approach used in this thesis where
spectra were fitted to particular values of τ^{-1},
considerable reliance must be placed on the
temperature measurements. The use of the JEOL
temperature chart gave an estimate of the error of
$\pm$ 0.5 K. Temperature gradients in the NMR probe
itself were investigated to see how large their
contribution was to the error in measurement. They
were measured using copper-constantan thermocouples
which had voltages measured by a potentiometer bridge
(W.G. Pye and Co.). One thermocouple was positioned
in the probe near the receiver coil, while the other
was positioned at different heights in a spinning sample
tube.

Table 4.7
Temperature gradients in the sample tube in the JEOL JNM-C-60HL probe at different temperatures for a gas flow pressure of 30 g cm^{-2}

The probe thermocouple is represented by (B)

The sample tube thermocouple is represented by (A)

Room temperature (A) - 774 μV

(B) - 774 μV

(A)/μV (cm) height above the bottom of tube					(B)/ μV	ΔE	$\Delta(\Delta E)$	Temp. Control
0	1	2	3	4				
1454					1416	38	0	313 K
	1449				1409	40	2	
		1485			1431	54	16	
			1495		1435	60	22	
				1465	1400	65	27	
				1971	1866	105	38	323 K
			1965		1871	94	27	
		1951			1865	86	19	
	1951				1876	75	8	
1945					1878	67	0	
2402					2296	106	0	333 K
	2410				2295	115	9	
		2442			2317	125	19	
			2427		2286	141	35	
			2425		2284	141		
				2441	2288	153	47	
				2888	2664	224	78	343 K
				2890	2667	223		
			2872		2672	200	54	
			2872		2672	200		
		2825			2647	178	32	
		2843			2665	178		
	2814				2652	162	15	
	2814				2654	160		
2806					2660	146	0	
2807					2661	146	0	
3228					3041	173	0	353 K
	3255				3051	204	31	
	3251				3045	205	32	
		3277			3050	227	54	
		3280			3052	228	55	
			3298		3042	256	83	
			3305		3051	254	84	
				3354	3064	290	117	
				3354	3064	290	117	

Measurements for a range of temperatures are shown in Table (4.7). A plot of $\Delta(\Delta E)$ versus the height of the thermocouple (A) above the bottom of the sample tube is shown in Figure (4.12) for a temperature of 353 K. The temperature gradient is nearly 0.6 K cm^{-1}. The conversion factor for voltage (μV) to temperature was obtained from the "Handbook of Chemistry and Physics" by the Chemical Rubber Company. With the temperature controller registering 313 K the gradient was 0.2 K cm^{-1}. The extremes of the temperature range indicate a further contribution to the experimental temperature error of about 0.5 K. The temperature gradient of 0.6 K cm^{-1} was the extreme of the temperature measurements. Figures (4.9) and (4.10) show the data points with an error bar of $\pm$ 1.0 K. All these plots have a correlation coefficient of less than -0.999.

Since τ^{-1} was one of the parameters fed into the density matrix program it was difficult to estimate errors in this parameter. Possible physical problems arising from the particular approach of matching experimental spectra to the theoretical are the twin problems of phasing and saturation.

Saturation problems arise when the power output from the observation and locking channels start to decrease the spectral signal from the sample. To minimize saturation effects, spectra were run at minimum modulation and maximum amplitude. This resulted in all spectra having a large noise pattern which was reduced by using the appropriate electronic

Figure 4.12 The variation of temperature in a spinning NMR sample tube at 353 K

gradient = 29 μV cm^{-1}
≡ 0.6 K cm^{-1}

Distance along tube in cm
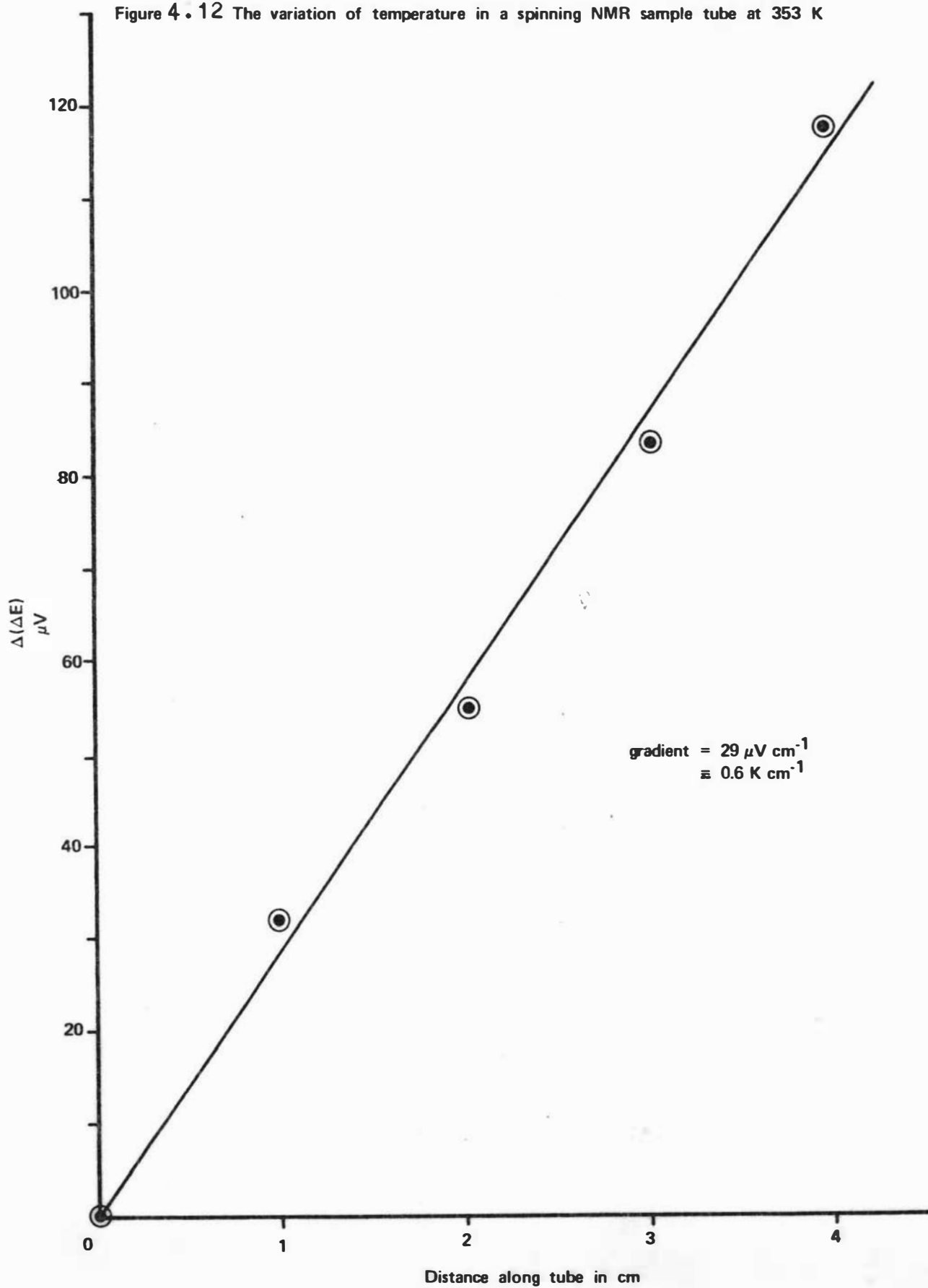
filter control on the spectrometer.   One method to
check if saturation effects were occurring was to
place the recorder pen on top of a spectral signal
and observe the movement, if any, of the recorder
pen.   A movement downwards would indicate that
saturation effects were taking place.   Another simple
way of checking saturation effects was to rerun the
same spectrum on top of the first spectrum.   If
there was saturation the peak heights of the signals
would be different.

The other problem that can affect τ^{-1} is the
phasing of the signal.   By having very high gain on
the amplitude controls, phasing was a real problem.
Proper phasing means that the spectrum does not deviate
from its base line after passing through an absorption
peak.   Any slight change in power and changes in
temperature affected the phasing of a spectrum.
The mode control between absorption and dispersion had
to be adjusted each time a spectrum was run at a
different temperature.   Incorrect phasing alters the
positions of peaks (essential input for the density
matrix program) and distorts the appearance of the
experimental line-shape which will affect τ^{-1}.   The
early problems of not using enough base-line resulted
in obtaining a non-linear plot of log τ^{-1} versus
inverse temperature.

The error in E_a and $\Delta H^{\ddagger}$ was estimated to be
$\pm$ 1.6 kJ mol^{-1} by graphical variation in the slopes of
the Arrhenius plots.

The particular method employed in this project,

of generating theoretical curves from the slow exchange parameters, could contribute to errors in τ^{-1}. It was found to be not possible to make systematic measurements of the temperature dependence of the chemical shifts and T_2 values in the region of slow exchange, because of solubility and solvent viscosity problems. The coupling constants are assumed to be independent of temperature[62]. Any temperature dependence in T_2 was minimised by the choice of broad bands in the spectra. Dahlquist and Forsen[38] in their study of N-acetyl pyrrole found that the theoretical spectra at both high and low temperatures could be well reproduced with the same set of T_2 and spin-spin coupling constants. They used these parameters for the calculation of theoretical spectra at all intermediate temperatures.

For acetone and chloroform the shift difference $(\nu_5 + \nu_3)/2 - (\nu_2 + \nu_6)/2$ showed a small change of about 1 Hz over the observable temperature range. Thus, the slow exchange chemical shifts were used, or had to be used, in all cases. Again Dahlquist and Forsen[38] with their vastly superior computing facilities used the slow exchange chemical shifts at all temperatures, as they found that a small temperature variation in the chemical shifts had no detectable effect on the calculated spectra. In this investigation peak fitting was performed by shifting the calculated NMR spectra one or two hertz when this proved necessary to ensure that the maximum intensity positions coincided. Such a procedure should

be valid provided the relative frequency shifts in the part of the spectrum which is being fitted are in the same direction.   This conclusion is supported by the excellent fits that were obtained for all the NMR spectra.

4.1.15 <u>Summary</u>

The use of the density matrix treated has cleared up the discrepancy between Korver et al[51] and MacNicol et al's[50] results for N,N-dimethyl-p-nitrosoaniline. MacNicol et al's values for the activation parameters in acetone have been found to be erroneous while Korver et al's values have been confirmed.   The correlation of Korver et al's results with the data from the density matrix treatment provide a good testimony for the reliability of the method.

The starting point of the investigation had been to examine the solvent effects that were supposedly occurring in the nitrosoanilines.   Korver et al[51], unable to explain their results, had suggested that further experiments were necessary to establish whether there was a significant correlation between the rotational barrier and the nature of the solvent.

For other systems like the 1-acyl pyrroles, different substituents had been observed to raise the barrier to internal rotation through increased double bond character[68].   The possibility of other factors, such as solvation, affecting the barrier was also raised.   Small but significant solvent effects have been observed for rotation about the N - CO band in amides[69,70].   A solvent effect on the inversion barrier

in N-benzyl-O, N-dimethyl hydroxylamine[71] was so marked
that the rate of inversion could only be studied with
solvents of low dielectric constant. Cooney et al[72]
observed a solvent effect on the barrier to rotation of
bicyclic N-nitrosamines and suggested that the observed
effect may be due to the solvents of higher polarity
stabilizing the dipolar resonance structure II.

$$\text{\textbackslash}N - N = O \longleftrightarrow \text{\textbackslash}N^+ = N - O -$$

$$\quad\quad\text{I} \quad\quad\quad\quad\quad\quad\quad\quad \text{II}$$

Analogous resonance structures can be written for
the p-substituted nitrosoanilines. However in this
investigation no such effect of solvent polarity on
the barrier was observed. The significant result of
the present study for the p-nitrosoanilines is that
despite the widely different properties of the solvents
used (a polar hydrogen binding solvent, chloroform; a
dipolar aprotic solvent, acetone; and a non-polar
aromatic solvent, toluene) within experimental error,
no significant solvent effect on the barrier to
rotation about the Ar-NO band was observed. Further
studies of the effect of solvent on the barrier to
rotation in other molecules are needed in order to
demonstrate whether the behaviour of the substituted
p-nitrosoanilines is exceptional.

For N,N-diethyl-p-nitrosoaniline in toluene-d_8
there appears to be a slight solvent effect with slight
increases in the calculated values of the entropy and
enthalpy of activation. If this small effect is real
it may arise from a solvent-solute association[73]

stabilizing the ground state and giving a slightly
higher value of $\Delta H^{\ddagger}$ while disruption of the
association on rotation gives rise to a larger
$\Delta S^{\ddagger}$ value.

The results of the work on the p-nitrosoanilines
have been published[74,75] and these reports can be
found in an envelope at the back of this thesis.

4.2. The Anion Derived from p-nitrosophenol

An appreciable barrier to rotation has been found to exist for the sodium and potassium salts of p-nitrosophenol in D_2O [49,76]. The magnitude of the $\Delta G^{\ddagger}$ value obtained for this compound stands out in contrast to values for the other p-substituted nitrosobenzenes in Calder and Garratt's paper.[49] In fact the $\Delta G^{\ddagger}$ value obtained was 20 kJ mol^{-1} higher than that for the next nitrosobenzene.

It has been suggested that rotation may be acid catalysed due to rapid rotation of the protonated form.[76]

(I)   (II)
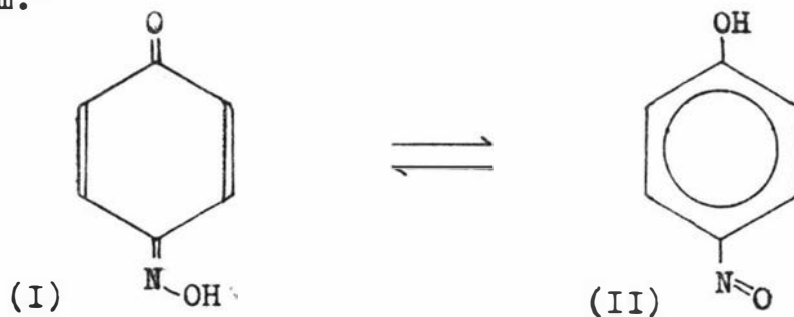
The following sections outline the study of p-nitrosophenol in potassium carbonate and discuss the results of attempts to alter the concentration of the free anion.

4.2.1 Purification of p-nitrosophenol

Approximately 10 g of commercial p-nitrosophenol (KOCH-LIGHT) was dissolved in 50 cm^3 of dry diethyl ether. This mixture was boiled with 1-2 g of decolourizing charcoal and then filtered through alumina. The clear green solution was evaporated down, under a stream of nitrogen gas, to give dull yellow crystals of p-nitrosophenol. These crystals were immediately collected by filtration, and stored in a dessicator.

The diethyl ether used in the above purification

was prepared in the following manner. A winchester of ether was divided into two approximately equal volumes, and each was shaken in a large separatory funnel with 20 cm^3 of ferrous solution (the concentrated solution of ferrous salt was prepared from 60 g of ferrous sulphate, 6 cm^3 of concentrated sulphuric acid and 110 cm^3 of water) diluted with 100 cm^3 of water. After the water was removed, the ether was transferred to the winchester and about 200 g of anhydrous calcium chloride was added. By leaving this mixture to stand for at least 24 hours most of the alcohol and water was removed. The ether was transferred by filtering through fluted filter paper to another clean dry winchester.

Sodium wire was then introduced directly into the ether. The bottle was sealed by a rubber stopper carrying a drying tube filled with cotton wool and calcium chloride (to allow the escape of hydrogen).

4.2.2 Preparation of NaOD.

Approximately 1 g of sodium metal was first cleaned in t-butyl alcohol. Under the conditions of a nitrogen atmosphere the sodium was added to a flask of D_2O. The addition took about half an hour. The solution was then filtered and made up to 25 cm^3 in a volumetric flask. Again, this was all done under nitrogen. The molarity of the NaOD was found by titrating with 0.1 M HCl to be 1.65 M.

4.2.3 Preparation of Samples.

7% w/v solutions of p-nitrosophenol were prepared in a 1 mol l^{-1} potassium carbonate solution and in the

1.65 mol l^{-1} sodium deuteroxide. These samples were made up for NMR measurement as previously discussed in Section 4.1.3. Anhydrous potassium carbonate was used in conjunction with deuterium oxide (Stohler Isotope Chemicals) for one sample. The pD of p-nitrosophenol in 1.65 mol l^{-1} NaOD was found to be 12.4.

Since tetramethylsilane is immiscible with water another internal reference standard had to be found. One proven NMR internal standard for D_2O is the internal standard 3-trimethyl-silylpropane sodium sulphonate. To obtain an adequate lock signal there must be a reasonable amount of reference compound present. However, such a quantity of reference compound was required that on lowering the temperature below 293 K (to obtain the slow exchange spectrum) this salt precipitated out of solution. This necessitated the choice of another NMR reference compound, hexamethyldisilane. This compound is immiscible with water but has a boiling point of 386 K. The hexamethyldisilane was sealed in a capillary tube centred in the NMR tube of p-nitrosophenol solution.

4.2.4 <u>Temperature Measurements</u>

While in previous work, 'super-dry' methanol in a sealed capillary tube in a sample of the same solvent had been used as the NMR thermometer, this section describes a different procedure. There were two reasons for this; one, was to check the reliability of measurements using the JEOL calibration chart which had to be relied on in all earlier temperature measurements. The other was to see how useful the

equations that applied to the glycol and methanol thermometers described below were.

The measuring thermometers were air-saturated methanol or glycol solvents containing concentrated aqueous hydrochloric acid (.03% by volume) sealed in NMR tubes. The spectrometer was locked to the CH_3 or CH_2 protons with the recorder centred on the OH resonance and the frequency difference ($\Delta\nu$) read on the frequency counter. A.L. Van Geet[77,78] has developed a number of equations to use in conjunction with these NMR thermometers.

For the ethylene glycol thermometer the chemical shift ($\Delta\nu$) between the CH_2 and OH groups fits a straight line, with a claimed error of $\pm$ 0.3 K over the range 310 - 410 K.

The equation is :

$$T = 466.0 - 1.694|\Delta\nu|$$

For the methanol NMR thermometer the ranges are :

175 - 225 K $T = 537.4 - 2.380|\Delta\nu|$

220 - 270 K $T = 498.4 - 2.083|\Delta\nu|$

265 - 313 K $T = 468.1 - 1.810|\Delta\nu|$

The claimed error in these equations is $\pm$ 0.8 K.

An advantage of Van Geet's NMR thermometers is that the hydrochloric acid causes a complete collapse of the multiplet structure thus obtaining sharp lines at all temperatures.

At temperatures over 273 K occasional temperature measurements were made using a calibrated thermometer. There was no detectable difference between measurements made in this way and those obtained using either the
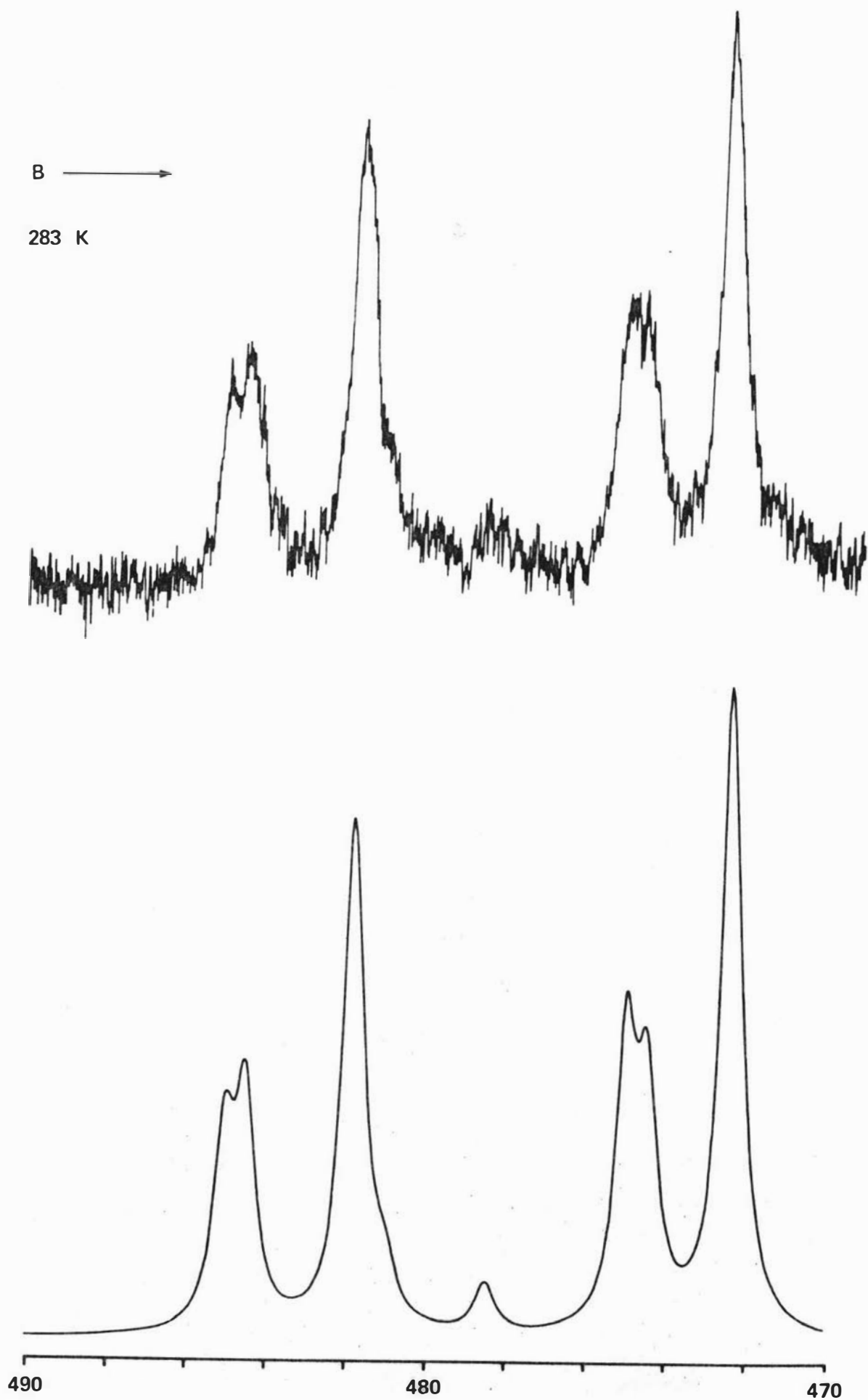
Figure 4.13a The spectrum of the anion of p-nitrosophenol, 7% w/v in D$_2$O containing excess K$_2$CO$_3$, in the slow exchange region.

B ⟶

283 K

450   440   430

Fig 4.13 b

B ⟶
283 K

402   390   378
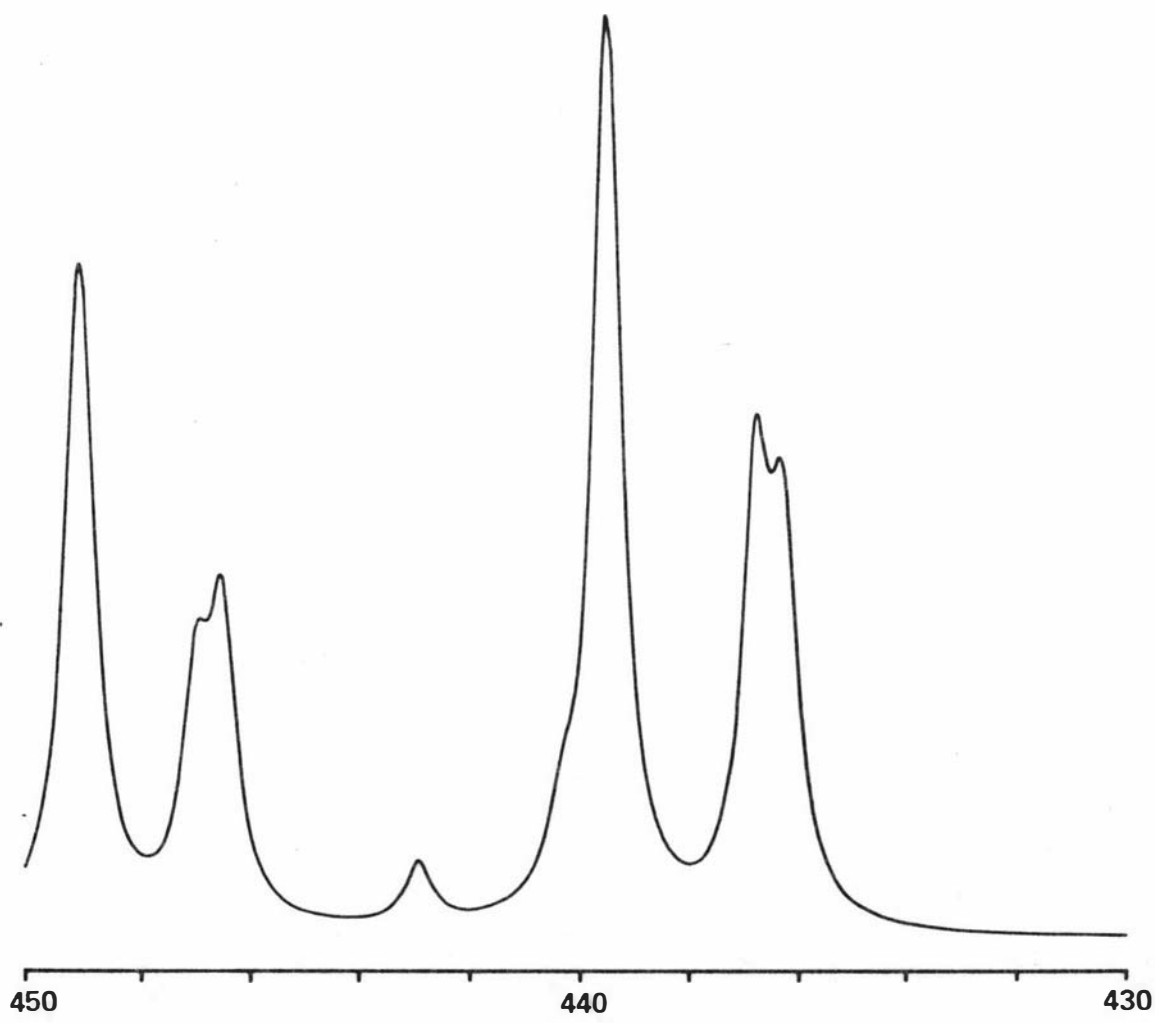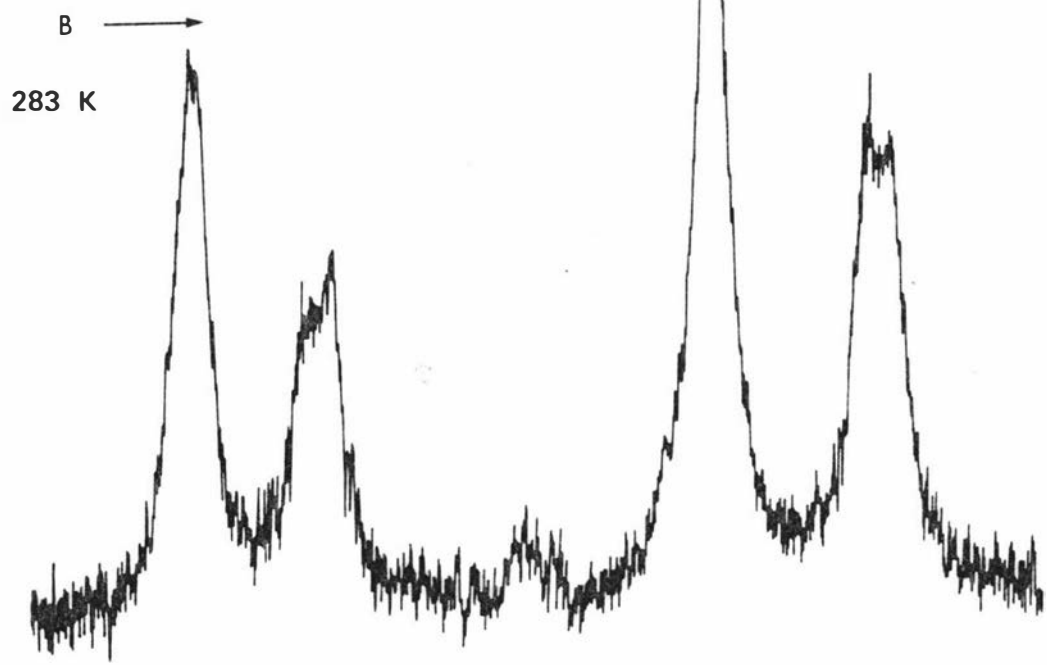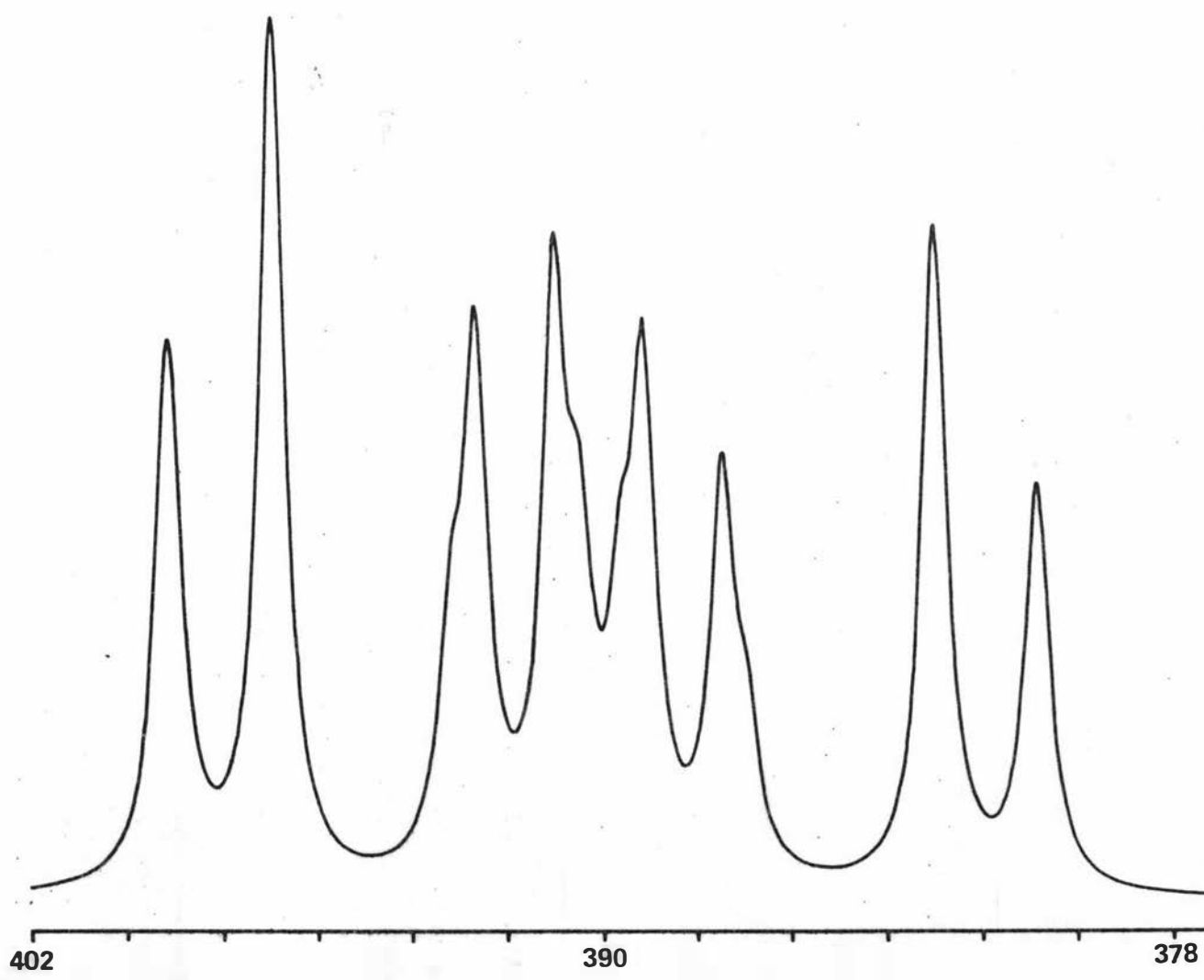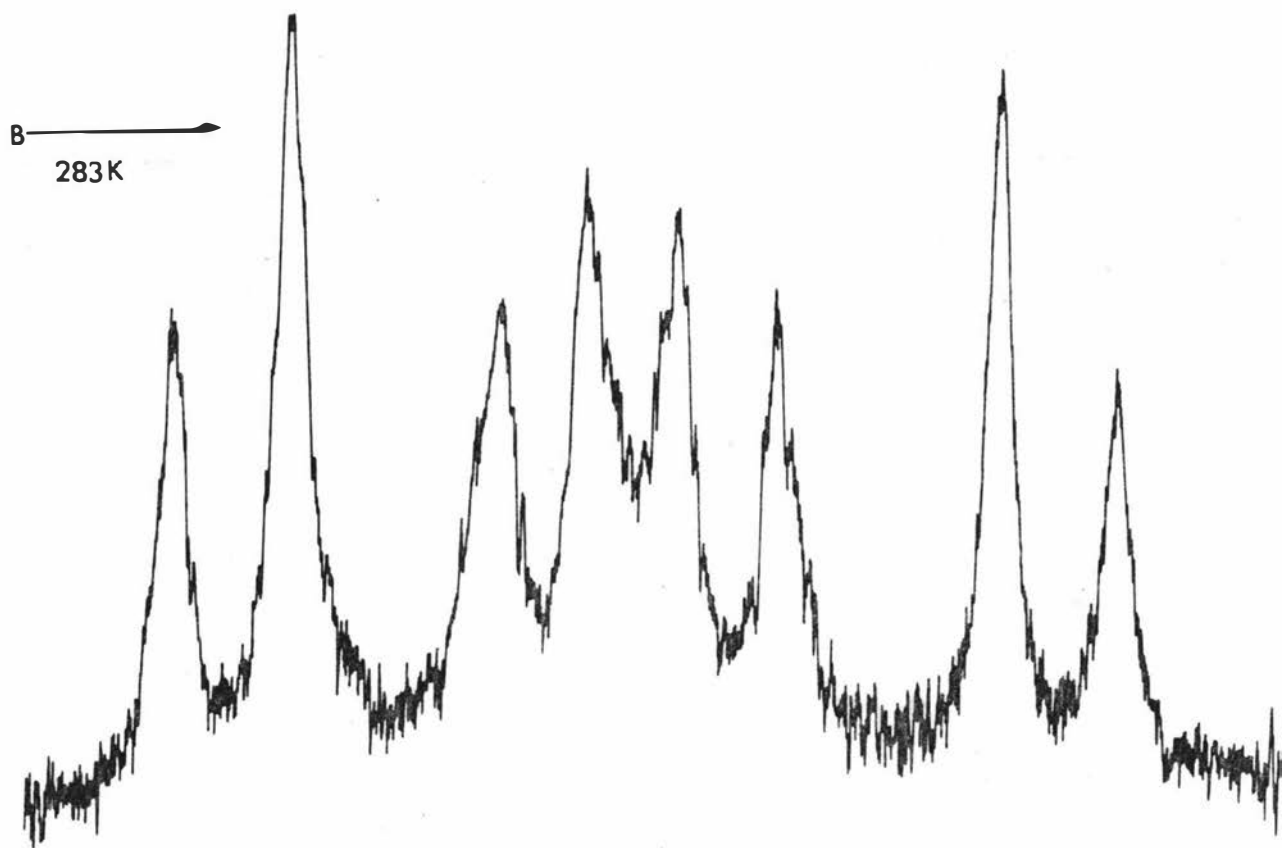
Fig 4.13 c

JEOL calibration chart for dry methanol or Van
Geet's equations for the methanol and glycol samples
containing hydrochloric acid.

4.2.5 Frequency Measurements

Frequency measurements on the spectra were carried
out in the same manner as that described for the
p-nitrosoanilines (Section 4.1.9).   The chemical
shifts, however, were measured in Hz from the
hexamethyldisilane in a sealed capillary tube inside
the NMR tube.

4.2.6 Analysis of the Slow Exchange Spectra

The slow exchange spectrum of p-nitrosophenol in
1 mol l^{-1} K_2CO_3 obtained at 283 K can be seen in
Figure (4.13).

With the higher concentration of p-nitrosophenol
(7% w/v), the spectra should exhibit a larger signal
to noise ratio.   The use of the capillary tube which
contains the hexamethyldisilane reduces the effective
concentration of the sample in the radiation coils by
about a half so that in fact all spectra obtained for
the p-nitrosophenols have quite low signal to noise
levels.

As can be seen from Figure (4.13) a typical ABMX
pattern for p-nitrosophenol was obtained at low
temperature.   The chemical shifts and coupling
constants for this system which were obtained by the
use of LAOCN3 (see Appendix II) are shown in Table 4.8.

The sample of p-nitrosophenol in sodium deuteroxide
in D_2O showed significant viscosity broadening below
293 K and when the temperature was lowered, further

Table 4.8

Chemical shifts and coupling constants for the ring protons of

the anions of p-nitrosophenol in 1 M K_2CO_3 in the slow exchange region.

Solvent	Chemical Shifts[A] (Hz from HMDS)				Coupling Constants (Hz)					
	H2	H3	H5	H6	J_{23}	J_{25}	J_{26}	J_{35}	J_{36}	J_{56}
D_2O	393.3	478.1	442.5	387.2	9.6	0	2.2	2.7	0	9.⌐

[A] HMDS = hexamethyldisilane

Estimated error in parameter is ±0.2 Hz

solid precipitated from the solution. It was not possible therefore, to directly measure the slow exchange spectra of p-nitrosophenol in this solvent, and the same parameters as those obtained in 1 mol l^{-1} K_2CO_3 solution were used (Table 4.8).

The spectra of p-nitrosophenol exhibit an AA'XX' pattern in the fast exchange region (373 K) for both the potassium carbonate and the sodium deuteroxide solutions.

4.2.7 The Exchange Rate (τ)

Theoretical spectra were generated by the density matrix program from the slow exchange parameters over a reasonably large range of rates.

Matching of spectra was made more difficult by the fact that the spectra had to be matched within a short time as the sample of p-nitrosophenol darkened and appeared to undergo significant decomposition over a period of only one to two weeks. A number of spectra generated by the density matrix program proved to be of no use as these had exchange rates which required temperatures above the boiling point of water.

As can be seen from Table (4.9) the range of rates that could be studied varied by a factor of only sixty (from 6.3 to 377 rads s^{-1}) even though the temperature changed by 70 K. For the nitrosoanilines the rate varied by a thousand for approximately the same temperature range.

In the study of p-nitrosophenol in NaOD higher temperatures were required for the corresponding exchange rate. Thus the theoretical spectrum that was

Table 4.9

Rotational rates as a function of temperature
for a 7% w/v solution of p-nitrosophenol.

In 1 M K_2CO_3 (made up in D_2O)

T (K)	τ^{-1}	$10^{-3} T^{-1}$ (K^{-1})	$\log_{10} \tau^{-1}$
305.6	6.3	3.273	0.7993
315.2	12.6	3.173	1.1004
336.1	50.3	2.975	1.7016
362.0	220.0	2.762	2.3424
368.3	314.2	2.715	2.4972
372.0	377.0	2.688	2.5763

In 1.65 M NaOD

T (K)	τ^{-1}	$10^{-3} T^{-1}$ (K^{-1})	$\log_{10} \tau^{-1}$
311.5	6.3	3.210	0.7993
322.0	12.6	3.106	1.1004
335.0	25.1	2.985	1.3997
358.5	50.3	2.790	1.7016

generated using an exchange rate of 12.6 s^{-1} matched
the experimental spectrum in NaOD solution at 322 K
and the experimental spectrum in potassium carbonate
at 315.2 K (Table 4.9). For the nitrosophenol in
this medium matching of experimental and theoretical
spectra proved difficult as the experimental spectrum
did not change significantly if the temperature was
changed by 1 or 2 K. This was in marked contrast
to the nitrosoanilines where a 1 K change of
temperature produced a significant effect in the
experimental spectrum. Matching was achieved for
the spectra with exchange rates up to 25.1 rads s^{-1}
but the value of the temperature at 50.3 rads s^{-1}
should only be regarded as an estimate. The
experimental spectrum matches the density matrix
theoretical spectrum about this temperature and remains
the same up to 373 K.

Examples of matched theoretical spectra for the
anion of p-nitrosophenol in potassium carbonate
solution can be seen in Figure (4.14).

4.2.8 <u>The Activation Parameters</u>

Figure (4.15) shows plots for the p-nitrosophenol
in potassium carbonate solution and sodium deuteroxide.
The curvature of the plot for the anion in NaOD is
quite marked in contrast to the plot obtained in K_2CO_3
solution. The activation parameters derived from
the Arrhenius plot for the K_2CO_3 solution are given in
Table (4.10). Errors in these activation parameters
were estimated as described in Section (4.1.14) for

B ⟶   10 Hz

372.0 K τ^{-1} 377.0 s^{-1}

368.3 K τ^{-1} 314.2 s^{-1}

305.6 K τ^{-1} 6.3 s^{-1}
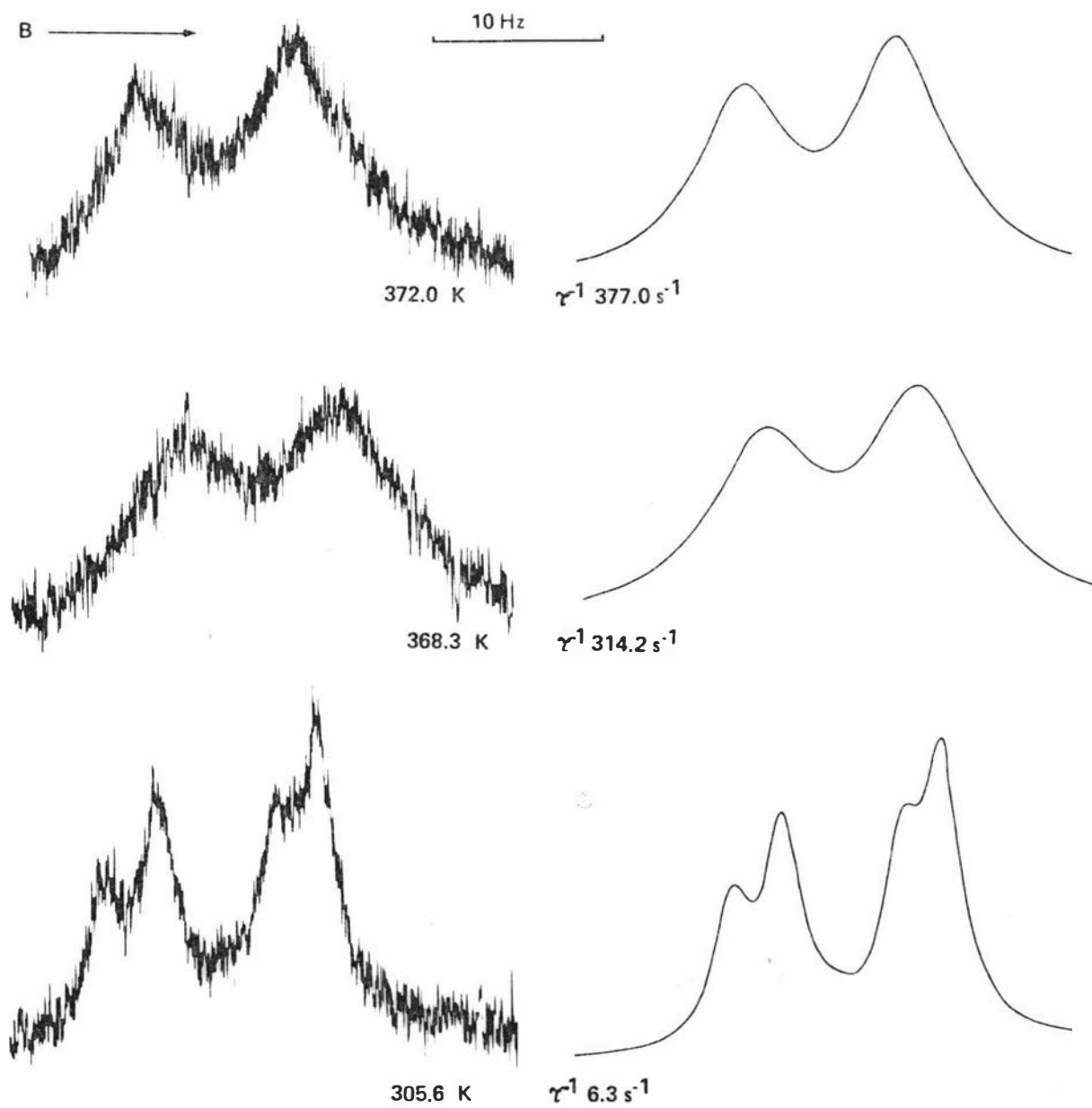
Figure 4.14 Examples of experimental and theoretical spectra for the H3,H5 nuclei of the anion of p-nitrosophenol in 1 mole l^{-1} K$_2$CO$_3$ (in D$_2$O).

the p-nitrosoanilines. Because of the curvature in the plot for the anion in NaOD it was not possible to obtain activation parameters from the data.

The values obtained for E_a and $\Delta H^{\ddagger}$ were not high, being 58.2 and 55.7 kJ mol^{-1} respectively. If Table (4.6) is examined it can be seen that these values are four or five thousand joules lower than that obtained for the p-nitrosoanilines. This was perhaps an unexpected result as, for such rotational processes, high values of $\Delta G^{\ddagger}$ are normally associated with high values of $\Delta H^{\ddagger}$. The value obtained for $\Delta G^{\ddagger}$ is in reasonable agreement with Calder and Garratt's[49] value of 72.5 kJ mol^{-1}. The high $\Delta G^{\ddagger}$ value gives rise to a negative $\Delta S^{\ddagger}$ value which is unusual if this four-spin system was simply undergoing intramolecular exchange. The expected value of $\Delta S^{\ddagger}$ in systems undergoing internal rotation is usually zero[49] or slightly positive as can be seen for example by the values obtained for $\Delta S^{\ddagger}$ for the p-nitrosoanilines (see Table 4.6).

4.2.9 <u>Summary</u>

For p-nitrosophenol, Havinga[79] writes that the equilibrium between the quinine monoxime form (I) and the nitroso form (II) as involving a common anion which can be written in the mesomeric forms (IIIa) and (IIIb).

(I)   (IIIa)   (IIIb)   (II)
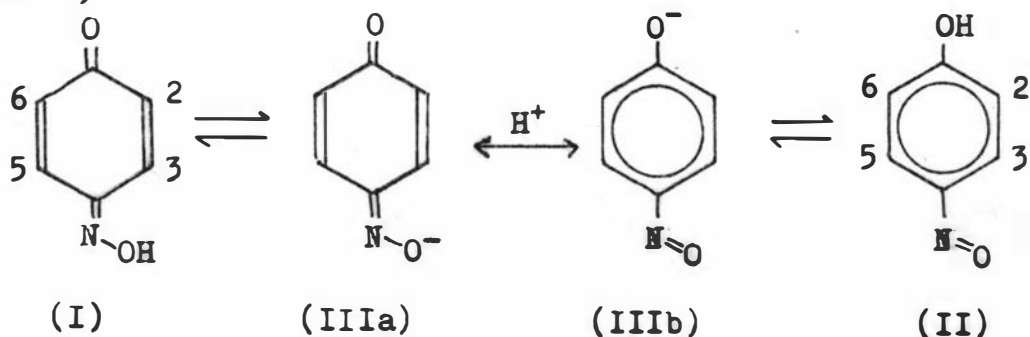
Figure 4.15 Arrhenius plots for rotation about the Ar-NO bond of the anion of p-nitrosophenol in 1M K_2CO_3 (1), and NaOD(2).
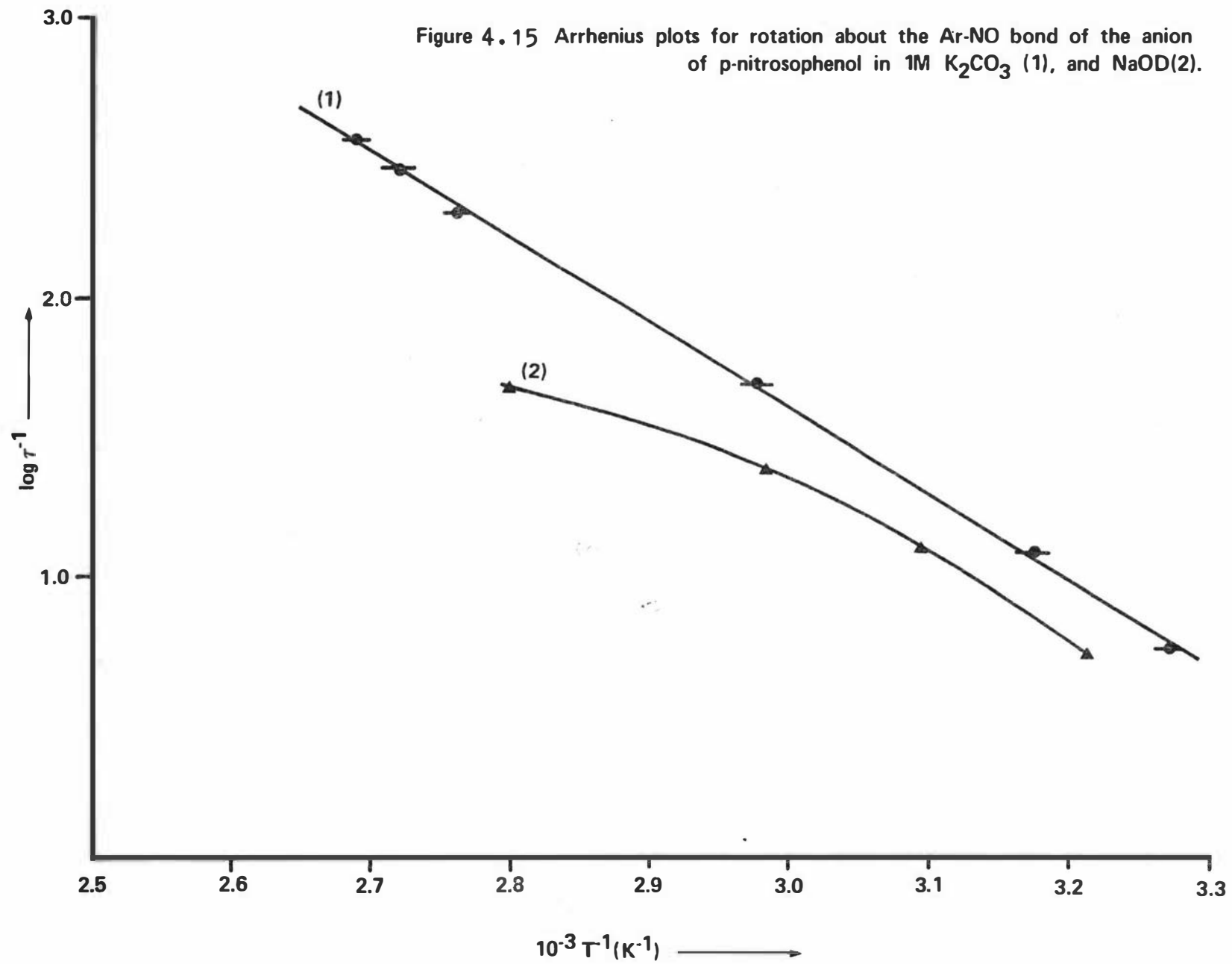
Table 4.10

Activation parameters for the anion of p-nitrosophenol in 1 M K_2CO_3

Solvent	E_a (kJ mol^{-1})	$\Delta H^{\ddagger}$ (kJ mol^{-1})	$\Delta G^{\ddagger}$ (kJ mol^{-1})[A]	$\Delta S^{\ddagger}$ (kJ mol^{-1} K^{-1})
D_2O	58.2	55.7	70.1	-0.048

[A] $\Delta G^{\ddagger}$ calculated at 298 K

Errors :- $\pm$ 1.6 kJ mol^{-1} in E_a and $\Delta H^{\ddagger}$

$\pm$ 0.2 kJ mol^{-1} in $\Delta G^{\ddagger}$

$\pm$ 0.006 kJ mol^{-1} K^{-1} in $\Delta S^{\ddagger}$

Norris and Sternhell[76] have suggested that exchange in the p-nitrosophenols was catalysed by protons and involves the syn-anti equilibrium of the monoxime form. The _syn_ configuration (N-OH) is defined with respect to the substituent at C-2. The percentage of the _syn_ isomer in the oxime form for the anion has been found to be 50%.[80] The observed appreciable barrier to rotation suggests that the canonical structure (IIIa) contributes more to the resonance hybrid than the canonical structure (IIIb).

Addition of solid sodium hydroxide to p-nitrosophenol in D_2O containing excess potassium carbonate, has been reported to cause sharpening of the NMR signals without any alterations in the peak positions.[76] From their observation Norris and Sternhell inferred that the process which leads to slight exchange broadening of the anion in potassium carbonate solutions at room temperature, and to a nearly symmetrical spectrum at 373 K, may involve the protonated form of the salt (II) as it appears to be suppressed by the presence of a strong base. They suggested that a quantitative study of the equilibrium between forms I and II was needed to settle this point.

The results obtained in this project represent an attempt to study the effect of such an equilibrium on the apparent barrier to rotation in p-nitrosophenol. The negative value of the entropy of activation could lend support to Norris and Sternhell's[76] claim that exchange in the p-nitrosophenols is catalysed by protons and does involve an equilibrium between the quinine

monoxime and the nitroso forms. The curved Arrhenius plot could arise due to a decrease in pD with increasing temperature (which has been shown to occur in concentrated base[81]) which will result in an increased amount of p-nitrosophenol in the protonated form. However, if such a decrease in pD is occurring the downward curvature of the log K versus $\frac{1}{T}$ plot for the anion in NaOD would not be consistent with Norris and Sternhell's suggestion that the rotation is acid catalysed.

To investigate this further attempts were made to study the p-nitrosophenol in a range of buffers containing added salt. Bates[81] has made available methods of making suitable buffers and tables showing the change in pH that occurs with temperature for each buffer. Attempts were made to utilize these buffers but calculations showed that the p-nitrosophenol needs to be in a concentration of 1% w/v to maintain a constant pH for these buffers. This is in contrast to the 7% w/v of p-nitrosophenol that had the spectrometer operating at the limits of its sensitivity (the sample contained the central capillary tube of hexamethyldisilane). Thus a more sensitive NMR spectrometer will be needed if the effect of pH on the barrier to rotation in p-nitrosophenol is to be studied in a more systematic way. The commercial availability of C-13 spectrometers could provide the solution to this problem. As discussed before, buffers can be made that have a certain known rate of decrease of pH with temperature. Using such buffers it should be possible to determine if

pH really effects this rotational process.

4.3 Conclusions.

The use of the density matrix method has for the first time provided the activation parameters of N,N-diethyl-p-nitrosoaniline in acetone, chloroform and toluene. The original values for the activation parameters of N,N-dimethyl-p-nitrosoaniline in acetone have been found to be erroneous while confirmation of the $\Delta H^{\ddagger}$ value in chloroform has been made. No effect of solvent on the barrier to rotation was observed for these compounds.

Activation parameter data has also been obtained for p-nitrosophenol in potassium carbonate solution. Attempts to systematically extend this work to other buffers showed that a more sensitive method was needed. This possibly could be obtained using the new pulse Fourier technique in NMR.

In comparison with approximate equations the density matrix approach involving a four-spin system is a time-consuming process. This can be balanced by the fact that approximate equations have not provided satisfactory solutions for activation parameters. The persistence in the use of approximate equations make comparisons of total line-shape methods and approximate methods a continuing subject of keen interest.[99,100]

The generation of theoretical spectra over the whole temperature range has proved to be a reliable method in finding the corresponding temperatures, in contrast to the standard technique of generating spectra from a computer until the one that matches the

experimental spectrum is found.

Approximate methods are still useful in obtaining kinetic data as the density matrix method requires that a system be studied over its entire spectral range. Information from the slow exchange region is required as input for the computer program, while spectra must be matched over the whole temperature range where significant spectral changes occur, to ensure the validity of the Arrhenius plot. The requirement of obtaining a slow exchange spectrum for a particular compound places a restriction on the solvents that can be used. Thus the density matrix approach requires a compound to satisfy a number of criteria. These are : solubility, thermal stability, and non-reactivity with the solvent. From this it can be seen that the density matrix method is not completely general in its applicability to obtaining rotational energy barriers. It is however, as this project shows, a powerful and useful tool in the obtaining of reliable kinetic data.

CHAPTER FIVE

Ligand Exchange in Cobalt (II)

Tetrahedral Complexes

The effect of rapid chemical exchange in an equilibrium situation on NMR spectra has given us the rates of many types of exchange that have not been accessible by other methods.[82] These types of reactions have included internal rotation and rates of ligand exchange in transition metal complexes.

The determination of rates of exchange in paramagnetic complexes depends upon the fact that the co-ordinated species has a shorter nuclear spin lifetime, resulting in a larger line-width than the unco-ordinated species in the bulk solution.

The nuclear spin lifetime is short in a paramagnetic environment because the nucleus is subjected to strong, fluctuating magnetic fields from the unpaired electrons which are responsible for the paramagnetism. These magnetic fields act on the dipole of the nucleus and change its orientation (spin-state).

Most studies have been concerned with octahedral complexes in aqueous solution or in the free ligand as solvent. A number of reviews have appeared on ligand substitution processes in octahedral complexes.[82,83]

Only a few detailed studies have investigated the rate of exchange of the free ligand in relatively inert solvents.[84,85] A qualitative investigation of thiourea tetrahedral cobalt (II) complexes has been made in acetone.[86]

The only complete line-shape study carried out so far is that of Zumdahl and Drago[85] on the exchange of

2-picoline with dichlorobis (2-picoline) cobalt (II).

The aim of this study was to find other tetrahedral complexes suitable for an NMR investigation by the line-shape technique. The following sections represent the more promising systems that were investigated in the first year of this project.

5.1 Phosphine Type Ligands

5.1.1 Preparation of dichlorobis(diphenylmethylphosphine) Cobalt(II)

This reaction was carried out under nitrogen (oxygen free). A solution of 3.2 g diphenylmethyl-phosphine (Maybridge Chemical Company), in hot ethanol and 2.08 g of anhydrous cobalt chloride also in hot ethanol, were combined together. The product, on being filtered, was washed alternately with ethyl acetate and ethanol. The complex was further dried on a vacuum line for two days.

The complex was then dissolved in freshly distilled chloroform and filtered twice to remove the impurities present.

Analytical results are reported for this compound:

calculated	C	58.86%	H	4.90%
found	C	58.34%	H	4.90%

These analyses were carried out by Dr A.E. Campbell of the Microanalytical Laboratory at Otago University.

5.1.2 Discussion

Pignolet and Horrocks[84] have studied ligand exchange for a range of tetrahedral nickel (II) and cobalt (II) tertiary phosphine complexes. The phosphines used by these investigators were triphenylphosphine, tri-p-tolylphosphine, and n-butyldiphenylphosphine.

It was hoped to extend this work using the commercially available diphenylmethyl and dimethylphenyl-phosphine ligands. A preliminary investigation was carried out using the ligand diphenylmethylphosphine. Using a concentration of 0.05 mol l^{-1} dichlorobis (diphenylmethylphosphine) cobalt (II) in deuterochloroform,

Figure 5.1

Plot of the observed chemical shift of the methyl protons
versus the mole fraction of ligand for 0.05 mol l^{-1}
dichlorobis(diphenylmethyl phosphine)cobalt (II)
in deuterochloroform at room temperature
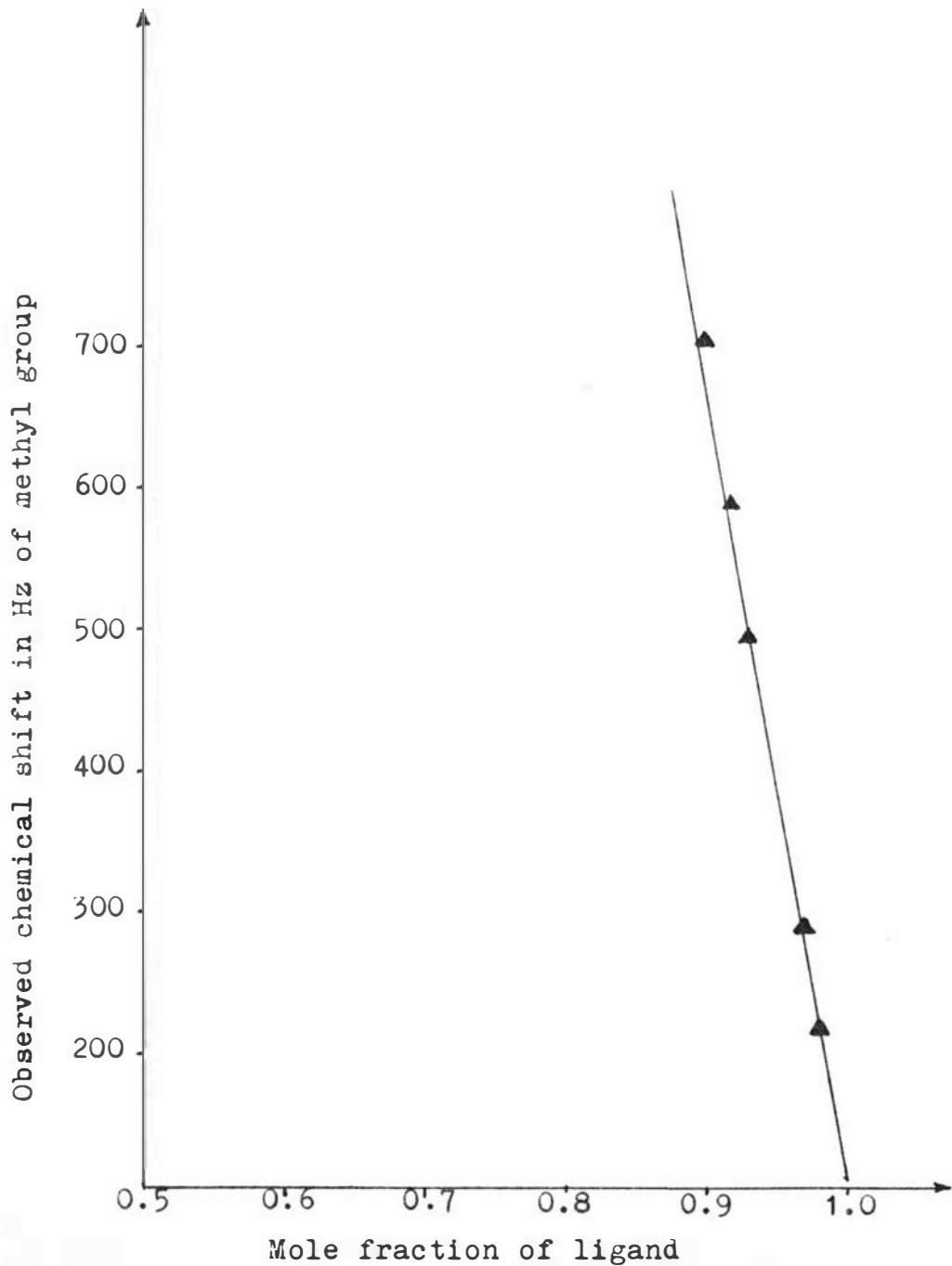
a range of solutions containing excess ligand was made up. These solutions covered a ligand mole fraction range from 0.64 to 0.97.

The reason for choosing these particular phosphines was that the methyl protons provide a simple AB exchange system. In contrast the aromatic protons were not examined as their spectra provide a complex and uninterpretable exchange pattern.

In this particular system enormous chemical shift effects were experienced. Figure 5.1 gives the magnitude of the chemical shifts experienced by the methyl protons in the mole fraction range over 0.9. Below the ligand mole fraction range of 0.9 the NMR signal of the methyl protons was partially obscured or completely obliterated by the NMR resonances of the phenyl ring protons.

Besides these problems, the phosphine complexes with associated ligand decomposed with precipitation, after only several days. It was found that no matter how carefully these samples were made up (the samples were prepared as in section 4.1.3) decomposition occurred. Pignolet and Horrocks[84] also reported decomposition problems with their systems.

From this initial study there were two requirements seen to be needed in choosing a particular Cobalt(II) complex for study. These were; thermal stability of the ligand and complex, and an interpretable NMR spectrum. In choosing a Cobalt(II) tetrahedral complex, a ligand was needed which contained only one or two different types of proton.

5.2 The ligand Trimethylarsine sulphide

5.2.1 Preparation of trimethylarsine sulphide[87]

All glassware was preheated and flushed with dry nitrogen. The reaction was carried out in a 3-litre flask fitted with a double-surface condenser, a nitrogen inlet and a dropping funnel. Methyl Iodide (190 cm^3) in dry di-n-butyl ether (200 cm^3) was added dropwise to magnesium turnings (73 g) in one litre of the same solvent. The reaction was initiated by adding iodine and heating to 50°C. The temperature of the reaction was maintained between 50-70° with the use of an ice-bath. On completion of the grignard, the condenser was replaced by a stirrer and the reaction was cooled to 0°C. Arsenic trichloride (50 cm^3) in di-n-butyl ether (100 cm^3) was then added dropwise over a period of two hours. Vigorous stirring was needed to prevent solidification of the reaction mixture. This stirring was continued at room temperature for an hour, after which the stirrer and dropping funnel were removed and a fractionating column was fitted. Owing to the height restriction of the fume hood the column did not prove to be very efficient. However solid impurities carried over in the distillation process were eliminated by using glass wool in the graduated dropping funnel.

After the fractionating column had been fitted, the temperature of the reaction mixture was gradually raised, using an oil bath, to 160°C. The arsine very quickly distilled off at a temperature of 70°C into a graduated dropping funnel. 65 cm^3 of trimethylarsine

were obtained.   The arsine was added directly to a
3-necked flask containing 19.5 g of sulphur in 200 cm^3
of "super-dry" ethanol.   The mixture was refluxed for
an hour and the excess sulphur then filtered off.   On
cooling, white crystals of trimethylarsine sulphide
(m.p. 183° lit. value 183.4°) were obtained.

5.2.2 <u>Preparation of dihalobistrimethylarsine sulphide
Cobalt(II) Complexes.</u>

The above complexes were prepared by mixing two
hot ethanolic solutions of Me_3AsS and CoX_2 (X = Cl, Br, I)
in a 2:1 molar ratio.   The complexes readily precipitated
on cooling.

5.2.3 <u>Discussion</u>

With the requirement of only one type of proton
satisfied, this ligand appeared to be very suitable.
The ligand trimethylarsine sulphide has been found to
form a number of tetrahedral Cobalt(II) complexes.[87]
The inducement to examine this hard to prepare ligand
was through the reported solubility of these tetrahedral
complexes.   The lengthy preparation of the
trimethylarsine sulphide was carried out and a range of
halo Cobalt(II) complexes was prepared.   The arsine
sulphide ligand was found to be quite soluble in acetone
and chloroform but the Cobalt(II) complexes prepared
from this ligand were not.   The iodo complex of
Cobalt(II) had a solubility in acetone of only 0.01 mol l^{-1},
this being the solvent it was most soluble in.   The
solubility was even further reduced with the addition of
excess trimethylarsine sulphide.   It was not possible to
obtain any NMR information on these insoluble complexes.

Thus a further requirement, that of adequate solubility, must be added in the search for a suitable Cobalt(II) tetrahedral complex.

5.3 Pyrazole type ligands

The following series of compounds represent the most promising of the systems studied in this project. These particular ligands and their associated complexes have good solubility in most solvents. This property is further commented on in the discussion. The ligand preparations (and their Cobalt(II) complexes) are considered in the following order :

3,5-dimethylpyrazole;

1,3,5-trimethylpyrazole;

4-bromo-1, 3,5-trimethylpyrazole;

3,5-dimethyl-1-phenylpyrazole; and

1,4-dimethylpyrazole.

5.3.1 Preparation of 3,5-dimethylpyrazole[88]

65 g (0.5 mole) of hydrazine sulphate was dissolved in 400 cm^3 of 10% NaOH in a one litre round-bottomed flask fitted with separatory funnel, thermometer and stirrer. The flask was immersed in an ice-bath and the mixture was cooled to 15°C. 50 g (0.5 mole) of acetylacetone was added dropwise (temperature being maintained at 15°C) over a period of 30 minutes with subsequent stirring for an hour.

The contents were diluted with 200 cm^3 of water to dissolve the precipitated inorganic salts and then transferred to a one litre separatory funnel and shaken with 125 cm^3 of ether. The aqueous layer was further

extracted with 4 x 40 cm^3 portions of ether. The
ether extracts were combined, washed with saturated
sodium chloride solution and dried over anhydrous
potassium carbonate.

The ether was removed by distillation and the
residue was dried at reduced pressure. The melting
point obtained was 107°C (lit. value 107° - 108°).

Preparation of the dibromobis 3,5-dimethylpyrazole Cobalt(II) Complex[59]

The complex was prepared by mixing two hot
ethanolic ("super-dry" ethanol) solutions of the ligand
(3,5 dimethyl-pyrazole) and cobaltous bromide in the
molar ratio of 2:1. On reducing the volume, dark blue
crystals of the complex were obtained.

5.3.2 Preparation of 1,3,5-trimethyl pyrazole (m.p. 37°C)

The procedure for this preparation is exactly the
same as that for 3,5 dimethyl-pyrazole with
methylhydrazine sulphate being used instead of hydrazine
sulphate. The preparation of methylhydrazine sulphate
is listed below.

Preparation of methylhydrazine sulphate[90]

(A) Benzalazine

The reaction was carried out in a 5-litre round-
bottomed flask fitted with a glass mechanical stirrer.
In this flask were placed 240 g (1.85 moles) of powdered
hydrazine sulphate, 1800 cm^3 of water, and 230 g (207 g,
3.4 moles) of 28% aqueous ammonia (sp. gr. 0.90).
When the hydrazine sulphate was dissolved, 440 cm^3
(460 g, 4.35 moles) of benzaldehyde was added, over a
period of 5 hours, from a separatory funnel. After the

mixture was stirred for a further two hours the
precipitated benzalazine was filtered with suction,
washed with water, and pressed thoroughly on a Buchner
funnel.   This product was dissolved in 800 cm^3 of
boiling 95% ethyl alcohol which on cooling precipitated
the benzalazine in long yellow needles.   The yield of
360 g after drying in a dessicator corresponds very
well with the lit. value of 350-360 g.

(B)   Methyl hydrazine sulphate

200 g (0.96 mole) of the previously prepared
benzalazine, 350 cm^3 of dry, thiophene-free benzene and
100 cm^3 (133 g, 1.05 moles) of dimethyl sulphate were
mixed in a 3-litre round-bottomed flask, provided with
a reflux condenser bearing a calcium chloride tube.
The mixture was heated continuously, with occasional
shaking, on a water bath to gentle refluxing for five
hours.   The mixture was cooled, and the solid addition
product was decomposed by adding 600 cm^3 of water
followed by shaking.   The benzene and the benzaldehyde
were then removed by steam distillation.   The residual
liquor, after cooling, was treated with 20 cm^3 of
benzaldehyde and left overnight.   The resin and
benzalazine were then filtered off.   The filtrate was
checked for unreacted hydrazine sulphate by the addition
of benzaldehyde (5 cm^3).   It was found to take about
six cycles of filtering, addition of benzaldehyde,
filtering again to remove any remaining unreacted
hydrazine sulphate.

The treated filtrate was then evaporated under
reduced pressure (rotary-evaporator) until a viscous

mass remained which was further dessicated by evaporating twice, in vacuo, with 50 cm^3 portions of absolute ethyl alcohol. The crystalline mass was filtered and purified by dissolving in 250 cm^3 of boiling 80% ethanol. On cooling, white crystals of methyl hydrazine sulphate precipitated and were filtered and dried. The yield was 38 g (25% of theoretical) with melting point 142°C (lit. value 141-142°).

5.3.3 <u>Preparation of 4-bromo-1,3,5-trimethyl pyrazole</u>

7.75 g (72.5 mmoles) of 1,3,5-trimethyl pyrazole was dissolved in 50 cm^3 of chloroform and was then slowly mixed with 11.6 g (145 m moles) of bromine in 30 cm^3 of chloroform under ice-cooling.

After refluxing for 90 minutes the solution was cooled and a saturated sodium carbonate solution was added until the mixture was colourless. The chloroform layer with the pyrazole was separated and on removal of the chloroform, 1,3,5-trimethyl-4-bromo-pyrazole (m.p. 32°C, lit. value 32-34°C) was obtained.

<u>Preparation of dichlorobis (1,3,5-trimethyl-4,bromo) -pyrazole Cobalt(II)</u>

This complex was prepared in a similar manner to the previous pyrazole cobalt complexes, with the ligand to complex mole ratio 2:1. Dark blue crystals were obtained.

5.3.4 <u>Preparation of 3,5-dimethyl-1-phenylpyrazole</u>[91]

10.8 g (0.1 mole) of phenyl hydrazine and a solution of 5,7-dimethyl-2,3-benzo-1,4-diazepinium chloride dihydrate (9.78 g, 0.04 mole) in 400 cm^3 of

water was shaken vigorously. The mixture was extracted with ether, and the extract was washed with aqueous sodium carbonate and then with water, dried over sodium sulphate and evaporated. The residual orange oil was distilled at 269-270°C to give the dimethylphenylpyrazole.

Preparation of dichloro bis(3,5-dimethyl-1-phenyl pyrazole) Cobalt(II)

This complex was formed from mixing two hot ethanolic solutions of the ligand and anhydrous cobalt chloride (mole ration 2:1). A blue complex was formed.

5.3.5 Attempted Preparation of 1,4-dimethyl pyrazole.

This preparation was attempted by two different methods, both of which are described in the following sections.

Method One[92]

This first method is the reaction of α-methyl-β-dimethyl amino-acrolein with methyl hydrazine sulphate to form 1,4 dimethyl pyrazole.

Preparation of α-methyl-β-dimethylamino-acrolein

To a 3-litre round-bottomed flask fitted with dropping funnel and mechanical stirrer containing 183 g (2.5 moles) of N,N-dimethyl formamide dissolved in 400 cm^3 of dichloroethane, 110 g (1.1 mole) of phosgene was introduced under ice-cooling and vigorous stirring. The resulting white precipitate was diluted with 200 cm^3 of dichloroethane and then mixed dropwise over an hour with 132 g (150 cm^3) of propionaldehyde acetal (see the following section for a description of the preparation of

this compound).

The solution was slowly warmed to $75^{\circ}C$ (bath temperature) and maintained at this temperature for fifteen minutes. During this time the adduct dissolved. Thirty grams of ice were now added, and the solution was decomposed with a concentrated potassium carbonate solution (158 g in 150 cm^3 of water). A vigorous evolution of fumes was observed initially. The reaction mixture was left overnight and the following day was reduced in volume from approximately 2.5 litres to 500 cm^3.

The now precipitated KCl was dissolved in 350 cm^3 H_2O and was extracted with 7 x 100 cm^3 portions of chloroform. The chloroform was dried with anhydrous potassium carbonate and was distilled off. The remaining dimethyl formamide was removed by vacuum distillation (water-pump). Less than 1% of the expected product was obtained.

The phosgene used in the experiment was a 20% solution in toluene. The conclusion reached was that the excess toluene (volume used 550 cm^3) quenched the reaction. A further attempt was made by boiling the phosgene out of the toluene and into the reaction mixture (the reaction mixture kept under cooling conditions). This attempt was also unsuccessful. Further attempts were not possible as no other supply of phosgene was available in New Zealand.

Preparation of propionaldehyde acetal[93]

In a 2.5 litre bottle, 525 g (650 cm^3 10.85 moles) of 95% ethanol and 100 g (0.9 moles) of granular anhydrous

calcium chloride were placed. The mixture was cooled to below $8^{\circ}C$ by an ice-bath and 330.6 g (413 cm^3, 5.2 moles) of propionaldehyde (B.D.H. and R.D.H. Hanover) was added slowly down the sides of the bottle so that it formed a layer on the alcoholic calcium chloride. The bottle was then tightly stoppered (cork-stopper) and shaken vigorously for a few minutes. It was then allowed to stand at room temperature with intermittent shaking for two days.

The upper layer was then separated and washed three times with 200 cm^3 portions of water. The oil was dried by standing over 24 g of anhydrous potassium carbonate and the fraction distilling at $123^{\circ}C$ (lit. value $123^{\circ}C$) was collected in good yield.

Method Two[94]

This method uses the procedure of methylation of the 4-methyl-3(5)-pyrazole carbonic acid ester by dimethyl sulphate (freshly distilled) in a 20% NaOH solution. Several attempts at this method were made without success. Methods of preparation for the compounds that were required to be made for this preparation are as follows.

Preparation of 4-methyl-3(5) pyrazolecarbonic ester[a]

10 g (0.1 mole) of crotonic acid methyl ester[b] was introduced into an equimolar amount of ethereal diazomethane[c] solution (from nitroso-methyl urea[d]). After three hours an equimolar amount of Br_2 (16 g) was dropped into the cooled solution. The oxidation product precipitated as a colourless paste, and was digested with sodium carbonate solution and recrystallised from diluted alcohol to give the ester of m.p. $170^{\circ}C$.

Preparation of crotonic acid methyl ester[b]

100 g of crotonic acid was dissolved in 1000 cm^3 methanol containing 10 cm^3 of H_2SO_4. This mixture was refluxed for 3.5 hours. The excess of methanol was then removed by distillation and the ester liberated by the addition of water (500 cm^3). The ester was extracted by ether, washed with water, and then dried over $MgSO_4$. The ether was removed and the residue was distilled yielding 40 g of ester at 120°C.

Preparation of diazomethane[c] [95]

100 cm^3 of ether was added to 30 cm^3 of 40% KOH and the mixture was cooled to 5°C. To this, with continued cooling and shaking, was added 10 g of finely powdered nitrosomethyl urea over a period of two minutes. The deep yellow layer, containing 2.8 g of diazomethane, together with some dissolved impurities and water, was then decanted.

Preparation of nitrosomethyl urea[d] [96]

In a tared 1-litre flask, 200 g (1.5 mole) of 25% aqueous (w/v) methylamine solution was placed. To this flask concentrated HCl was added until the solution was acid to methyl red (approximately 155 cm^3 of acid was required). Water was then added until the total weight was 500 g. 300 g of urea was added, and the solution was boiled gently for three hours and vigorously for 1/4 hour. The solution was cooled to room temperature, 110 g of $NaNO_2$ (98% $NaNO_2$) was dissolved in it, and the mixture was cooled to 0°C. The mixture of 600 g of ice and 100 g of concentrated H_2SO_4 in a 3-litre beaker was surrounded by a salt-ice-bath mixture

and the cold methyl urea-nitrate solution was run in slowly with mechanical stirring such that the temperature did not rise above $0^{\circ}C$.

The nitrosomethyl urea rose to the surface as a crystalline foamy precipitate which was filtered quickly. The crystals were stirred to a paste with about 50 cm^3 of cold water and sucked as dry as possible. The product was then dried on a vacuum line.

5.3.6 Discussion.

The first tetrahedral cobalt(II) complexes of the pyrazoles were reported in 1970.[89] The ligands that were used were 3,5-dimethylpyrazole and 1,3,5-trimethyl-pyrazole. Bagley et al[89] reported the solubility and retention of tetrahedral configuration in solution of these complexes. The failure of these two ligands to give six-co-ordinate complexes was attributed to the steric effects of the substituents on the 3 and 5 (or 1) positions.

The 3,5-dimethylpyrazole was the first ligand prepared and the dichloro cobalt(II) complex made. An NMR study of the complex and free ligand showed ligand exchange taking place as there was no separation of the free and co-ordinated NMR signals. A ligand mole fraction range was made using a concentration of 0.05 mol l^{-1} for the complex. Figure (5.2) shows the results of this investigation at one temperature.

As can be seen from the figure, the plot of observed chemical shift versus mole fraction of ligand was not linear. This meant that information such as the chemical shift of the complex (mole fraction of ligand equals zero) was unobtainable. As this is

Figure 5.2

Plot of the observed chemical shift of the methyl protons
versus the mole fraction of ligand for 0.05 mol l^{-1}
dichlorobis(3,5-dimethyl pyrazole)cobalt (II)
in deuterochloroform at 53.5°C
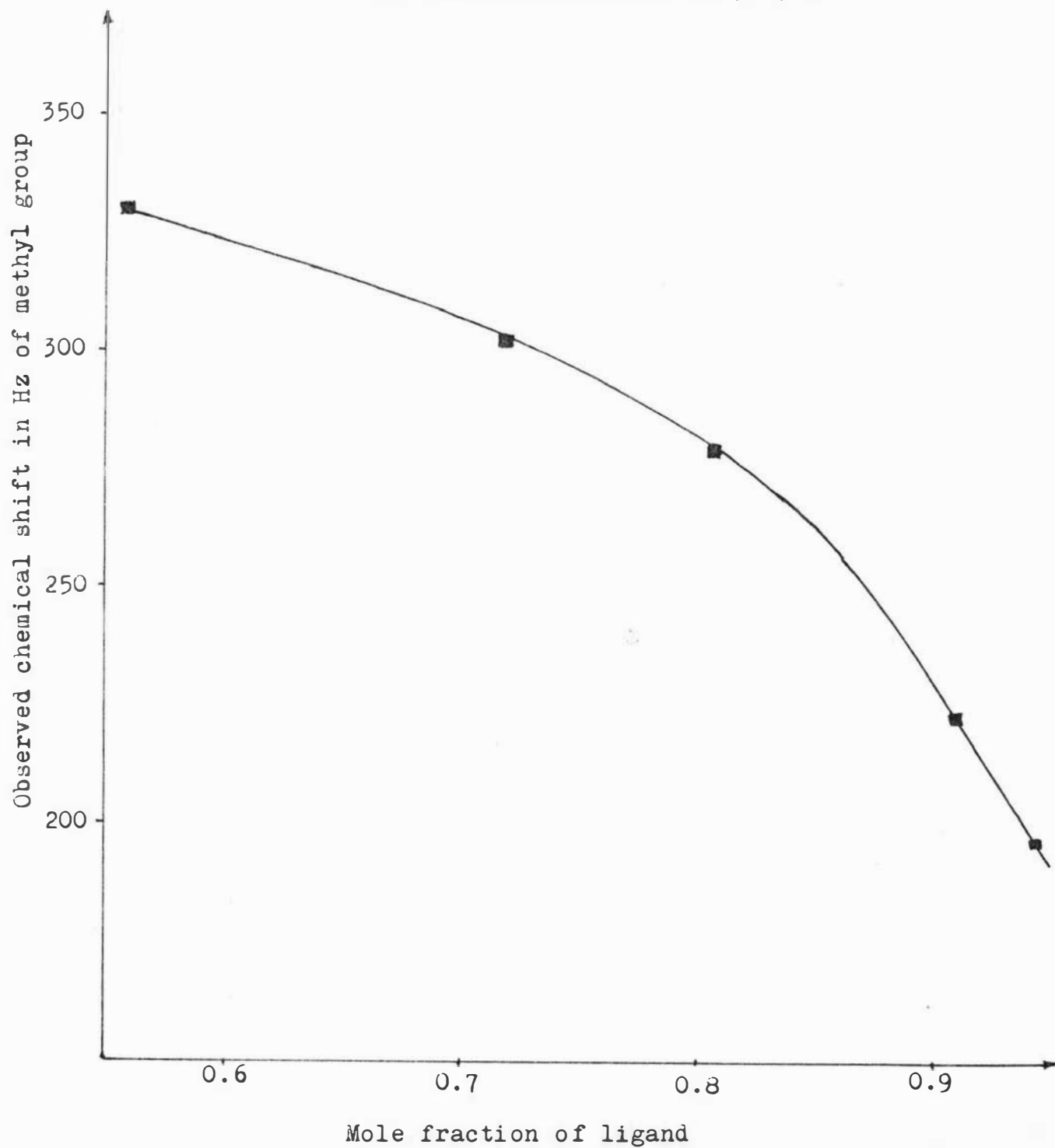
essential to obtaining accurate rate information this particular ligand was not suitable.

A possible cause of the curvature in Figure (5.2) is the effect of dimerization. Dimerization is known to occur in 3,5-dimethylpyrazole resulting in chains of ligands in solution thus making uncertain the mole fraction of free ligand at any concentration or temperature.

An important result of this study was that exchange was seen to take place in these systems. The ligand, 1,3,5-trimethylpyrazole and its associated Cobalt(II) halo-complexes were then made as the methyl in the one position would eliminate the hydrogen bond associative effects.

For any temperature, separation of the free and co-ordinated ligand signals occurred in a deuterochloroform solution of dichlorobis (1,3,5-trimethylpyrazole) Cobalt(II) containing excess trimethylpyrazole. The addition of the methyl group to pyrazole is known to have an additive incremental effect on the $pK_{BH}+$ value[97] (in other words it makes the pyrazole a better base). For the condition of "fast exchange" in an NMR experiment the ligand 1,3,5-trimethylpyrazole was non-labile.

An attempt to reduce the basicity of the trimethylpyrazole was made by brominating the 4-position. A new Cobalt (II) complex was formed, dichlorobis (1,3,5-trimethyl-4-bromo-pyrazole) Cobalt (II). Again, like the other pyrazoles, this complex proved to be very soluble. On a preliminary NMR investigation this complex and excess ligand again showed separation of the free and unco-ordinated ligand signals (ligand non-lability).

A last attempt was made to find a suitable ligand for a definitive study. With the pyrazole type ligand readily forming complexes and not suffering from the problems of chemical instability and decomposition, the ligand 1,4-dimethylpyrazole was selected. With this ligand the hydrogen bonding problems of the 3,5 dimethyl-pyrazole should be eliminated. Also the ligand should prove to be labile in contrast to the 1,3,5-trimethylpyrazole as it contains only two methyl groups.

As can be seen from the preparative section, several attempts were made to prepare this ligand without success. Another pyrazole was made at the same time, 3,5-dimethyl-1-phenylpyrazole.[98] This ligand forms a tetrahedral complex with anhydrous cobaltous chloride but unfortunately the excess ligand (impurities in the oil) reacts with the complex in making up samples for NMR measurement.

5.4 Conclusions

In finding a suitable Cobalt(II) tetrahedral complex for an NMR rate study a number of problems arose. Firstly the complex and ligand must be reasonably soluble and stable. In particular the complex must be stable and soluble in the presence of a significant excess of the free ligand. The second point is that the complex must remain in a tetrahedral conformation over a large temperature range and in the presence of excess ligand. The final point relating to the ligand is that its NMR spectrum must be interpretable, that is the ligand should not contain more than two types of proton.

With these requirements, the pyrazoles seem to be the most suitable ligands presently available.

If the problem of obtaining a satisfactory method of preparation for 1,4-dimethylpyrazole is solved, perhaps a new ligand exchange system involving Cobalt(II) will be found.

APPENDIX 1

INPUT FOR PROGRAM DENSITY MATRIX

The data cards are as follows:

First card: This card contains the case number (NCASE) signifying the number of jobs and an identifying name, e.g. 4-NITROSO-K-SALT IN D_2O Aug, 74. NCASE may be between 1 and 99. The FORMAT of the card is (I2, 19A4).

Second card: The coupling constants (AJ12, AJ13, AJ14, AJ23, AJ24, AJ34) are punched on this card. FORMAT (8F 10.6).

Third card: This card contains the chemical shifts (W1, W2, W3, W4). FORMAT (8F10.6).

Fourth card: The inverse of the spin-spin relaxation rate TTWO is read on this card. FORMAT (8F10.6).

Fifth card: The lower (WI) and upper (WU) limits of the frequency range for which the density matrix is to calculate a theoretical spectrum is read on this card. Also read is DELTA. DELTA is the amount by which the frequency increases for each successive data point till WU is reached. FORMAT (8F10.6)

Sixth card: This card reads RTOR (inverse τ) or the rotational rate. FORMAT (8F10.6).

If different frequency ranges and rotational rates are wanted (a range of theoretical spectra), this is signified by the case number. Thus if there is more than one job the seventh card contains (WI)', (WU)', and (DELTA)'. The eighth (RTOR)' ... eleventh card (WI)", (WU)", (DELTA)", twelth card (RTOR)" and so on till the number of cases is finished.

An END OF JOB card signifies the end of the run.

STRUCTURE OF THE PROGRAM

Statement number or comment (C)	Comment
C READ IN INPUT DATA 500	Following this the data are read in from punched cards, chemical shifts, coupling constants, etc.
501-503	Print instructions for output; headings, frequencies and calculated intensities.
C SET UP MATRIX	As mentioned in Chapter Three the 112 x 112 matrix is divided into four matrices for solving. Here the first 8 x 8 matrix is set up.
1050-1051	This is setting up the B matrix as discussed in Chapter Three for the AB case (AX = B). The terms in the matrix can be set equal to one as this merely alters the scale of the theoretical spectrum.
1020-1021	The first A matrix (8 x 8) is set up by initially setting all the elements of the matrix to zero and then building up the matrix.
1008-1037	This holds the A and B matrices for solution by the subroutine SIMQ which is a standard matrix inversion program.
1100	SUM(L) is the solution of the matrix inversion ($X = A^{-1} B$) : for the 8 x 8 matrix this is $B(2) + B(4) + B(6) + B(8)$. For a particular frequency, this is the intensity.
1010-1013	This enables the first 8 x 8 matrix to be solved for the whole frequency range.

Statement number or comment (C)	Comment
2011	This is the commencement of the second 8 x 8 matrix. The frequency is reset to WI.
2020	The matrix elements are set equal to 0.0 for A.
2021 - C SOLUTION ...	The second 8 x 8 A matrix is set up.
2008-2037	The subroutine SIMQ solves $(X = A^{-1}B)$.
2100	SUM(L) is the addition of the intensities plus the previous SUM(L) from the first matrix.
2010-2013	The second 8 x 8 matrix is solved for the frequency range WI to WU.
C ORIGINAL KWJO2 3011	This is the commencement of the third matrix (48 x 48). All the elements of the B matrix are set at 0.0.
3050	The B matrix is set up.
99	The 48 x 48 A matrix is set up with all elements equal to 0.0.
20-44 to C ORIGINAL KWJO1	The third A (48 x 48) matrix is set up.
3008-3016	The third matrix is solved by matrix inversion (SIMQ).
3100	The intensity SUM(L) is found. To this is added the previous intensity found for that particular frequency.

Statement number or comment (C)	Comment
3010 3007-3006	This enables the frequency range (WI-WU) to be solved.
C PDB02 4011	This fourth B matrix is set up for the final 48 x 48 A matrix. The frequency is initialized at WI.
239	The A matrix elements are set equal to O.O.
266 - C ORIGINAL PDB01	The final A matrix is set up.
4008-4016	SIMQ solves $(X = A^{-1}B)$.
4100	The total intensity for each frequency is found by SUM(L).
WRITE (3,4) W, SUM(L)	The results are printed out of frequency with corresponding intensity.
4010-4006	The fourth matrix is solved for the frequency range WI to WU.
5011-5012	If the number of cases is finished the results are printed. If not the next job involving a new frequency range and rotational rate is commenced.
SUBROUTINE SIMQ.	This subroutine is a matrix inversion program.

PROGRAM LISTING

The listing of DENSITY MATRIX appears on the remaining pages of this Appendix.

```
FILE   2=LINEINPUTDATA,UNIT=READER                                          1
FILE   3=LINEOUTPUTDATA,UNIT=PRINTER
C       ORIGINAL KWJ03
       INTEGER G
       INTEGER P
       DIMENSION A(2304),AA(2304),B(48),BB(48),SUM(500),NAME(19)
       NCAS=1
C READ IN INPUT DATA
       READ(2,2000)NCASE,NAME
       READ (2,1)AJ12,AJ13,AJ14,AJ23,AJ24,AJ34
       READ (2,1)W1,W2,W3,W4
       READ(2,1)TTWO
   500 READ(2,1)WI,WU,DELTA
       READ(2,1)RTOR
C WRITE PRELIMINARY DATA
       IF(NCAS-1)502,502,501
   501 WRITE(3,5500)NCAS,RTOR
       GO TO 503
   502 WRITE(3,2500)NAME
       WRITE(3,3000)
       WRITE(3,4000)W1,W2,W3,W4
       WRITE(3,7000)
       WRITE(3,8000)AJ12,AJ13,AJ14,AJ23,AJ24,AJ34
       WRITE(3,5000)TTWO,RTOR
   503 WRITE(3,6000)
C SET UP MATRIX
       DO 1050 I=1,9
  1050 BB(I)=0.0
       DO 1051 I=2,9,2
  1051 BB(I)=1.0
       W=WI
       BJ12=0.5*AJ12
       BJ13=0.5*AJ13
       BJ14=0.5*AJ14
       BJ23=0.5*AJ23
       BJ24=0.5*AJ24
       BJ34=0.5*AJ34
       DO 1020 I=1,64
  1020  AA(I)=0.0
       DO 1021 I=1,64,9
  1021  AA(I)=-TTWO-RTOR
       AA(3)=RTOR
```

```
      AA(12)=RTOR
      AA(17)=RTOR
      AA(26)=RTOR
      AA(39)=RTOR
      AA(48)=RTOR
      AA(53)=RTOR
      AA(62)=RTOR
      AA(4)=BJ34
      AA(6)=BJ24
      AA(8)=BJ14
      AA(11)=-BJ34
      AA(13)=-BJ24
      AA(15)=-BJ14
      AA(18)=BJ34
      AA(22)=BJ23
      AA(24)=BJ13
      AA(25)=-BJ34
      AA(29)=-BJ23
      AA(31)=-BJ13
      AA(34)=BJ24
      AA(36)=BJ23
      AA(40)=BJ12
      AA(41)=-BJ24
      AA(43)=-BJ23
      AA(47)=-BJ12
      AA(50)=BJ14
      AA(52)=BJ13
      AA(54)=BJ12
      AA(57)=-BJ14
      AA(59)=-BJ13
      AA(61)=-BJ12
      AA(2)=-BJ14-BJ24-BJ34+W-W4
      AA(9)=-AA(2)
      AA(20)=-BJ13-BJ23-BJ34+W-W3
      AA(27)=-AA(20)
      AA(38)=-BJ12-BJ23-BJ24+W-W2
      AA(45)=-AA(38)
      AA(56)=-BJ12-BJ13-BJ14+W-W1
      AA(63)=-AA(56)
C SOLUTION OF THE MATRIX AND PRINT OUT OF THE SOLUTION
      N=8
      L=0
 1008 DO 1009 J=1,64
 1009 A(J)=AA(J)
      DO 1037 J=1,8
 1037 B(J)=BB(J)
      CALL SIMQ(A,B,N,KS)
```

```
      IF (KS) 999,1100,999
 1100 L=L+1
      SUM(L)=B(2)+B(4)+B(6)+B(8)
      P=2
      W=W+DELTA
      IF(W-WU)1010,1010,2011
 1010  AA(P)=AA(P)+DELTA
      IF(P-55) 1007,1014,1014
 1007 P=P+18
       GO TO 1010
 1014 P=9
 1012 AA(P)=AA(P)-DELTA
      IF(P-62)1013,1008,1008
 1013 P=P+18
      GO TO 1012
C     ORIGINAL KWJ04
 2011 CONTINUE
      W=WI
      DO  2020 I=1,64
 2020 AA(I)=0.0
      DO 2021 I=1,64,9
 2021 AA(I)=-TTWO-RTOR
      AA(3)=RTOR
      AA(12)=RTOR
      AA(17)=RTOR
      AA(26)=RTOR
      AA(39)=RTOR
      AA(48)=RTOR
      AA(53)=RTOR
      AA(62)=RTOR
      AA(4) =-BJ12
      AA(6)=-BJ13
      AA(8)=-BJ14
      AA(11)=BJ12
      AA(13)=BJ13
      AA(15)=BJ14
      AA(18)=-BJ12
      AA(22)=-BJ23
      AA(24)=-BJ24
      AA(25)=BJ12
      AA(29)=BJ23
      AA(31)=BJ24
      AA(34)=-BJ13
      AA(36)=-BJ23
      AA(40)=-BJ34
      AA(41)=BJ13
      AA(43)=BJ23
```

```
       AA(47)=BJ34
       AA(50)=-BJ14
       AA(52)=-BJ24
       AA(54)=-BJ34
       AA(57)=BJ14
       AA(59)=BJ24
       AA(61)=BJ34
       AA(2)=BJ12+BJ13+BJ14+W-W1
       AA(9)=-AA(2)
       AA(20)=BJ12+BJ23+BJ24+W-W2
       AA(27)=-AA(20)
       AA(38)=BJ13+BJ23+BJ34+W-W3
       AA(45)=-AA(38)
       AA(56)=BJ14+BJ24+BJ34+W-W4
       AA(63)=-AA(56)
C SOLUTION OF THE MATRIX AND PRINT OUT OF THE SOLUTION
       L=0
  2008 DO 2009 J=1,64
  2009 A(J)=AA(J)
       DO 2037 J=1,8
  2037 B(J)=BB(J)
       CALL SIMQ(A,B,N,KS)
       IF(KS)999,2100,999
  2100 L=L+1
       SUM(L)=B(2)+B(4)+B(6)+B(8)+SUM(L)
       P=2
       W=W+DELTA
       IF(W-WU) 2010,2010,3011
  2010 AA(P)=AA(P)+DELTA
       IF(P-55)2007,2014,2014
  2007 P=P+18
       GO TO 2010
  2014 P=9
  2012 AA(P)=AA(P)-DELTA
       IF(P-62) 2013,2008,2008
  2013 P=P+18
       GO TO 2012
C         ORIGINAL KWJ02
  3011 DO 3050 I=1,48
  3050 BB(I)=0.0
       BB(2)=1.0
       BB(4)=1.0
       BB(8)=1.0
       BB(14)=1.0
       BB(18)=1.0
       BB(22)=1.0
       BB(28)=1.0
```

```
      BB(30)=1.0
      BB(36)=1.0
      BB(44)=1.0
      BB(46)=1.0
      BB(48)=1.0
      W=WI
      DO 99 G=1,2304
99    AA(G)=0.0
      DO 20 G=38,528,98
20    AA(G)=-BJ14
      DO 21 G=85,575,98
21    AA(G)= BJ14
      DO 22 G=26,516,98
22    AA(G)=-BJ24
      DO 23 G=73,563,98
23    AA(G)= BJ24
      DO 24 G=614,1104,98
24    AA(G)=-BJ13
      DO 25 G=661,1151,98
25    AA(G)= BJ13
      DO 26 G=14,504,98
26    AA(G)=-BJ34
      DO 27 G=61,551,98
27    AA(G)= BJ34
      DO 28 G=602,1092,98
28    AA(G)=-BJ23
      DO 29 G=649,1139,98
29    AA(G)= BJ23
      DO 30 G=1190,1680,98
30    AA(G)=-BJ12
      DO 31 G=1237,1727,98
31    AA(G)= BJ12
      DO 32 G=1730,2220,98
32    AA(G)=-BJ14
      DO 33 G=1777,2267,98
33    AA(G)= BJ14
      DO 34 G=1154,1644,98
34    AA(G)=-BJ24
      DO 35 G=1201,1691,98
35    AA(G)= BJ24
      DO 36 G=1742,2232,98
36    AA(G)=-BJ13
      DO 37 G=1789,2279,98
37    AA(G)= BJ13
      DO 38 G=578,1068,98
38    AA(G)=-BJ34
      DO 39 G=625,1115,98
```

```
39 AA(G)= BJ34
   DO 40 G=1166,1656,98
40 AA(G)=-BJ23
   DO 41 G=1213,1703,98
41 AA(G)= BJ23
   DO 42 G=1754,2244,98
42 AA(G)=-BJ12
   DO 43 G=1801,2291,98
43 AA(G)= BJ12
   DO 44 G=1,2304,49
44 AA(G)=-TTWO-RTOR
   AA(4)= BJ23
   AA(6)= BJ24
   AA(8)= BJ13
   AA(10)=BJ14
   AA(51)=-BJ23
   AA(53)=-BJ24
   AA(55)=-BJ13
   AA(57)=-BJ14
   AA(98)= B 23
   AA(102)= B 34
   AA(104)= BJ12
   AA(108)= BJ14
   AA(145)=-BJ23
   AA(149)=-BJ34
   AA(151)=-BJ12
   AA(155)=-BJ14
   AA(194)= BJ24
   AA(196)= BJ34
   AA(202)= BJ12
   AA(204)= BJ13
   AA(241)=-BJ24
   AA(243)=-BJ34
   AA(249)=-BJ12
   AA(251)=-BJ13
   AA(290)= BJ13
   AA(292)= BJ12
   AA(298)= BJ34
   AA(300)= BJ24
   AA(337)=-BJ13
   AA(339)=-BJ12
   AA(345)=-BJ34
   AA(347)=-BJ24
   AA(386)= BJ14
   AA(390)= BJ12
   AA(392)= BJ34
   AA(396)= BJ23
```

6

```
AA(433)=-BJ14
AA(437)=-BJ12
AA(439)=-BJ34
AA(443)=-BJ23
AA(484)= BJ14
AA(486)= BJ13
AA(488)= BJ24
AA(490)= BJ23
AA(531)=-BJ14
AA(533)=-BJ13
AA(535)=-BJ24
AA(537)=-BJ23
AA(592)= BJ23
AA(594)= BJ24
AA(596)= BJ13
AA(598)= BJ14
AA(639)=-BJ23
AA(641)=-BJ24
AA(643)=-BJ13
AA(645)=-BJ14
AA(686)= BJ23
AA(690)= BJ34
AA(692)= BJ12
AA(696)= BJ14
AA(733)=-BJ23
AA(737)=-BJ34
AA(739)=-BJ12
AA(743)=-BJ14
AA(782)= BJ24
AA(784)= BJ34
AA(790)= BJ12
AA(792)= BJ13
AA(829)=-BJ24
AA(831)=-BJ34
AA(837)=-BJ12
AA(839)=-BJ13
AA(878)= BJ13
AA(880)= BJ12
AA(886)= BJ34
AA(888)= BJ24
AA(925)=-BJ13
AA(927)=-BJ12
AA(933)=-BJ34
AA(935)=-BJ24
AA(974)= BJ14
AA(978)= BJ12
AA(980)= BJ34
```

```
AA(984)= BJ23                                    8
AA(1021)=-BJ14
AA(1025)=-BJ12
AA(1027)=-BJ34
AA(1031)=-BJ23
AA(1072)= BJ14
AA(1074)= BJ13
AA(1076)= BJ24
AA(1078)= BJ23
AA(1119)=-BJ14
AA(1121)=-BJ13
AA(1123)=-BJ24
AA(1125)=-BJ23
AA(1180)= BJ23
AA(1182)= BJ24
AA(1184)= BJ13
AA(1186)= BJ14
AA(1227)=-BJ23
AA(1229)=-BJ24
AA(1231)=-BJ13
AA(1233)=-BJ14
AA(1274)=+BJ23
AA(1278)=+BJ34
AA(1280)=+BJ12
AA(1284)=+BJ14
AA(1321)=-BJ23
AA(1325)=-BJ34
AA(1327)=-BJ12
AA(1331)=-BJ14
AA(1370)= BJ24
AA(1372)= BJ34
AA(1378)= BJ12
AA(1380)= BJ13
AA(1419)=-BJ34
AA(1425)=-BJ12
AA(1427)=-BJ13
AA(1466)= BJ13
AA(1468)= PJ12
AA(1474)= BJ34
AA(1476)= BJ24
AA(1513)=-BJ13
AA(1515)=-BJ12
AA(1521)=-BJ34
AA(1523)=-BJ24
AA(1562)= BJ14
AA(1566)= BJ12
AA(1568)= PJ34
```

```
AA(1572)= BJ23
AA(1609)=-BJ14
AA(1613)=-BJ12
AA(1615)=-BJ34
AA(1619)=-BJ23
AA(1660)= BJ14
AA(1662)= BJ13
AA(1664)= BJ24
AA(1666)= BJ23
AA(1707)=-BJ14
AA(1709)=-BJ13
AA(1711)=-BJ24
AA(1713)=-BJ23
AA(1768)= BJ23
AA(1770)= BJ24
AA(1772)= BJ13
AA(1774)= BJ14
AA(1815)=-BJ23
AA(1817)=-BJ24
AA(1819)=-BJ13
AA(1821)=-BJ14
AA(1862)= BJ23
AA(1866)= BJ34
AA(1868)= BJ12
AA(1872)= BJ14
AA(1909)=-BJ23
AA(1913)=-BJ34
AA(1915)=-BJ12
AA(1919)=-BJ14
AA(1958)= BJ24
AA(1960)= BJ34
AA(1966)= BJ12
AA(1968)= BJ13
AA(2005)=-BJ24
AA(2007)=-BJ34
AA(2013)=-BJ12
AA(2015)=-BJ13
AA(2054)= BJ13
AA(2056)= BJ12
AA(2062)= BJ34
AA(2064)= BJ24
AA(2101)=-BJ13
AA(2103)=-BJ12
AA(2109)=-BJ34
AA(2111)=-BJ24
AA(2150)= BJ14
AA(2154)= BJ12
```

9

```
AA(2156)= BJ34
AA(2160)= BJ23
AA(2197)=-BJ14
AA(2201)=-BJ12
AA(2203)=-BJ34
AA(2207)=-BJ23
AA(2248)= BJ14
AA(2250)= BJ13
AA(2252)= BJ24
AA(2254)= BJ23
AA(2295)=-BJ14
AA(2297)=-BJ13
AA(2299)=-BJ24
AA(2301)=-BJ23
AA(2)=BJ34-BJ23-BJ13+W-W3
AA(49)=-AA(2)
AA(100)=BJ24-BJ23-BJ12+W-W2
AA(147)=-AA(100)
AA(198)=BJ14-BJ13-BJ12+W-W2-W3+W4
AA(245)=-AA(198)
AA(296)=BJ14-BJ12-BJ13+W-W1
AA(343)=-AA(296)
AA(394)=BJ24-BJ23-BJ12+W-W1-W3+W4
AA(441)=-AA(394)
AA(492)=BJ34-BJ13-BJ23+W-W1-W2+W4
AA(539)=-AA(492)
AA(590)=BJ34-BJ24-BJ14+W-W4
AA(637)=-AA(590)
AA(688)=BJ13-BJ12-BJ14+W-W2-W4+W3
AA(735)=-AA(688)
AA(786)=BJ23-BJ12-BJ24+W-W2
AA(833)=-AA(786)
AA(884)=BJ23-BJ12-BJ24+W-W1-W4+W3
AA(931)=-AA(884)
AA(982)=BJ13-BJ12-BJ14+W-W1
AA(1029)=-AA(982)
AA(1080)=BJ34-BJ24-BJ14+W-W1-W2+W3
AA(1127)=-AA(1080)
AA(1178)=BJ12-BJ13-BJ14+W-W3-W4+W2
AA(1225)=-AA(1178)
AA(1276)=BJ24-BJ14-BJ34+W-W4
AA(1323)=-AA(1276)
AA(1374)=BJ23-BJ13-BJ34+W-W3
AA(1421)=-AA(1374)
AA(1472)=BJ23-BJ13-BJ34+W-W1-W4+W2
AA(1519)=-AA(1472)
AA(1570)=BJ24-BJ34-BJ14+W-W1-W3+W2
```

```
AA(1617)=-AA(1570)                              11
AA(1668)=BJ12-BJ14-BJ13+W-W1
AA(1715)=-AA(1668)
AA(1766)=BJ12-BJ24-BJ23+W-W3-W4+W1
AA(1813)=-AA(1766)
AA(1864)=BJ13-BJ34-BJ23+W-W2-W4+W1
AA(1911)=-AA(1864)
AA(1962)=BJ14-BJ34-BJ24+W-W2-W3+W1
AA(2009)=-AA(1962)
AA(2060)=BJ14-BJ34-BJ24+W-W4
AA(2107)=-AA(2060)
AA(2158)=BJ13-BJ34-BJ23+W-W3
AA(2205)=-AA(2158)
AA(2256)=BJ12-BJ24-BJ23+W-W2
AA(2303)=-AA(2256)
AA(13)=RTOR
AA(62)=RTOR
AA(117)=RTOR
AA(166)=RTOR
AA(211)=RTOR
AA(260)=RTOR
AA(305)=RTOR
AA(354)=RTOR
AA(399)=RTOR
AA(448)=RTOR
AA(503)=RTOR
AA(552)=RTOR
AA(577)=RTOR
AA(626)=RTOR
AA(681)=RTOR
AA(730)=RTOR
AA(775)=RTOR
AA(824)=RTOR
AA(869)=RTOR
AA(918)=RTOR
AA(963)=RTOR
AA(1012)=RTOR
AA(1067)=RTOR
AA(1116)=RTOR
AA(1189)=RTUR
AA(1234)=RTOR
AA(1293)=RTOR
AA(1342)=RTOR
AA(1387)=RTUR
AA(1436)=RTOR
AA(1481)=RTOR
AA(1530)=RTOR
```

```
       AA(1575)=RTOR
       AA(1624)=RTOR
       AA(1679)=RTOR
       AA(1728)=RTOR
       AA(1753)=RTOR
       AA(1802)=RTOR
       AA(1857)=RTOR
       AA(1906)=RTOR
       AA(1951)=RTOR
       AA(2000)=RTOR
       AA(2045)=RTOR
       AA(2094)=RTOR
       AA(2139)=RTOR
       AA(2188)=RTOR
       AA(2243)=RTOR
       AA(2292)=RTOR
C        ORIGINAL KWJ01
       N=48
       L=0
 3008 DO 3009 J=1,2304
 3009 A(J)=AA(J)
       DO 3016  K=1,48
 3016 B(K)=BB(K)
       CALL SIMQ(A,B,N,KS)
       IF(KS) 999,3100,999
 3100 L=L+1
       SUM(L)=B(2)+B(4)+B(8)+B(14)+B(18)+B(22)+B(28)+B(30)+B(36)+B(44)+B
      1(46)+B(48)+SUM(L)
       P=2
       W=W+DELTA
       IF(W-WU) 3010,3010,4011
 3010  AA(P)=AA(P)+DELTA
 3007 P=P+47
       AA(P)=AA(P)-DELTA
       IF(P-2300) 3006,3008,3008
 3006 P=P+51
       AA(P)=AA(P)+DELTA
       GO TO 3007
C        ORIGINAL PDB02
 4011 BB(8)=0.0
       BB(10)=1.0
       BB(22)=0.0
       BB(24)=1.0
       BB(40)=1.0
       BB(44)=0.0
       W=WI
       DO 239 L=1,2304
```

```
239 AA(L)=0.0
    DO266 L=34,720,98
266 AA(L)=-0.5*AJ14
    DO217 L=81,767,98
217 AA(L)=0.5*AJ14
    DO218 L=26,320,98
218 AA(L)=-0.5*AJ13
    DO219 L=73,367,98
219 AA(L)=0.5*AJ13
    DO220 L=810,1104,98
220 AA(L)=-0.5*AJ13
    DO221 L=857,1151,98
221 AA(L)=0.5*AJ13
    DO222 L=18,1488,98
222 AA(L)=-0.5*AJ24
    DO223 L=65,1535,98
223 AA(L)=0.5*AJ24
    DO224 L=10,304,98
224 AA(L)=-0.5*AJ23
    DO285 L=57,351,98
285 AA(L)=0.5*AJ23
    DO286 L=402,696,98
286 AA(L)=-0.5*AJ34
    DO227 L=449,743,98
227 AA(L)=0.5*AJ34
    DO228 L=1186,1480,98
228 AA(L)=-0.5*AJ34
    DO229 L=1233,1527,98
229 AA(L)=0.5*AJ34
    DO230 L=1578,1872,98
230 AA(L)=-0.5*AJ23
    DO231 L=1625,1919,98
231 AA(L)=0.5*AJ23
    DO232 L=1538,2224,98
232 AA(L)=-0.5*AJ14
    DO233 L=1585,2271,98
233 AA(L)=0.5*AJ14
    DO234 L=1154,1448,98
234 AA(L)=-0.5*AJ13
    DO235 L=1201,1495,98
235 AA(L)=0.5*AJ13
    DO236 L=1938,2232,98
236 AA(L)=-0.5*AJ13
    DO237 L=1985,2279,98
237 AA(L)=0.5*AJ13
    DO238 L=770,2240,98
238 AA(L)=-0.5*AJ12
```

```
      DO 1239 L=817,2287,98                        14
1239  AA(L)=0.5*AJ12
      DO240 L=386,680,98
 240  AA(L)=-0.5*AJ23
      DO241 L=433,727,98
 241  AA(L)=0.5*AJ23
      DO242 L=778,1072,98
 242  AA(L)=-0.5*AJ34
      DO243 L= 825,1119,98
 243  AA(L)=0.5*AJ34
      DO244 L=1562,1856,98
 244  AA(L)=-0.5*AJ34
      DO245 L=1609,1903,98
 245  AA(L)=0.5*AJ34
      DO246 L=1954,2248,98
 246  AA(L)=-0.5*AJ23
      DO247 L=2001,2295,98
 247  AA(L)=0.5*AJ23
      DO248 L=1,2304,49
 248  AA(L)=-RTOR-TTWO
      AA(6)=0.5*AJ13
      AA(8)=0.5*AJ14
      AA(53)=-0.5*AJ13
      AA(55)=-0.5*AJ14
      AA(102)=0.5*AJ23
      AA(104)=0.5*AJ24
      AA(149)=-0.5*AJ23
      AA(194)=0.5*AJ13
      AA(196)=0.5*AJ23
      AA(200)=0.5*AJ34
      AA(241)=-0.5*AJ13
      AA(243)=-0.5*AJ23
      AA(247)=-0.5*AJ34
      AA(290)=0.5*AJ14
      AA(337)=-0.5*AJ14
      AA(341)=-0.5*AJ34
      AA(4)=0.5*AJ12
      AA(51)=-0.5*AJ12
      AA(98)=0.5*AJ12
      AA(145)=-0.5*AJ12
      AA(151)=-0.5*AJ24
      AA(292)=0.5*AJ24
      AA(294)=0.5*AJ34
      AA(339)=-0.5*AJ24
      AA(396)=0.5*AJ12
      AA(398)=0.5*AJ13
      AA(400)=0.5*AJ14
```

```
AA(443)=-0.5*AJ12
AA(445)=-0.5*AJ13
AA(447)=-0.5*AJ14
AA(490)=0.5*AJ12
AA(494)=0.5*AJ23
AA(496)=0.5*AJ24
AA(537)=-0.5*AJ12
AA(541)=-0.5*AJ23
AA(543)=-0.5*AJ24
AA(586)=0.5*AJ13
AA(588)=0.5*AJ23
AA(592)=0.5*AJ34
AA(633)=-0.5*AJ13
AA(635)=-0.5*AJ23
AA(639)=-0.5*AJ34
AA(682)=0.5*AJ14
AA(684)=0.5*AJ24
AA(686)=0.5*AJ34
AA(729)=-0.5*AJ14
AA(731)=-0.5*AJ24
AA(733)=-0.5*AJ34
AA(788)=0.5*AJ12
AA(790)=0.5*AJ13
AA(792)=0.5*AJ14
AA(835)=-0.5*AJ12
AA(837)=-0.5*AJ13
AA(839)=-0.5*AJ14
AA(882)=0.5*AJ12
AA(886)=0.5*AJ23
AA(888)=0.5*AJ24
AA(929)=-0.5*AJ12
AA(933)=-0.5*AJ23
AA(935)=-0.5*AJ24
AA(978)=0.5*AJ13
AA(980)=0.5*AJ23
AA(984)=0.5*AJ34
AA(1025)=-0.5*AJ13
AA(1027)=-0.5*AJ23
AA(1031)=-0.5*AJ34
AA(1074)=0.5*AJ14
AA(1076)=0.5*AJ24
AA(1078)=0.5*AJ34
AA(1121)=-0.5*AJ14
AA(1123)=-0.5*AJ24
AA(1125)=-0.5*AJ34
AA(1180)=0.5*AJ12
AA(1182)=0.5*AJ13
```

```
AA(1184)=0.5*AJ14
AA(1227)=-0.5*AJ12
AA(1229)=-0.5*AJ13
AA(1231)=-0.5*AJ14
AA(1274)=0.5*AJ12
AA(1278)=0.5*AJ23
AA(1280)=0.5*AJ24
AA(1321)=-0.5*AJ12
AA(1325)=-0.5*AJ23
AA(1327)=-0.5*AJ24
AA(1370)=0.5*AJ13
AA(1372)=0.5*AJ23
AA(1376)=0.5*AJ34
AA(1417)=-0.5*AJ13
AA(1419)=-0.5*AJ23
AA(1423)=-0.5*AJ34
AA(1466)=0.5*AJ14
AA(1468)=0.5*AJ24
AA(1470)=0.5*AJ34
AA(1513)=-0.5*AJ14
AA(1515)=-0.5*AJ24
AA(1517)=-0.5*AJ34
AA(1572)=0.5*AJ12
AA(1574)=0.5*AJ13
AA(1576)=0.5*AJ14
AA(1619)=-0.5*AJ12
AA(1621)=-0.5*AJ13
AA(1623)=-0.5*AJ14
AA(1666)=0.5*AJ12
AA(1670)=0.5*AJ23
AA(1672)=0.5*AJ24
AA(1713)=-0.5*AJ12
AA(1717)=-0.5*AJ23
AA(1719)=-0.5*AJ24
AA(1762)=0.5*AJ13
AA(1764)=0.5*AJ23
AA(1768)=0.5*AJ34
AA(1809)=-0.5*AJ13
AA(1811)=-0.5*AJ23
AA(1815)=-0.5*AJ34
AA(1858)=0.5*AJ14
AA(1860)=0.5*AJ24
AA(1862)=0.5*AJ34
AA(1905)=-0.5*AJ14
AA(1907)=-0.5*AJ24
AA(1909)=-0.5*AJ34
AA(1964)=0.5*AJ12
```

16

```
AA(1966)=0.5*AJ13
AA(1968)=0.5*AJ14
AA(2011)=-0.5*AJ12
AA(2013)=-0.5*AJ13
AA(2015)=-0.5*AJ14
AA(2058)=0.5*AJ12
AA(2062)=0.5*AJ23
AA(2064)=0.5*AJ24
AA(2105)=-0.5*AJ12
AA(2109)=-0.5*AJ23
AA(2111)=-0.5*AJ24
AA(2154)=0.5*AJ13
AA(2156)=0.5*AJ23
AA(2160)=0.5*AJ34
AA(2201)=-0.5*AJ13
AA(2203)=-0.5*AJ23
AA(2207)=-0.5*AJ34
AA(2250)=0.5*AJ14
AA(2252)=0.5*AJ24
AA(2254)=0.5*AJ34
AA(2297)=-0.5*AJ14
AA(2299)=-0.5*AJ24
AA(2301)=-0.5*AJ34
AA(2)=-0.5*(AJ12-AJ23-AJ24)+W-W2
AA(49)=0.5*(AJ12-AJ23-AJ24)-W+W2
AA(100)=-0.5*(AJ12-AJ13-AJ14)+W-W1
AA(147)=0.5*(AJ12-AJ13-AJ14)-W+W1
AA(198)=-0.5*(AJ34-AJ14-AJ24)+W+W3-W2-W1
AA(245)=0.5*(AJ34-AJ14-AJ24)-W-W3+W2+W1
AA(296)=-0.5*(AJ34-AJ13-AJ23)+W+W4-W2-W1
AA(343)=0.5*(AJ34-AJ13-AJ23)-W-W4+W2+W1
AA(394)=-0.5*(AJ13-AJ23-AJ34)+W-W3
AA(441)=0.5*(AJ13-AJ23-AJ34)-W+W3
AA(492)=-0.5*(AJ24-AJ14-AJ34)+W+W2-W3-W1
AA(539)=0.5*(AJ24-AJ14-AJ34)-W-W2+W3+W1
AA(590)=-0.5*(AJ13-AJ12-AJ14)+W-W1
AA(637)=0.5*(AJ13-AJ12-AJ14)-W+W1
AA(688)=-0.5*(AJ24-AJ12-AJ23)+W+W4-W3-W1
AA(735)=0.5*(AJ24-AJ12-AJ23)-W-W4+W3+W1
AA(786)=-0.5*(AJ14-AJ24-AJ34)+W-W4
AA(833)=0.5*(AJ14-AJ24-AJ34)-W+W4
AA(884)=-0.5*(AJ23-AJ13-AJ34)+W+W2-W4-W1
AA(931)=0.5*(AJ23-AJ13-AJ34)-W-W2+W4+W1
AA(982)=-0.5*(AJ23-AJ12-AJ24)+W+W3-W4-W1
AA(1029)=0.5*(AJ23-AJ12-AJ24)-W-W3+W4+W1
AA(1080)=-0.5*(AJ14-AJ12-AJ13)+W-W1
AA(1127)=0.5*(AJ14-AJ12-AJ13)-W+W1
```

```
AA(1178)=-0.5*(AJ14-AJ24-AJ34)+W+W1-W3-W2
AA(1225)=0.5*(AJ14-AJ24-AJ34)-W-W1+W3+W2
AA(1276)=-0.5*(AJ23-AJ13-AJ34)+W-W3
AA(1323)=0.5*(AJ23-AJ13-AJ34)-W+W3
AA(1374)=-0.5*(AJ23-AJ12-AJ24)+W-W2
AA(1417)=-BJ24
AA(1421)=0.5*(AJ23-AJ12-AJ24)-W+W2
AA(1472)=-0.5*(AJ14-AJ12-AJ13)+W+W4-W3-W2
AA(1519)=0.5*(AJ14-AJ12-AJ13)-W-W4+W3+W2
AA(1570)=-0.5*(AJ13-AJ23-AJ34)+W+W1-W4-W2
AA(1617)=0.5*(AJ13-AJ23-AJ34)-W-W1+W4+W2
AA(1668)=-0.5*(AJ24-AJ14-AJ34)+W-W4
AA(1715)=0.5*(AJ24-AJ14-AJ34)-W+W4
AA(1766)=-0.5*(AJ13-AJ12-AJ14)+W+W3-W4-W2
AA(1813)=0.5*(AJ13-AJ12-AJ14)-W-W3+W4+W2
AA(1864)=-0.5*(AJ24-AJ12-AJ23)+W-W2
AA(1911)=0.5*(AJ24-AJ12-AJ23)-W+W2
AA(1962)=-0.5*(AJ12-AJ23-AJ24)+W+W1-W4-W3
AA(2009)= 0.5*(AJ12-AJ23-AJ24)-W-W1+W4+W3
AA(2060)=-0.5*(AJ12-AJ13-AJ14)+W+W2-W4-W3
AA(2107)= 0.5*(AJ12-AJ13-AJ14)-W-W2+W4+W3
AA(2158)=-0.5*(AJ34-AJ14-AJ24)+W-W4
AA(2205)= 0.5*(AJ34-AJ14-AJ24)-W+W4
AA(2256)=-0.5*(AJ34-AJ13-AJ23)+W-W3
AA(2303)= 0.5*(AJ34-AJ13-AJ23)-W+W3
AA(3)=RTOR
AA(52)=RTOR
AA(97)=RTOR
AA(146)=RTOR
AA(199)=RTOR
AA(248)=RTOR
AA(293)=RTOR
AA(342)=RTOR
AA(419)=RTOR
AA(468)=RTOR
AA(513)=RTOR
AA(562)=RTOR
AA(615)=RTOR
AA(664)=RTOR
AA(709)=RTOR
AA(758)=RTOR
AA(795)=RTOR
AA(844)=RTOR
AA(889)=RTOR
AA(938)=RTOR
AA(991)=RTOR
AA(1040)=RTOR
```

```
      AA(1085)=RTOR
      AA(1134)=RTOR
      AA(1171)=RTOR
      AA(1220)=RTOR
      AA(1265)=RTOR
      AA(1314)=RTOR
      AA(1367)=RTOR
      AA(1416)=RTOR
      AA(1461)=RTOR
      AA(1510)=RTOR
      AA(1547)=RTOR
      AA(1596)=RTOR
      AA(1641)=RTOR
      AA(1690)=RTOR
      AA(1743)=RTOR
      AA(1792)=RTOR
      AA(1837)=RTOR
      AA(1886)=RTOR
      AA(1963)=RTOR
      AA(2012)=RTOR
      AA(2057)=RTOR
      AA(2106)=RTOR
      AA(2159)=RTOR
      AA(2208)=RTOR
      AA(2253)=RTOR
      AA(2302)=RTOR
C       ORIGINAL PDB01
      L=0
 4008 DO 4009 J=1,2304
 4009 A(J)=AA(J)
      DO 4016 K=1,48
 4016 B(K)=BB(K)
      CALL SIMQ(A,B,N,KS)
      IF(KS) 999,4100,999
 4100 L=L+1
      SUM(L)=B(2)+B(4)+B(10)+B(14)+B(18)+B(24)+B(28)+B(30)+B(36)+B(40)+
     1B(46)+B(48)+SUM(L)
      SUM(L)=-SUM(L)
      WRITE(3,4)W,SUM(L)
      P=2
      W=W+DELTA
      IF(W-WU) 4010,4010,5011
 4010 AA(P)=AA(P)+DELTA
 4007 P=P+47
      AA(P)=AA(P)-DELTA
      IF(P-2300) 4006,4008,4008
 4006 P=P+51
```

```
      AA(P)=AA(P)+DELTA                                           20
      GO TO 4007
5011  IF(NCASE-1) 6011,6011,5012
5012  WRITE(3,9000)NCAS
      NCAS=NCAS+1
      NCASE=NCASE-1
      GO TO 500
 999  WRITE(3,1000)
6011  WRITE(3,9000)NCAS
   1  FORMAT(8F10.6)
   4  FORMAT(22X,F6.2,35X,F10.3)
1000  FORMAT('1SINGULAR SET OF EQUATIONS')
2000  FORMAT(I2,19A4)
2500  FORMAT(1H1,30X,19A4//)
3000  FORMAT(5X,'CHEMICAL SHIFTS',20X,'1',20X,'2',20X'3',20X'4')
4000  FORMAT(36X,F8.3,3(13X,F8.3))
5000  FORMAT(//5X,'INVERSE T(2)=',F8.3///5X,'RELAXATION RATE=',F10.3//)
5500  FORMAT(1H1,5X,'START OF CASE ',I2//5X,'RELAXATION RATE 'F10.3//)
6000  FORMAT(20X,'FREQUENCY',35X,'INTENSITY')
7000  FORMAT(//5X,'COUPLING CONSTANTS',17X,'12',10X,'13',10X,'14',10X,'2
     13',10X,'24',10X,'34')
8000  FORMAT(38X,F6.3,5(6X,F6.3))
9000  FORMAT(////5X,'END OF CASE ',I2)
      CALL EXIT
      END
```

```
      SUBROUTINE SIMQ(A,B,N,KS)                                        21
      DIMENSION A(1),B(1)
C         FORWARD SOLUTION
      TOL=0.0
      KS=0
      JJ=-N
      DO 65 J=1,N
      JY=J+1
      JJ=JJ+N+1
      BIGA=0
      IT=JJ-J
      DO 30 I=J,N
C         SEARCH FOR MAXIMUM COEFFICIENT IN COLUMN
      IJ=IT+I
      IF(ABS(BIGA)-ABS(A(IJ))) 20,30,30
   20 BIGA=A(IJ)
      IMAX=I
   30 CONTINUE
C         TEST FOR PIVOT LESS THAN TOLERANCE (SINGULAR MA
      IF(ABS(BIGA)-TOL) 35,35,40
   35 KS=1
      RETURN
C         INTERCHANGE ROWS IF NECESSARY
   40 I1=J+N*(J-2)
      IT=IMAX-J
      DO 50 K=J,N
      I1=I1+N
      I2=I1+IT
      SAVE=A(I1)
      A(I1)=A(I2)
      A(I2)=SAVE
C         DIVIDE EQUATION BY LEADING COEFFICIENT
   50 A(I1)=A(I1)/BIGA
      SAVE=B(IMAX)
      B(IMAX)=B(J)
      B(J)=SAVE/BIGA
C         ELIMINATE NEXT VARIABLE
      IF(J-N) 55,70,55
   55 IQS=N*(J-1)
      DO 65 IX=JY,N
      IXJ=IQS+IX
      IT=J-IX
      DO 60 JX=JY,N
      IXJX=N*(JX-1)+IX
      JJX=IXJX+IT
   60 A(IXJX)=A(IXJX)-(A(IXJ)*A(JJX))
```

```
   65 B(IX)=B(IX)-(B(J)*A(IXJ))
C         BACK SOLUTION
   70 NY=N-1
      IT=N*N
      DO 80 J=1,NY
      IA=IT-J
      IB=N-J
      IC=N
      DO 80 K=1,J
      B(IB)=B(IB)-A(IA)*B(IC)
      IA=IA-N
   80 IC=IC-1
      RETURN
      END
```

APPENDIX 2.

LAOCN3

    The program has two capabilities, direct calculation and iterative calculation.

    For a trial direct calculation the program accepts as data a case number, the number of spin nuclei in the system, an identification title, the range of frequencies of transitions of interest, the isotopic variety of each nucleus, a set of chemical shifts and coupling constants (Hz) and control variables, (i) specifying that no iterative fitting is to be done, and (ii) whether output on punched cards is required. The program yields for output, all input data and a table of transitions with an identifying number for each transition, its frequency, and its intensity. Punched cards with these frequencies and intensities can also be produced if so desired.

    If the trial calculation has yielded a calculated spectrum bearing a resemblance to an observed spectrum, an iterative calculation can be attempted.

    The program for an iterative calculation requires the same data as the trial calculation plus specifications on which sets of parameters are to be varied. Also experimental frequencies corresponding to line numbers obtained in the preliminary trial direct calculation must be fed in.

    As output the program yields the root mean square error in fitting of assigned lines for the trial calculation and after each cycle of adjustment, a table of the probable errors associated with the values of each parameter set with the table of the adjusted parameters. A table containing for each transition the line identification number, the assigned experimental frequency, the calculated frequency, the calculated intensity, and the error in fitting, if an experimental frequency was given, is also given as output.

Best Value Cases

Compound (1) = N, N-dimethyl-p-nitrosoaniline
Compound (2) = N, N-diethyl-p-nitrosoaniline

R

4   1

3   2

N = O
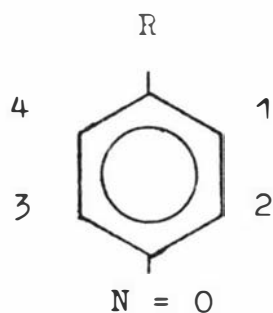
The program requires the
chemical shifts in this
sequence.

Compound (1) in acetone-d$_6$

$$
\begin{aligned}
W(1) &= 420.387 \pm .015 \\
W(2) &= 535.804 \pm .014 \\
W(3) &= 397.067 \pm .058 \\
W(4) &= 402.688 \pm .056 \\
A(1,2) &= 9.043 \pm .020 \\
A(1,3) &= 0.155 \pm .058 \\
A(1,4) &= 2.835 \pm .059 \\
A(2,3) &= 2.497 \pm .043 \\
A(2,4) &= 0.040 \pm .042 \\
A(3,4) &= 9.533 \pm .034
\end{aligned}
$$

Iteration 3 RMS error = .045

Compound (2) in acetone-d$_6$

$$
\begin{aligned}
W(1) &= 423.950 \pm .018 \\
W(2) &= 533.619 \pm .016 \\
W(3) &= 399.607 \pm .065 \\
W(4) &= 406.316 \pm .081 \\
A(1,2) &= 9.113 \pm .024 \\
A(2,3) &= 0.055 \pm .060 \\
A(1,4) &= 2.862 \pm .062 \\
A(2,3) &= 2.455 \pm .050 \\
A(2,4) &= 0.002 \pm .050 \\
A(3,4) &= 9.411 \pm .045
\end{aligned}
$$

Iteration 3 RMS error = .052

Compound (1) in chloroform-d$_1$

$$
\begin{aligned}
W(1) &= 409.291 \pm .049 \\
W(2) &= 534.393 \pm .021 \\
W(3) &= 407.049 \pm .036 \\
W(4) &= 391.616 \pm .026 \\
A(1,2) &= 8.920 \pm .050 \\
A(1,3) &= -0.018 \pm .055 \\
A(1,4) &= 2.638 \pm .042 \\
A(2,3) &= 2.377 \pm .044 \\
A(2,4) &= -0.047 \pm .034 \\
A(3,4) &= 9.546 \pm .041
\end{aligned}
$$

Iteration 3 RMS error = .066

Compound (2) in chloroform-d$_1$

$$
\begin{aligned}
W(1) &= 409.704 \pm .030 \\
W(2) &= 531.759 \pm .024 \\
W(3) &= 410.447 \pm .028 \\
W(4) &= 392.304 \pm .028 \\
A(1,2) &= 9.025 \pm .039 \\
A(1,3) &= 0.0 \\
A(1,4) &= 2.528 \pm .042 \\
A(2,3) &= 2.394 \pm .037 \\
A(2,4) &= 0.0 \\
A(3,4) &= 9.492 \pm .035
\end{aligned}
$$

Iteration 2 RMS error = .088

Compound (2) in toluene-d$_8$

$$W(1) = 360.441 \pm .015$$
$$W(2) = 537.450 \pm .015$$
$$W(3) = 404.326 \pm .019$$
$$W(4) = 340.425 \pm .016$$
$$A(1,2) = 8.998 \pm .022$$
$$A(1,3) = -0.063 \pm .023$$
$$A(1,4) = 2.667 \pm .022$$
$$A(2,3) = 2.371 \pm .025$$
$$A(2,4) = -0.064 \pm .022$$
$$A(3,4) = 9.508 \pm .025$$

Iteration 2 RMS error = .053

p-nitrosophenol in 1 M K$_2$CO$_3$ (in D$_2$O)

$$W(1) = 393.317 \pm .044$$
$$W(2) = 478.077 \pm .024$$
$$W(3) = 442.522 \pm .024$$
$$W(4) = 387.222 \pm .047$$
$$A(1,2) = 9.599 \pm .047$$
$$A(1,3) = -0.041 \pm .044$$
$$A(1,4) = 2.220 \pm .048$$
$$A(2,3) = 2.691 \pm .034$$
$$A(2,4) = -0.084 \pm .042$$
$$A(3,4) = 9.648 \pm .051$$

Iteration 3 RMS error = 0.076

N.B.   The actual error in these parameters as
        discussed in Chapter Four, is $\pm$ 0.2 Hz.

References

1.   F. Bloch, W.W. Hansen and M.E. Packard.
Phys. Rev. 69, 127 (1946).

2.   E.M. Purcell, H.C. Torrey and R.V. Pound.
Phys. Rev. 69, 37 (1946).

3.   W. Pauli.
Naturwisschaften, 12, 741 (1924).

4.   Ruth M. Lynden-Bell and Robin K. Harris.
Nuclear magnetic resonance spectroscopy, p. 12,
Thomas Nelson (1969).

5.   W.G. Proctor and F.C. Yu.
Phys. Rev. 81, 20, (1951).

6.   H.S. Gutowsky and D.W. McCall.
Phys. Rev. 82, 748 (1951).

7.   E.L. Hahn and D.E. Maxwell.
Phys. Rev. 84, 1246 (1951).

8.   N.F. Ramsey and E.M. Purcell.
Phys. Rev. 85, 143 (1952).

9.   P.D. Buckley, K.W. Jolley and D.N. Pinder.
Progress in NMR spectroscopy, 10, 11 (1975).

10.   Ruth M. Lynden-Bell and Robin K. Harris.
Chapter 4, nuclear magnetic resonance spectroscopy
Thomas Nelson (1969).

11.   P. Meakin, D.O. Harris and Eizi Hirota.
J. Chem. Phys. 51, 3775 (1969).

12.   E.B. Wilson.
Advances Chem. Phys. 2, 367 (1969).

13.   S. Muzishima.
Structure of Molecules and Internal Rotation.
Academic Press, New York (1954).

14. Horst Kessler.

    Angew. Chem. Internat. Edit. Vol. 9 (1970), no. 3.

15. T.C. Farrar and E.D. Becker.

    Pulse and Fourier Transform NMR, Academic Press (1971).

16. Charles S. Johnson, Jnr.

    Advances in Magnetic Resonance Vol. 1, p. 33.

17. S. Glasstone, K.J. Laidler and H. Eyring.

    The Theory of Rate Processes, pp 184-201, McGraw-Hill.

18. H.S. Gutowsky and C.H. Holm.

    J. Chem. Phys. 25, 1228 (1956).

19. H.S. Gutowsky, D.W. McCall and C.P. Slichter.

    J. Chem. Phys. 21, 279 (1953).

20. H.S. Gutowsky and A. Saika.

    J. Chem. Phys. 21, 1688 (1953).

21. J.W. Emsley, J. Feeney and L.H. Sutcliffe.

    High Resolution Nuclear Magnetic Resonance Spectroscopy.

    Pergamon Press.

22. S. Alexander.

    J. Chem. Phys. 37, 967 (1962)

                   38, 1787 (1963)

                   40, 2741 (1964)

23. Matsami Takeda and E.O. Stejskal.

    J. Am. Chem. Soc. 82, 25 (1960).

24. Tables of Exchange Broadened NMR Multiplets

    technical note No. 2, contract No. AF61(052)-03,

    Weizmann Institute of Sciences.

25. Max T. Rogers and James C. Woodbrey.

    J. Phys. Chem., 540 (1966).

26. Adam Allerhand, H.S. Gutowsky, J. Jonas and
                                    R.A. Meinzer

    J. Am. Chem. Soc. 88, 3185 (1966).

27.   L.H. Piette and W.A. Anderson.

       J. Chem. Phys. 30, 899 (1959).

28.   F.A.L. Anet and A.J.R. Bourn.

       J. Am. Chem. Soc. 89, 760 (1967).

29.   F.R. Jensen, D.S. Noyce, C.H. Sederholm and
                                    A.J. Berlin

       J. Am. Chem. Soc. 82, 1256 (1960)

                          84, 386 (1962).

30.   R.K. Harris and N. Sheppard.

       Proc. Chem. Soc., 419 (1961).

31.   S. Meiboom.

       Paper presented at the Symposium on High

       Resolution NMR, Boulder, Colo, July 1962.

32.   F.A.L. Anet, M. Ahmad and L.D. Hall.

       Proc. Chem. Soc., 145 (1964).

33.   F.A. Bovey, F.P. Hood, E.W. Anderson and
                                    R.L. Kornegay

       Proc. Chem. Soc., 146 (1964)

       J. Chem. Phys. 41, 2041 (1964).

34.   A. Allerhand, F. Chen and H.S. Gutowsky.

       J. Chem. Phys. 42, 3040 (1965).

35.   F.A.L. Anet.

       J. Am. Chem. Soc. 86, 458 (1964).

36.   R.M. Lynden-Bell.

       Progress in NMR Spectroscopy, 2, 163 (1967).

37.   P.D. Buckley, K.W. Jolley and D.N. Pinder.

       Progress in NMR Spectroscopy, 10, pp 1-26 (1975).

38.   Kjell-Ivar Dahlquist and Sture Forsen.

       J. Phys. Chem. 73, 4124 (1969).

39.   R.M. Lynden-Bell.

       Progress in NMR Spectroscopy, 2, 166 (1967).

40. R.M. Lynden-Bell.

    Progress in NMR Spectroscopy, $\underline{2}$, 166 (1967).

41. R.M. Lynden-Bell.

    Progress in NMR Spectroscopy, $\underline{2}$, 169 (1967).

42. R.M. Lynden-Bell.

    Progress in NMR Spectroscopy, $\underline{2}$, 171 (1967).

43. P.D. Buckley, K.W. Jolley and D.N. Pinder.

    Progress in NMR Spectroscopy, $\underline{10}$, 10 (1975).

44. R.M. Lynden-Bell.

    Progress in NMR Spectroscopy, $\underline{2}$, (1967).

45. P.D. Buckley, K.W. Jolley and D.N. Pinder.

    Progress in NMR Spectroscopy, $\underline{10}$, 14 (1975).

46. Kjell-Ivar Dahlquist and Sture Forsen.

    Acta. Chem. Scand. $\underline{24}$, 654 (1970).

47. D.N. Pinder.

    J. Phys. Chem., $\underline{77}$, 567 (1973).

48. Annual Review of NMR Spectroscopy Vol 1, p. 8.

    Ed. E.F. Mooney, Academic Press (1968) London

    and New York.

49. I.C. Calder and P.J. Garratt.

    Tetrahedron, $\underline{25}$, 4023 (1969).

50. D.D. MacNicol, R. Wallace and J.C.D. Brand.

    Trans. Farad. Society, $\underline{1}$, 1 (1965).

51. P.K. Korver, P.J. van der Haak and Th. J. De Boer.

    Tetrahedron $\underline{22}$, 3157 (1966).

52. Pesteiner and Brüek in Landolt-Bernstein, Tabellen

    Zahlen werte und Funktionen, I. Band, 3 Teil

    (Molekeln II), (Springer-Verlag, Berlin, 1951).

53. Mason and Dunderdale.

    J. Chem. Soc., 754 (1956).

54. Nakomoto and Rundle.

J. Am. Chem. Soc. $\underline{78}$, 1113 (1956).

55. Keussler and Lüttke.

Z. Elektrochem. $\underline{63}$, 614 (1959).

56. A.I. Vogel.

Practical Organic Chemistry, 3rd Edn (Longmans,
London 1956).

57. Dictionary of Organic Compounds, pub.

Eyre and Spottiswoode, London.

58. A.A. Bothner-By and S.M. Castellano.

Computer Programs for Chemistry, editor P.F. De Tar,

Benjamin, New York, Vol. 1, p. 16, (1968).

59. R.E. Klinck, D.H. Marr and J.B. Stothers.

Chem. Comm. 409 (1967).

60. T. Drakenberg, K.-I. Dahlquist and S. Forsen.

Acta Chemica Scandinavica $\underline{24}$, 694 (1970).

61. R.K. Harris and N. Sheppard.

J. Mol. Spectroscopy $\underline{23}$, 231 (1967).

62. J.W. Emsley, J. Feeney and L.H. Sutcliffe,

p. 63   High Resolution Nuclear Magnetic

Resonance Spectroscopy.   Pergamon Press.

63. G. Fraenkel and C. Franconi.

J. Am. Chem. Soc. $\underline{82}$, 4478 (1960).

64. R.C. Neumann Jnr and L.B. Young.

J. Phys. Chem. $\underline{69}$, 2570 (1965).

65. A.G. Wittaker and S. Siegel.

J. Chem. Phys. $\underline{42}$, 3320 (1965).

66. M. Rabinowitz and A. Pines.

J. Am. Chem. Soc. $\underline{91}$, 1585 (1969).

67. F. Conti and W.V. Philipsborn.

Helv. Chim. Acta. $\underline{50}$, 603 (1967).

68. T. Matsuo and H. Shosenji.

Chem. Comm., 501 (1969).

69. T. Drakenberg, K.I. Dahlquist and S. Forsen.

J. Phys. Chem. $\underline{76}$, 2178 (1972).

70. Torbjörn Drakenberg.

Tetrahedron Letters, 1743 (1972).

71. D.L. Griffith and J.D. Roberts.

J. Am. Chem. Soc. $\underline{87}$, 4089 (1965).

72. J.D. Cooney, S.K. Brownstein and J.W. Apsimon.

Canad. J. Chem. $\underline{52}$, 3028 (1974).

73. R.G. Wilson and D.H. Williams.

J. Chem. Soc. B, 1163 (1968).

74. P.D. Buckley, A.R. Furness, K.W. Jolley and
                                    D.N. Pinder.

Aust. J. Chem., 1974, $\underline{27}$, 21-6.

75. Alan R. Furness, Paul D. Buckley and Ken W. Jolley.

Aust. J. Chem., 1975, 28, 2303-6.

76. R.K. Norris and S. Sternhell.

Aust. J. Chem. $\underline{19}$, 841 (1966).

77. A.L. Van Geet.

Analytical Chemistry, $\underline{40}$, 2227 (1968).

78. A.L. Van Geet.

Analytical Chemistry, $\underline{42}$, 679 (1970).

79. E. Havinga and A. Schors.

Rec. Trav. Chim. Pays-Bas $\underline{69}$, 457 (1950)
                           $\underline{70}$, 59 (1951).

80. R.K. Norris and S. Sternhell.

Tetrahedron Letters, 97 (1967).

81. Determination of pH - Theory and Practice.

R.G. Bates, John Wiley and Sons, New York (1965).

82. R.G. Pearson and M.M. Anderson.
     Angew. Chem. Internat. Edit. $\underline{4}$, 281 (1965).

83. T.R. Stengle and C.H. Langford.
     Co-ordination Chemistry Reviews $\underline{2}$, 349 (1967).

84. L.H. Pignolet and W. De W. Horrocks Jnr.
     J. Am. Chem. Soc. $\underline{90}$, 922 (1968)
                        $\underline{88}$, 5929 (1966).

85. S.S. Zumdahl and R.S. Drago.
     J. Am. Chem. Soc. $\underline{89}$, 4319 (1967).

86. D.R. Eaton and K. Zaw.
     Canad. J. of Chem. $\underline{49}$, 3315 (1971).

87. A.M. Brodie, S.H. Hunter, G.A. Rodley and
                                    C.J. Wilkins.
     J. Chem. Soc. A, 987 (1968).

88. Organic Syntheses Coll. Vol. 4, 351.
     John Wiley and Sons, N.Y.

89. M.J. Bagley, D. Nicholls, and B.A. Warburton.
     J. Chem. Soc. A, 2694 (1970).

90. Organic Syntheses Coll. Vol. 2, 395
     John Wiley and Sons, N.Y.

91. I.L. Finar.
     J. Chem. Soc. part 4, 4094 (1958).

92. H. Bredereck, H. Herlinger and E.H. Schweizer.
     Chemische Berichte, $\underline{93}$, 1208 (1960).

93. Organic Syntheses Coll. Vol. 1, 1.
     John Wiley and Sons, N.Y.

94. C.A. Rojahn.
     Chemische Berichte, 607 (1926).

95. Organic Syntheses, Coll. Vol. 2, 165.
     John Wiley and Sons, N.Y.

96. Organic Syntheses Coll. Vol. 2, 461.
    John Wiley and Sons, N.Y.

97. F.T. Boyle and Richard A.Y. Jones.
    Perkin Transactions II $\underline{2}$, 165 (1973).

98. I.L. Finar.
    J. Chem. Soc., 4094 (1958).

99. Douglas G. Bickly and Nick Serpone.
    Canad. J. of Spectroscopy $\underline{19}$, 40 (1974).

100. A. Jaeschke, H. Muensch, H.G. Schmid, H. Friebolin
                                   and A. Mannschreck.
    Journal of Mol. Spectroscopy $\underline{31}$, 14 (1969).